

DISSERTATION

SUBSTRATE CONTROLLED INTERACTIONS BETWEEN HYDRAULICS, SEDIMENT
TRANSPORT, AND EROSIONAL FORMS IN BEDROCK RIVERS

Submitted by

Jaime Ruth Goode

Department of Geosciences

In partial fulfillment of the requirements

For the Degree of Doctor of Philosophy

Colorado State University

Fort Collins, Colorado

Fall 2009

UMI Number: 3401011

All rights reserved

INFORMATION TO ALL USERS

The quality of this reproduction is dependent upon the quality of the copy submitted.

In the unlikely event that the author did not send a complete manuscript and there are missing pages, these will be noted. Also, if material had to be removed, a note will indicate the deletion.



UMI 3401011

Copyright 2010 by ProQuest LLC.

All rights reserved. This edition of the work is protected against unauthorized copying under Title 17, United States Code.



ProQuest LLC
789 East Eisenhower Parkway
P.O. Box 1346
Ann Arbor, MI 48106-1346

COLORADO STATE UNIVERSITY

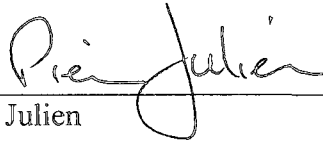
May 14, 2009

WE HEREBY RECOMMEND THAT THE DISSERTATION PREPARED UNDER OUR SUPERVISION BY JAIME RUTH GOODE ENTITLED SUBSTRATE CONTROLLED INTERACTIONS BETWEEN HYDRAULICS, SEDIMENT TRANSPORT, AND EROSIONAL FORMS IN BEDROCK RIVERS BE ACCEPTED AS FULFILLING IN PART REQUIREMENTS FOR THE DEGREE OF DOCTOR OF PHILOSOPHY.

Committee on Graduate work



Daniel Cenderelli



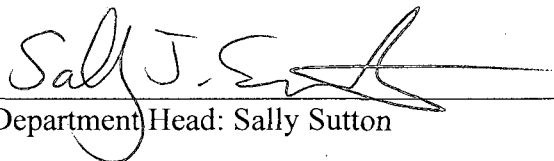
Pierre Julien



Sara Rathburn



Advisor: Ellen Wohl



Department Head: Sally Sutton

ABSTRACT OF DISSERTATION

SUBSTRATE CONTROLLED INTERACTIONS BETWEEN HYDRAULICS, SEDIMENT TRANSPORT, AND EROSIONAL FORMS IN BEDROCK RIVERS

Bedrock rivers are important components of the landscape that are distinguished from alluvial rivers by high sediment transport capacity relative to supply, and a direct link between the underlying geology and forms and processes. This dissertation examines how independent substrate controls influence the interactions among bedrock channel morphology, hydraulics, sediment transport, and incision processes. Three distinct, but related chapters focus on hydraulics, sediment transport dynamics, and incision processes at inter-reach and intra-reach scales. The majority of this research was conducted on the Ocoee River, Tennessee, which flows through the Blue Ridge province of the southern Appalachians. Four main study reaches were designated based on differences in bedrock erodibility controlled by lithologic and structural variation.

The results indicate that substrate differences correlate with variation in reach morphology (i.e., gradient, bedform orientation and amplitude), such that less erodible substrates are associated with steeper reach gradient and with transversely oriented ribs of greater amplitude. One-dimensional hydraulic modeling indicates that in the reach with the least erodible substrate, and greatest bed slope and rib amplitude, the reach-averaged hydraulic roughness was the greatest. Increased hydraulic roughness in steeper reaches points to the importance of positive and negative feedbacks in these systems: Greater substrate erosional resistance limits profile lowering, which likely creates steeper bed slopes and greater stream

power, creating a self-enhancing feedback. This local increase in stream power is balanced by increased roughness resulting from the erosional processes that produce bedrock ribs, which represents a self-regulating feedback. The overall result reflects quantifiable adjustments between substrate resistance and hydraulic driving forces in bedrock channels.

Focusing on sediment transport dynamics, the results indicate that transport distance is not a significant function of grain size, as has been reported for alluvial channels. Reach-scale differences in channel morphology correlate with transport distance. At different intra-reach scales, the smallest spatial resolution was the best predictor of transport distance. The highly complex bed topography in this system leads to widely varying coarse sediment transport dynamics. Complex interactions among gradient and bed roughness appear to govern reach-scale differences in the degree of alluvial cover.

Inter-reach differences in lithology and channel morphology lead to differences in both the size and spatial patterns of potholes. In reaches with more resistant rock and heterogeneous bed topography, pothole dimensions are larger and follow an aggregated spatial pattern. Intermediate bed elevations show the highest likelihood of pothole formation, suggesting that local hydraulics and tools versus cover relationships govern pothole formation and maintenance. At different spatial scales, substrate characteristics play a key role in controlling the forms and processes of the bedrock channels examined in this study.

Jaime Ruth Goode
Department of Geosciences
Colorado State University
Fort Collins, CO 80523
Fall 2009

ACKNOWLEDGEMENTS

Absolutely, the first to thank is my advisor, Ellen Wohl. I am enormously grateful for her inspiration, efficiency, open accessibility for questions throughout this research, and friendship. The opportunities to work on different projects in other regions, which she provided, greatly broadened my research scope.

Friends and family provided unyielding support. I am very fortunate to have such loving and supportive parents, Richard and Ruth Goode. They have been with me every step of the way, always encouraging me to push myself and work hard.

I thank my husband, Nate Pickens, for his support especially in the final phases of this work; the many friends in Fort Collins, Steamboat and the Ocoee for keeping my mind fresh with play time in the mountains and rivers; and fellow graduate students for humor and stimulating scientific discussions.

I owe many thanks to Doug Thompson for introducing me to the field of Fluvial Geomorphology as an undergraduate at Connecticut College, and showing me that I could make a career out of my passion for rivers. Doug has been a continual supporter through my graduate work.

I greatly appreciated all the hard work that three main field assistants supplied: Will Stubblefield, Will Lyons, and Roy Szymanski. Thanks are owed for their high thresholds of

boredom during intense channel geometry surveys. Without their hard work, this project would not have been possible.

Thanks to Sara Rathburn, Dan Cenderelli and Pierre Julien for serving on my committee and providing valuable comments and reviews of this research, and for challenging me through this process. Robin Reich was instrumental in developing the spatial statistic approach to study potholes, presented in Chapter 5.

This work was funded by the National Science Foundation grant EAR-0507098, without which, this research and my graduate program would not have been possible.

TABLE OF CONTENTS

CHAPTER 1. INTRODUCTION.....	1
1.1 Study objectives.....	2
1.1.1 Research overview.....	3
CHAPTER 2. BACKGROUND	5
2.1 Bedrock channels.....	5
2.2. Bedrock channel morphology.....	8
2.3. Incision processes.....	11
2.3. Bedrock incision models	13
3.3.1. Saltation-abrasion model of bedrock incision.....	16
2.3. Sediment transport.....	17
2.4. Substrate controls	19
2.5 Bedforms and sculpted forms.....	21
CHAPTER 3. SUBSTRATE CONTROLS ON THE LONGITUDINAL PROFILE OF BEDROCK CHANNELS: IMPLICATIONS FOR REACH-SCALE ROUGHNESS.....	30
3.1 Introduction	31
3. 2. Study Area	34
3.3. Methods	40
3.3.1. Longitudinal variation in substrate and channel morphology.....	40
3.3.2. Hydraulic modeling of reach-scale roughness	42
3.4. Results	46
3.4.1. Reach-scale differences in erodibility	46
3.4.2. Substrate properties in relation to channel morphology	49
3.5 Discussion.....	59
3.6. Conclusions	63
CHAPTER 4: COARSE SEDIMENT TRANSPORT DYNAMICS AT THREE SPATIAL SCALES OF BEDROCK CHANNEL BED COMPLEXITY	68
4.1. Introduction	69

4.2.	Study Area	73
4.3.	Methods	77
4.4.	Results	82
4.4.1.	Transport distance and tracer size (H1)	87
4.4.2.	Inter-reach variability in transport distance (H2)	89
4.4.3.	Intra-reach variability in transport distance (H3)	93
4.5.	Discussion.....	101
4.5.1.	Controls on transport distance.....	101
4.5.2.	Limitations and uncertainties	101
4.5.3.	Consideration of dam effects on sediment supply and alluvial cover.....	104
4.5.4.	Factors influencing alluvial cover in bedrock channels.....	105
4.6.	Conclusion.....	109
CHAPTER 5. SUBSTRATE INFLUENCES ON THE SIZE AND SPATIAL PATTERNS OF STREAM POTHOLES: A FIELD EXAMPLE.....		115
5.1.	Introduction	116
5.2.	Study Area	120
5.3.	Methods	123
5.3.1.	Field Methods.....	123
5.3.2.	Statistical Analyses	125
5.3.3.	Modeling the probability of pothole formation.....	126
5.4.	Results	129
5.4.1.	Inter-reach variability.....	129
5.4.2.	Intra-reach variability.....	134
5.4.3.	Probability of pothole occurrence	135
5.4.4.	Relative abrasional efficiency	139
5.5.	Discussion.....	141
5.5.1.	Pothole variability as a function of rock characteristics: Reach-scale differences.....	142
5.5.2.	Relative elevation and optimal locations for pothole formation	144
5.5.3.	Interactions between potholes and bedrock ribs	145
5.6.	Conclusion.....	147
Chapter 6: CONCLUSIONS		152
6.1.	Future directions.....	157
APPENDIX.....		159

LIST OF TABLES

Table 3.1. Blue Ridge Streams.....	34
Table 3.2. HEC-RAS one-dimensional modeling results and summary data for Upper Ocoee subreaches.....	45
Table 4.1. Summary of transport distances and tracer sizes transported	83
Table 4.2. Summary of reach differences including percent cover.....	85
Table 4.3. Summary of transport distances and tracer sizes transported	86
Table 4.4. Summary of ANOVA analysis of transport distance by intra-reach spatial scale.....	94
Table 5.1. Reach variable summary.....	123
Table 5.2. Dimension regression statistics.....	129
Table 5.3. Summary statistics from segregation by size analysis	134

LIST OF FIGURES

Figure 3.1. Conceptual model end members.....	32
Figure 3.2. Study area site map.....	35
Figure 3.3. Photographs of bedrock ribs along the Upper Ocoee section.....	38
Figure 3.4. Photograph of longitudinal ribs in Upper Ocoee R2 showing alluvial patches in sculpted forms and between ribs.....	39
Figure 3.5. Three-dimensional plots of the four Upper Ocoee subreaches.....	44
Figure 3.6. Comparison of substrate resistance (A. Schmidt hammer reading; B. Selby Score) among reaches along the Upper and Middle Ocoee sections.....	48
Figure 3.7. Reach gradient adjusted by drainage area as a function of rock erodibility.....	50
Figure 3.8. Longitudinal profile plots showing bed elevation variation according to rib orientation.....	53
Figure 3.9. Comparison of bed slope among reaches with different rib orientations.....	54
Figure 3.10. Detailed longitudinal profile plot of the Little River reach illustrating rib amplitude and spacing.....	55
Figure 3.11. Positive logarithmic relationship between reach gradient and rib amplitude.....	56

Figure 3.12. Comparison of calculated n-values from the upper Ocoee subreaches. Rib orientations are indicated above each plot.....	57
Figure 3.13. Substrate controls on reach-scale roughness	58
Figure 4.1. Digital Orthophoto of the Ocoee River study area (<i>USGS</i> , 1997).....	74
Figure 4.2. a) Photograph illustrating the coarse sediment deposition in between ribs in Reach 3. b) Tracer clast (circled) downstream of a bedrock rib in a local hydraulic environment classified as shielded.	76
Figure 4.3. Annual hydrograph for Ocoee No. 3 for three years of study. Note the systematic fluctuations in summer recreational release flows..	79
Figure 4.4. Size distribution of tracer clasts sampled from the existing bed material in each reach.....	85
Figure 4.5. Transport distance (normalized by the transport distance of the D_{50} <small>mobile</small> tracer for that flow period) versus the tracer size (standardized by the D_{50} <small>mobile</small>).....	88
Figure 4.6. Size distribution of mobile tracers from each reach	89
Figure 4.7. Cumulative distributions of transport distances after six re-surveys for all three reaches (a, b and c, respectively).....	91
Figure 4.8. Reach-scale variation in transport distances.	92
Figure 4.9. Box plot comparing the transport distance of tracers by cross section hydraulics in Reach 1	95
Figure 4.10. Box plot comparing tracer transport distance by zone topographic metrics in Reach 1.	97
Figure 4.11. Box plot comparing tracer transport distance by local hydraulic environment classification in Reach 1	99
Figure 5.1. Study area. Location of study section on the Ocoee River is indicated by the star, and the reach locations are shown on the Digital Orthophoto of the Ocoee River study area	121

Figure 5.2. Photograph of pothole in Reach 4 on the downstream side of a massive rib.....	124
Figure 5.3. Schematic showing how pothole elevations relative to some arbitrary flow depth were calculated.....	127
Figure 5.4. Pothole dimension relationships: Depth versus radius power functions for all four reaches.....	130
Figure 5.5. Boxplots comparing pothole dimensions between reaches (n = 105, 295, 176, and 146, respectively).....	132
Figure 5.6. K-functions plotted in reference to simulated Poisson process based on 100 replications.	133
Figure 5.7 a) Cumulative distribution function of pothole elevations relative ($Z_{relative}$) to an arbitrary water surface elevation that parallels the mean bed slope (Figure 5.2). b) Probability density function pothole $Z_{relative}$ for all four reaches.....	137
Figure 5.8. Probability plot of reach areas	138
Figure 5.9. Relationship between grinder size and pothole radius.....	140
Figure 5.10. Relative experimental grinder abrasion.....	141
Figure 5.11. Coalesced potholes between longitudinal ribs. Flow is top to bottom.	146
Figure 6.1. Flow diagram of the interactions among channel morphology, sediment transport, pothole incision, and hydraulics, which are all influenced directly or indirectly by rock properties.....	155

CHAPTER 1. INTRODUCTION

Bedrock channels are important components of the landscape, as they control the rates of landscape evolution by setting the base level for hillslopes and translating the overall response to external forces of climate and tectonics (Molnar and England, 1990; Howard et al., 1994; Whipple et al., 2000a). Bedrock channels are characterized as having little alluvial cover and conditions of high sediment transport capacity relative to supply, leaving the characteristics of the bedrock geology to play an important role in shaping the channel. Typically, bedrock channels occur in regions of relatively high tectonic uplift and are common to higher elevation, lower order watersheds; they comprise a significant portion of the landscape (Montgomery et al., 1996). A recent explosion in bedrock channel studies has been driven by this importance. Still, little is known regarding the processes of incision and controls on bedrock channel form, especially from field studies; the majority of the research has focused on constraining parameters specific to bedrock channels in order to model overall landscape evolution. These models initially focused on simple scaling of drainage area and slope (i.e., stream power or shear stress) to predict incision rates (Howard and Kirby, 1983; Howard et al., 1994; Whipple and Tucker, 1999). Recognition of the importance of alluvial material in bedrock systems led to further development of incision models that included bedload and suspended load effects (Sklar and Dietrich, 1998, 2004, Lamb et al., 2008, Turowski et al., 2007; Turowski, 2009). Still, there is a need to further constrain the processes and interactions between the underlying geology, hydraulics, sediment transport, and erosion

that control channel form and incision at different scales. Advances in these studies will therefore enhance our understanding and prediction of landscape evolution.

1.1 Study objectives

Overall, it is important to distinguish processes that operate differently in alluvial and bedrock channels, and to explore the controls on those differences. I followed a multi-scaled approach to attack this problem and isolate different processes at different spatial scales. The three main scales of focus are the channel segment, inter-reach and intra-reach scales. For the channel segment scale, variability is examined along the channel profile at distances ranging from 100 m to 5 km. This scale includes examinations of four streams within the main study region, the Blue Ridge Province of the southern Appalachians. This scale highlights how regional differences in substrate erosional resistance reflect geologic structure and influence the type and relative effectiveness of channel erosion.

At the inter-reach scale, comparisons between hydraulics, sediment transport and erosional forms are made based on differences in reach morphology and rock resistance that have direct links to the underlying independent substrate control. Reaches 75m to 200 m in length were designated based on internal consistency of bedrock substrate and channel geometry. The main substrate differences between the four reaches of focus on the Ocoee River are the orientation of structurally influenced bedrock ribs (explained in detail in Chapter 3) and dominant lithology (e.g., massive metagreywacke or densely foliated phyllite). Differences in the dynamics of coarse sediment transport dynamics, as well as the size and spatial patterns of potholes, can be compared among the reaches and

linked to variability in substrate characteristics. This scale highlights how local differences in substrate influence channel erosion.

At the intra-reach scale of 10^{-1} to 10^1 m, comparisons between sediment transport dynamics and erosional forms are based on differences in local channel topography that ultimately reflects the underlying bedrock geology. This scale highlights how the feedbacks among substrate resistance, hydraulics, and small-scale bed topography influence channel erosion.

Combined comparisons of substrate resistance, hydraulics, sediment dynamics, and bedrock erosion at different scales provide useful insights into the controls on bedrock channel processes. These insights can ultimately lead to better process parameterizations and numerical simulations of bedrock incision.

1.1.1 Research overview

In order to investigate the independent influence of bedrock substrate on the interactions between channel morphology, hydraulics, sediment transport and erosional processes, the dissertation is broken into three chapters which attempt to isolate each component. Chapter 3 examines the controls on rock properties and structurally influenced bed topography on reach-scale hydraulics and longitudinal variability in channel morphology. In Chapter 4, the focus turns to the interactions between channel morphology, hydraulics and coarse sediment transport at the inter- and intra-reach scales. Chapter 5 examines the influence of rock properties and channel morphology on the efficacy of erosion focused in potholes. Finally, Chapter 6 links all components in a conceptual model for bedrock channel adjustment given highly influential substrate

parameters. Because each of the three chapters has been submitted for publication, the journal article structure was maintained within each chapter. The study focuses on the Ocoee River, Tennessee and the description of the study area is maintained in each chapter so that the flow of each paper is not disrupted.

CHAPTER 2. BACKGROUND

This dissertation, which examines the influences of substrate on hydraulics, sediment transport and erosional forms in bedrock channels based on field studies, adds to the existing research on bedrock channel forms and processes. This research includes: basin- and reach-scale analyses that characterize bedrock channel morphology; studies of different erosional processes and the efficacy of these processes; numerical models of bedrock incision; process studies of the relationship between coarse alluvial material and bedrock incision patterns (tools vs. cover effects); and experimental studies of incision processes and interactions between hydraulics, sediment transport and channel form. This chapter provides background information and reviews key literature related to these topics in order to set the stage for the three main study chapters. The results from this field-based dissertation will enhance our understanding of bedrock channel processes and form.

2.1 Bedrock channels

The recent surge in the study of bedrock rivers has largely been driven by recognition that these systems occupy a significant portion of the landscape (Montgomery et al., 1996; Wohl, 1998; Whipple, 2004) and that they are integral components of landscape change because they set the base level for hillslope response to tectonic and climatic forcing (Whipple, 2004; Whipple and Tucker, 1999, 2002). Overall,

the evolution of landscapes is governed by rates and processes of fluvial incision into bedrock.

Bedrock-dominated channels largely occur in headwater regions in the high elevation zones of tectonically active mountain belts (e.g., Howard et al., 1994; Montgomery et al., 1996; Sklar and Dietrich, 1998; Turowski et al., 2008b). Although Montgomery et al. (1996) suggest that bedrock reaches occur at higher channel slopes for a given drainage area over alluvial reaches with the same drainage area, an inherent problem arises of what defines a bedrock reach. Whipple (2004) followed a definition that is consistent with some of the earlier definitions (Gilbert, 1877; Howard et al., 1994; Montgomery, et al., 1996): “Bedrock-channels lack a continuous cover of alluvial sediments, even at low flow, and exist only where transport capacity exceeds sediment flux over a long term.” Tinkler and Wohl (1998) provide a similar definition based on sediment supply and capacity: “Bedrock channels are those reaches along which a substantial portion of the boundary (>50%) is exposed bedrock, or is covered by an alluvial veneer which is largely mobilized at high flows such that the underlying bedrock geometry strongly influences patterns of flow hydraulics and sediment movement.” Turowski et al. (2008b) go further and provide a quantitative description according to hydraulic geometry-based sediment transport relationships. They indicate that this type of definition is dynamic and not a function of channel conditions at a static state in space or time. Regardless of the intricacies of these definitions, the central idea is that the inherent bedrock properties provide an independent control on bedrock channel form and processes, which are centrally linked to sediment supply and capacity. As with any other classification, a gradual transition should exist between bedrock and alluvial channels as

dominant controls on channel dynamics shift from one to another (Turowski et al., 2008b).

Studies in alluvial systems dominate fluvial geomorphology, but recent studies examine fluvial processes in mountainous terrains. A central tenet to the expansion of research in mountain rivers, and more specifically bedrock rivers, is that the long-developed theories developed for alluvial systems are not applicable in these other systems; central concepts such as dominant discharge (Langbein, 1964) and hydraulic geometry (Leopold and Maddock, 1953) developed for alluvial streams may not model bedrock systems in the same way. The logical assumption behind these differences is that consolidated and unconsolidated boundaries are deformed by different mechanisms and over largely different time scales.

Bedrock channel morphology reflects hydraulic driving forces acting across different time scales compared to alluvial systems (Baker and Ritter 1975; Baker, 1977; O'Connor et al., 1986). The width and location of active incision of natural bedrock channels should change with the magnitude and frequency relationship between flow and sediment discharge (Hartshorn et al., 2002). Independent substrate properties such as local lithologic and structural heterogeneity (Wohl and Achyuthan, 2002; Kobor and Roering, 2004; Frankel et al., 2007), jointing (Miller, 1991; Ehlen and Wohl, 2002), bedding, and base level history (Wohl et al., 1994 Lave and Avouac, 2002; Duvall et al., 2004) are important influences on the processes and form of bedrock channels. The starting assumption for self-adjusted alluvial channels is that discharge exerts the dominant influence on channel form (Leopold and Maddock, 1953). Despite the high erosional thresholds and substrate heterogeneity in bedrock channels, some evidence

exists that bedrock channel dimensions also scale with flow (Montgomery and Gran, 2001; Wohl and David, 2008). However, local bedrock properties also influence channel morphology (Montgomery and Gran, 2001). Therefore, feedbacks between hydraulic parameters and bedrock characteristics likely govern the balance between spatial variability of channel form and scaling of channel dimensions by flow.

2.2. Bedrock channel morphology

Studies of bedrock channel forms have focused on different scales. At the basin scale, studies have focused on the longitudinal profile of bedrock channels and the response to climatic and tectonic forces (e.g., Seidl et al., 1994; Snyder et al., 2000; Kobor and Roering, 2004). At the reach scale, several investigators have described step-pool and pool-riffle sequences (e.g., Keller and Melhorn, 1978; Duckson and Duckson, 1995; Wohl and Merritt, 2001). Other features such as inner channels (e.g., Baker, 1973; Wohl, 1993; Wohl and Achyuthan, 2002), knickpoints (e.g., Crosby et al., 2006; Frankel et al., 2007) and slot canyons with undulating walls (e.g., Wohl et al., 1999; Carter and Anderson, 1996) have also been described. Smaller-scale sculpted forms such as potholes, although receiving less attention, are also important features in bedrock rivers (e.g., Alexander, 1932; Wohl, 1993; Hancock et al., 1998; Whipple et al., 2000a; Richardson and Carling, 2005; Springer et al., 2005). At all scales these features can be influenced to differing degrees by the underlying rock characteristics.

At the basin scale, bedrock channels typically display abrupt downstream variation along and between reaches as a result of local or inter-reach variation in

lithology or structure (Ehlen and Wohl, 2002; Wohl et al., 1994; Duvall et al., 2004). Previous investigators have assumed that the boundaries of bedrock channels are sufficiently resistant and heterogeneous that channel form is dominated by substrate characteristics. Despite local variability, many others have documented that bedrock channel width varies systematically as a power function of drainage area (Hack 1957; Snyder et al., 2003; Tomkin et al., 2003; Wohl and David, 2008), where drainage area is used as a surrogate for discharge. Other recent studies have described downstream changes in bedrock channel width because the downstream hydraulic geometry (DHG) width relation is used in the derivation of the stream power incision law (described below). Therefore, understanding the downstream width variability in bedrock streams is important for modeling bedrock incision and landscape evolution. In weak sedimentary lithologies, Montgomery and Gran (2001) did not find differences in the width-drainage area functions among alluvial and bedrock reaches. Whipple (2004) argues that the same physics control channel width in alluvial and bedrock channels because of similarities in channel width for corresponding drainage areas.

In one of their study streams, Montgomery and Gran (2001) documented that lithologic differences led to significant changes in the channel width; they noted that downstream increases in width could be reset by a resistant lithology. Montgomery and Gran (2001) noted that width decreased when the channel transitioned to a more resistant lithology. In this case the transition was from limestone to granite.

In addition to relative rock resistance, others have noted that variations in uplift rate along the longitudinal profile are associated with channel width variability. In cases where uplift rate increases downstream, channel width narrows (Lave and Avouac, 2002).

Where uplift rates are high, bedrock channels tend toward steeper gradients because incision rates lag behind uplift (Whipple, 2004). Steeper channel reaches are associated with narrower channels (Wohl et al., 2004). Variations in channel width and slope can account for inferred differences in long term incision rates between rivers that are undergoing different uplift (Duvall et al., 2004). These studies all document that bedrock channels adjust dimensions such as width and gradient in response to independent controls, such as bedrock structure and lithology and uplift rates. In terms of the application of these results to the stream power incision law, Finnegan et al. (2005) concluded that bedrock channel width varies with both discharge and slope. Therefore, scaling width by only discharge in the stream power incision model underestimates stream power in areas where the river is steeper.

Many have argued that discharges of much greater magnitude and lower frequency are responsible for the form of bedrock channels (Baker, 1973, O'Connor et al., 1986). Indirect estimation of discharge in bedrock streams using various types of field indicators, including vegetation limits and breaks in slope, suggests that channel geometry is predominantly shaped by higher discharges of lesser frequency than predicted based on concepts of frequently recurring bankfull as the dominant discharge (Wolman and Miller, 1960; Wohl and Wilcox, 2005). In most bedrock-influenced channels, more resistant substrate leads to longer relaxation times and the morphology of a past flood may be preserved in the channel for longer time periods. Therefore, the field-determined bankfull stage, where discernible, is associated with a large magnitude, but less frequent return period, and the same 1-2 year frequency floods that are important for shaping alluvial streams are not as important in bedrock reaches. At flows above bankfull

in alluvial streams, the presence of a broad flood plain, usually with vegetation, lowers mean shear stress and velocity by increasing roughness as the water spreads over the wide, shallow section (Baker, 1977). Confinement in bedrock streams maintains high velocities and shear stresses, such that a lower-than-expected flood magnitude may be responsible for erosion of bedrock channel boundaries.

Through flume experiments aimed to investigate the collective adjustment of bedrock channel slope, width, roughness, alluvial cover and incision rate at the reach scale, Finnegan et al. (2007) observed that channels adjust their width through alterations in the location of vertical incision. The location within the channel and the width of the localized incision zone were directly related to the balance between bedload supply and transport capacity. Similarly, the experimental results of Dietrich et al. (1989) from alluvial channels demonstrated that reduction in sediment supply led to narrowing in the zone of active sediment transport and coarsening of the immobile sediment along the margins of this transport zone.

2.3. Incision processes

Fluvial incision into bedrock occurs through several processes: chemical weathering, cavitation, plucking of bedrock blocks, and abrasion by suspended and bed load sediment (e.g., Wohl, 1993; Hancock et al., 1998; Sklar and Dietrich, 1998; Wohl, 1998; Whipple, 2004). Chemical weathering, or corrosion, is most prevalent in carbonate lithologies, such as limestone; it occurs through chemical interaction between the water and rock surface. This process is important for either chemically dissolving such rocks, or

for weakening non-carbonate rock surfaces in preparation for other erosive processes, such as plucking or abrasion (Carling and Grodek, 1994).

Cavitation refers to a process whereby bedrock material is removed by high instantaneous pressure forces that result from the collapse of vapor-filled bubbles that form in turbulent flows (Barnes, 1956). Although this process has not been well documented in natural channels, Barnes (1956) developed an equation for its potential occurrence in natural streams based on the Bernoulli equation.

Plucking and abrasion are the two most studied bedrock erosional processes (e.g., Carling and Tinkler, 1998; Hancock et al., 1998; Tinkler, 1993; Sklar and Dietrich, 2001; Hartshorn et al., 2002). Plucking is an efficient mechanism for removing bedrock blocks where joints are closely spaced. Blocks are typically removed via lift generated from pressure differences in the flow around the blocks or sliding of the upper block in response to shear stress differences (Hancock et al., 1998).

Abrasion occurs as saltating bedload or sediment in suspension translates the kinetic energy of the mobile particle into removal of bedrock material; abrasion can be a dominant erosional mechanism in bedrock-dominated channels, especially in massive bedrock and where there is an intermediate supply of coarse bedload material. Given the importance of alluvial material in bedrock channel systems, the mechanics of bedload transport processes exert a strong influence on the rate and style of bedrock channel incision. Hancock et al. (1998) described a process of abrasion via suspended material that is flung against the bed in the turbulent wake zone behind sculpted features as a scenario called “attack from the back.”

Incision into bedrock is accomplished through a linked and interconnected set of physical processes that vary in their efficiency both in space and time (Hancock et al., 1998). These processes do not tend to be mutually exclusive and one process may prepare the rock surface for erosion via another process. Several studies have suggested that the dominance of one process over another is controlled by the hydraulics and rock characteristics (Hancock et al., 1998; Wohl; 1998; Whipple et al., 2000a). For example, Whipple et al. (2000a) suggested that plucking will dominate and abrasion will be insignificant where joints are spaced less than 1 m apart.

2.3. Bedrock incision models

The initial interest in bedrock channel erosion was driven by questions related to landscape evolution modeling. At the watershed scale, bedrock incision rate was modeled as a power law function of the boundary shear stress (Howard and Kerby, 1983; Howard et al., 1994; Howard, 1994). Many of the original models assumed steady-state fluvial incision where the incision rate keeps pace with the uplift rate. More recent models account for bedload transport capacity and supply (Sklar and Dietrich, 1998, 2004; Lamb et al., 2008, Turowski et al., 2008b, 2009). These recent models differ in the method used to describe sediment transport processes. These models also make different predictions about the response rate to climatic and tectonic forcing (Whipple and Tucker, 2002).

The earliest formulation of a bedrock incision model was developed based on simple scaling. Howard and Kerby (1983) described detachment limited rate of bedrock erosion, E , or dz/dt , modeled as a power law function of drainage area, A , and slope, S , with drainage area used as a proxy for discharge.

$$E = \frac{dz}{dt} = K\dot{A}^m S^n, \quad (2.1)$$

where the exponents m and n depend on whether stream power or shear stress drives incision (Whipple and Tucker, 2002), and K is a term used to describe resistance to incision and is a function of lithology. Variations in the appropriate values for K are poorly documented (Stock and Montgomery, 1999).

In their examination of rapidly eroding badlands topography, Howard and Kerby (1983) found that the local erosion rates were well explained by this model. They found a linear relation between incision rate and the bed shear stress, with the exponents m and n equaling $1/3$ and $2/3$, respectively. Using drainage area as a surrogate for discharge assumes that the time-averaged quantities of hydraulic parameters adequately integrate the effects of the whole history of flooding in that system.

Models developed for mountain landscape evolution largely focus on incision into bedrock because channels with a significant bedrock boundary (Turowski, et al., 2008a) dominate in these landscapes and set the base level for hillslope erosion processes (e.g., Howard, 1994; Tucker and Slingerland, 1994; Whipple and Tucker, 2002; Sklar and Dietrich, 2004; Lamb et al., 2008). The longitudinal profiles of these channels are strong indicators of the long time-scale fluvial response to climatic and tectonic drivers.

Whipple and Tucker (1999) argued that the best way to determine the underlying physics of fluvial processes is to study systems that are undergoing a transient response.

Many studies have focused on the vertical incision component through detachment-limited incision models (e.g., Howard, 1994). Expansion of these longitudinal incision models has focused on the role of alluvial cover and processes of abrasion via saltating bedload (Sklar and Dietrich, 1998, 2004; Gasparini et al., 2006;

Turowski et al., 2009), as well as the role of suspended sediment (Lamb, et al., 2008). Other studies have examined the lateral component to bedrock channel incision (Wobus et al., 2006; Finnegan et al., 2007; Turowski et al., 2008b) and the implications for rivers meandering through bedrock gorges (Stark, 2006). The data needed to evaluate different aspects of competing models are rare (van der Beek and Bishop, 2003; Tomkin et al., 2003). Many studies have taken an experimental or theoretical approach (Finnegan et al., 2007; Turowski, 2009), yet others have examined the bedrock properties measured in the field that are important controls on the rates and styles of incision.

Bedrock incision is typically modeled as a function of shear stress or unit stream power (e.g., Howard and Kerby, 1983; Howard, 1994; Whipple and Tucker, 1999). With some assumptions about the relationships between channel width and discharge as well as drainage area and discharge, both the shear stress and stream power models can be expressed as a function of only two variables: drainage area and slope (e.g., Tucker and Slingerland, 1997; Whipple and Tucker, 1999). Although the effects of sediment flux are also a function of drainage area and slope, the influence of sediment flux on incision rate is not specifically included in either the shear stress or stream power formulations. Sediment flux therefore has an influence on fluvial incision, which may affect the scaling relationship between incision rate and both drainage area and slope (Sklar and Dietrich, 1998; 2004; Tomkin et al., 2003; van der Beek and Bishop, 2003).

Modified versions of the stream power model incorporate the magnitude of the tools versus cover effects via a function of the volumetric sediment supply. If both tools and cover effects operate, this function is expected to follow a parabolic function of the ratio of the sediment supply to transport capacity. This ratio depends on hillslope

processes and rates, as well as the variability of hydrologic regime. Understanding the details of bedrock incision processes provides important information on the evolution of rivers and hillslopes in mountainous terrains. Stream power incision into bedrock groups a range of processes of incision into a simplified form. Given the wide range of processes by which bedrock erosion occurs, the suite of processes are not likely to vary identically with stream power (Sklar and Dietrich, 1998). This clearly reveals the simplifications made by stream power incision models, despite their usefulness and computational succinctness (Howard and Kerby, 1983; Seidl et al., 1994).

3.3.1. Saltation-abrasion model of bedrock incision

Different studies have examined different factors that limit the ability of bedrock channels to incise vertically. In one end-member case, vertical incision is limited by the ability of erosional processes to physically remove pieces of the bedrock; this is referred to as detachment-limited conditions. The other end of the spectrum which limits bedrock channels from vertically incising is the ability to transport the sediment supply, thereby setting up transport-limited conditions. It is unclear, however, which of these end members dominate. Alternatively, Sklar and Dietrich (1998; 2004) describe a model of bedrock incision that incorporates the role of bedload transport in bedrock channels. This model essentially combines concepts of alluvial streams and bedrock streams and describes these processes as an intermediate domain between transport-limited and detachment-limited end-member systems. The model predicts the instantaneous bedrock incision rate, E_i , as a function of flow discharge, channel width, hydraulic roughness, coarse sediment supply rate, and the representative grain size. In its simplest terms, the model describes the incision rate as the product of three terms: the average volume of

rock that is removed by bedload impacts (V_i), the rate of impacts per unit bed area per unit time (I_r), and the proportion of the bedrock surface exposed and not protected by alluvial cover (F_e),

$$E_i = V_i I_r F_e \quad (2.2)$$

2.3. Sediment transport

Particular interest has focused on the important role of bedload material in controlling incision via abrasion in bedrock systems (Sklar and Dietrich, 1998; 2001; Hartshorn et al., 2002). Recent research has focused on understanding reach-scale processes involved in bedrock channel incision (e.g., Johnson and Whipple, 2007; Finnegan et al., 2007; Chatanantavet and Parker, 2008) in order to better constrain parameters and assumptions required for landscape evolution models (e.g., Howard, 1994; Whipple and Tucker, 2002; Sklar and Dietrich, 2004; Turowski et al., 2007; Lamb et al., 2008).

The mechanics of bedload transport processes exert a strong influence on the rate and style of bedrock channel incision. Under conditions of low bedload supply relative to transport capacity, this material acts positively to abrade the bedrock channel surfaces, creating a tools effect. Conversely, when bedload supply increases, particle collisions and interactions favor deposition into alluvial patches, eventually covering the bedrock. In this case the bedload material inhibits bedrock incision and the cover effect dominates. At intermediate sediment supply rates, there are enough tools for abrasion, but not enough for alluvial cover to form. This dual role of sediment to enhance or inhibit bedrock incision was initially proposed by Gilbert (1877), and more recently quantified by Sklar

and Dietrich (1998). Although this threshold model is fairly simple conceptually, there are many nuances and details that arise when it is further examined experimentally (Johnson and Whipple, 2007; Finnegan et al., 2007; Chatanantavet and Parker, 2008) and in the field, as I present in this dissertation.

These effects have been incorporated into recent bedrock incision models. The model developed by Sklar and Dietrich (2004) is based on a linear decline in the fraction of the bed that is exposed as sediment supply increases and eventually falls to zero bedrock exposed when the supply equals the transport. The Whipple and Tucker (2002) model is also based on a linear decline. Turowski et al. (2007) proposed a similar model, but with an exponential decline in the fraction of alluviation. Their model introduced a dynamic cover term instead of the static cover term used by Sklar and Dietrich (2004). The dynamic cover term accounts for grain-grain interactions becoming more frequent as the concentration of mobile sediment increases, thereby reducing the grain impacts on the bed. The cover factor is used to account for regions of the bed that are intrinsically more or less favorable to deposition. Turowski et al. (2007) conclude that their model provides a better fit to the erosion data of Sklar and Dietrich (2001). Given the importance of the tools versus cover relationships, most of these models have focused on bedload transport. Suspended sediment may also be an important abrasional tool (Whipple et al., 2000b; Hartshorn et al., 2000), and Lamb et al. (2008) have developed a model that incorporates both suspended and bedload sediment transport. With the inclusion of a sediment flux variable in recent bedrock incision models, it becomes paramount to investigate these sediment transport dynamics in the field, especially if sediment transport processes differ from alluvial systems.

Several investigators have studied the interactions between bedrock channel morphology, sediment transport and the degree of alluvial cover (Finnegan et al., 2007; Johnson and Whipple, 2007; Chatanantavet and Parker, 2008). According to the formulations of Chatanantavet and Parker (2008), sediment supply from hillslopes in steep, actively uplifting mountain ranges maintains antecedent sediment patches between floods, thus preventing bedrock exposure in the channel bed. In the other end-member bedrock channel setting, where uplift rates are low, the corresponding low denudation rates and sediment delivery lead to maintained exposure of the bedrock (e.g., Wohl, 1993).

2.4. Substrate controls

Substrate plays a major role in controlling the shape of bedrock rivers, but this parameter must be considered in reference to the flow regime and hydraulic forces driving erosion. If the forces of discharge (hydraulic driving forces) far outweigh the controls of substrate resistance, then it is likely that relationships such as downstream hydraulic geometry (DHG) will be similar among bedrock and alluvial streams. Wohl and Merritt (2001) discriminated bedrock-channel geometry according to gradient, substrate heterogeneity, and Selby rock mass strength. Their results suggested that, similar to alluvial streams, bedrock channel morphology reflects a balance between hydraulic driving and substrate resisting forces. Wohl (2004) used the ratio of total stream power (hydraulic driving force) to D_{84} (substrate resistance) as a discriminator of mountain streams with well developed and poorly developed DHG. In mountain streams where this ratio was greater than $10,000 \text{ Kg/s}^3$, DHG was well developed. The inherent

connection between bedrock river form and the rock into which they incise can lead to strong substrate influences, such that substrate resistance exceeds the hydraulic driving forces in controlling channel morphology.

Wohl et al. (1999) did not find differences in substrate characteristics, which included intact rock strength, orientation and spacing, bedding and porosity, among bedrock reaches with undulating walls and straight reaches. From this they concluded that the hydraulic mechanisms dominated over substrate controls, and the canyon wall undulations were formed primarily by hydraulic forces. Also, in these channels the grain size is small and large boulders or bedforms are either lacking or are not enough to control energy dissipation. Instead, the hydraulics interact with the substrate to form undulations in the channel wall that are analogous to undulations in the channel bed. Along the Cache la Poudre River, Colorado, lithologic and structural variation corresponds to variation in channel and valley width. Reaches with higher joint density, which are controlled by the relative location of the channel to a shear zone, tend to be wider than reaches with low joint density where the channel veers away from the shear zone (Ehlen and Wohl, 2002).

A comparison of substrate resistance to hydraulic driving forces must be based on a certain flow magnitude. If the form of bedrock channels is adjusted to the larger, less frequent flows, then it is important to realize that the hydraulic driving force of these large flows may overcome the resistant boundary. However, the heterogeneities in resistance may also initiate energy dissipation mechanisms such as the formation of bedforms. Given the independent substrate controls on some bedrock channels, if

substrate variability exerts the strongest control on channel morphology, then it might not be possible for these channels to develop toward a uniformity in energy expenditure.

2.5 Bedforms and sculpted forms

Localized erosion in bedrock channels can result in reach- and subreach-scale bed and bank forms such as knick points or knickzones along the profile (Gardner, 1983; Frankel et al., 2007), inner channels within the cross section (Baker, 1973; Shepherd and Schumm, 1974; Wohl and Ikeda, 1997; Johnson and Whipple, 2007), or sculpted abrasional forms such as potholes, flutes and grooves (Richardson and Carling, 2005). Another expression of focused erosion, which I explore for the first time in this dissertation, is the formation of undulating, structurally-controlled bedrock ribs that are intermediate in scale between sculpted forms and either knickpoints or inner channels. The bedforms in alluvial rivers and bedforms, wall undulations, knickzones, or sculpted forms in bedrock channels behave similarly, with the main effect being energy dissipation. Wohl et al. (1999) showed that periodicity in the flow structure created by bed or bank forms perpetuates bedforms in the downstream direction, which leads to a feedback between forms and hydraulics. This may lead to flow conditions that oscillate around critical flow (Grant, 1997). In this dissertation, I focus on bedrock rib bedforms, which likely act as hydraulic energy diffusers much like bedforms in alluvial channels, effectively reducing velocity and minimizing energy expenditure between topographic undulations (Yang, 1971; Carling, 1989; Wohl et al., 1993; 1999).

Because of the close coupling between bedrock characteristics and fluvial processes, bedforms in bedrock channels can be influenced to varying degrees by either hydraulic or rock properties. In their thorough evaluation of sculpted bedrock channel

forms, Richardson and Carling (2005) describe this in the context of two end members, “structurally controlled” channel morphologies and “hydrodynamically controlled” types of morphologies. These end members also coincide with the dominant incision process expected: where there is structural control (i.e., joints, bedding planes or foliations), plucking should dominate, whereas in the hydrodynamic controlled morphologies, abrasion should dominate. In this dissertation, I examine a bedform that is an intermediate to these end members, having structural influence, but experiencing alterations via abrasion.

The previous discussion highlights the tight interactions among bedrock substrate properties, channel form, hydraulics, sediment transport and erosional processes. It is even difficult to isolate one component in discussion without reference to the others. Because it has been widely recognized that bed load transport plays a key role in shaping bedrock channels, it is increasingly important to examine the interactions among the bedrock and coarse sediment transport in these systems (Johnson and Whipple, 2007; Finnegan et al., 2007; Chatanantavet and Parker, 2008; Turowski et al., 2007).

References

- Alexander H.S. (1932) Pothole erosion. *J. of Geology* 40, 305–337.
- Baker, V.R. (1973), Erosional forms and processes for the catastrophic Pleistocene Missoula floods in eastern Washington, in *Fluvial Geomorphology*, edited by M. Morisawa, pp.123-148, Publications in Geomorphology, State University of New York, Binghamton.
- Baker, V.R. (1977), Stream-channel response to floods, with examples from central Texas. *Bulletin of the Geological Society of America*, 88, 1057-1071.
- Baker, V.R. and D. F. Ritter (1975), Competence of rivers to transport coarse bedload material, *Geological Society of America Bulletin* 86, 975-978.
- Barnes, H.L. (1956), Cavitation as a geological agent, *American Journal of Science*, 254, 493-505.
- Carling., P.A. and T. Grodek (1994), Indirect estimation of ungauged peak discharges in a bedrock channel with reference to design discharge selection, *Hydrological Processes* 8, 497-511.
- Carling, P.A. and K. Tinkler (1998), Conditions for the entrainment of cuboid boulders in bedrock streams: An historical review of literature with respect to recent investigations, in *Rivers Over Rock: Fluvial Processes in Bedrock Channels*, edited by K. J. Tinkler and E. E. Wohl, Geophys. Monogr. Ser., vol. 107, pp. 35–60, AGU, Washington, D. C.
- Carter, C.L., and R.S. Anderson (2006), Fluvial erosion of physically modeled abrasion-dominated slot canyons, *Geomorphology* 81, 89-113.
- Chatanantavet, P., G. Parker (2008), Experimental study of bedrock channel alleviation under varied sediment supply and hydraulic conditions, *Water Resour. Res.*, 44, W12446, doi:10.1029/2007WR006581.
- Crosby, B.T. and K.X. Whipple (2006), Knickpoint initiation and distribution within fluvial: 236 waterfalls in the Waipaoa, North Island, New Zealand, *Geomorphology* 82, 16-38.
- Davies, T.R. and A.J. Southerland (1980), Resistance to flow past deformable boundaries. *Earth Surface Processes* 5, 175-179.
- Dietrich, W. E., J. W. Kirchner, H. Ikeda, and F. Iseya (1989), Sediment supply and the development of the coarse surface layer in gravel-bedded rivers, *Nature* 340, 215–217.

- Duckson, D.W. and L.J. Duckson (2001), Channel bed steps and pool shapes along Soda Creek, Three Sisters Wilderness, Oregon, *Geomorphology*, 38, 267-279.
- Duvall, A., E. Kirby, and D. Burbank (2004), Tectonic and lithologic controls on bedrock channel profiles and processes in coastal California, *J. Geophys. Res.*, 109, F03002, doi:10.1029/2003JF000086.
- Ehlen, J. and E.E. Wohl (2002), Joints and landform evolution in bedrock canyons. *Transactions of the Japanese Geomorphological Union* 23(2), 237-255.
- Finnegan N.J., G. Roe, D.R. Montgomery, and B. Hallet (2005), Controls on channel width of rivers: Implications for modeling fluvial incision into bedrock. *Geology* 33(3), 229-232.
- Finnegan, N. J., L. S. Sklar, and T. K. Fuller (2007), Interplay of sediment supply, river incision, and channel morphology revealed by the transient evolution of an experimental bedrock channel, *J. Geophys. Res.*, 112, F03S11, doi:10.1029/2006JF000569.
- Frankel, K.L., F.J. Pazzaglia, J.D. Vaughn (2007), Knickpoint evolution in a vertically bedded substrate, upstream-dipping terraces, and Atlantic slope bedrock channels. *Geological Society of America Bulletin* 119 (1-3), 476-486.
- Gardner, T.W. (1983), Experimental study of knickpoint and longitudinal profile evolution in cohesive, homogeneous material. *Geological Society of America Bulletin*, 94, 664-672.
- Gasparini, N. M., R. L. Bras, and K. X. Whipple (2006), Numerical modeling of non-steady-state river profile evolution using a sediment flux-dependent incision model, in *Tectonics, Climate and Landscape Evolution*, Geol. Soc. Am. Spec. Pap., vol. 398, edited by S. D. Willett et al., pp. 27- 141, Geol. Soc. Am., Boulder, Colo.
- Gilbert, G. K. (1877), Land sculpture, in *The Geology of the Henry Mountains, Utah*, edited by C. B. Hunt, chap. 5, *Mem. Geol. Soc. Am.*, 167, 99- 150.
- Grant, G.E. (1997), Critical flow constrains flow hydraulics in mobile-bed streams: A new hypothesis, *Water Resources Research* 33, 349-358.
- Hack, J.T. (1957), Studies of longitudinal stream profiles in Virginia Maryland, *U.S. Geological Survey Professional Paper* 294-B:97.
- Hancock, G., R. S. Anderson, and K. X. Whipple (1998), Beyond power: Bedrock river incision process and form, in *Rivers Over Rock: Fluvial Processes in Bedrock Channels*, edited by K. J. Tinkler and E. E. Wohl, Geophys. Monogr. Ser., vol. 107, pp. 35- 60, AGU, Washington, D. C.

- Hartshorn, K., N. Hovius, W.B. Dade, R.L. Slingerland (2002), Climate-driven bedrock incision in an active mountain belt. *Science* 297, 2036-2038.
- Howard, A. D. (1994), A detachment-limited model of drainage basin evolution, *Water Resources Research*, 30, 2261–2285.
- Howard, A. D., and G. Kerby (1983), Channel changes in badlands, *Geological Society of America Bulletin*, 94, 739– 752.
- Howard, A.D., M.A. Seidl, and W.E. Dietrich (1994), Modeling fluvial erosion on regional to continental scales, *Journal of Geophysical Research* 99, 13, 13,917-13,986.
- Johnson, J. P., and K. X. Whipple (2007), Feedbacks between erosion and sediment transport in experimental bedrock channels, *Earth Surf. Processes Landforms*, 32, 1048–1062.
- Keller, E.A. and Melhorn, W.N., 1978. Rhythmic spacing and origin of pools and riffles, *Geological Society of America Bulletin* 89, 723-730.
- Kobor, J.S., J.R. Roering (2004), Systematic variation of bedrock channel gradients in the central Oregon Coast Range: implications for rock uplift and shallow landsliding, *Geomorphology* 62, 239-256.
- Lague, D., N. Hovius, and P. Davy (2005), Discharge, discharge variability, and the bedrock channel profile, *Journal of Geophysical Research, Earth Surface*, 110, F04006, doi:10.1029/2004JF000259.
- Lamb, M. P., W. E. Dietrich, and L. S. Sklar (2008), A model for fluvial bedrock incision by impacting suspended and bedload sediment, *Journal of Geophysical Research, Earth Surface*, 113, F03025, doi:10.1029/2007JF000915.
- Lave, J., and J. P. Avouac (2001), Fluvial incision and tectonic uplift across the Himalayas of central Nepal, *Journal of Geophysical Research*, 106, 26,561–26,592.
- Leopold, L. B., and T. Maddock Jr. (1953), The hydraulic geometry of stream channels and some physiographic implications, *U.S. Geol. Surv. Prof.*, 252.
- Miller, J.R., (1991), The influence of bedrock geology on knickpoint development and channel bed configuration along downcutting streams in south-central India, *Journal of Geology* 99, 591-605.
- Molnar, P. and P. England (1990), Late Cenozoic uplift of mountain ranges and global climate change: Chicken or egg?, *Nature*, 364, 29-34.

- Montgomery, D.R., T.B. Abbe, J.M. Buffington, N.P. Peterson, K.M. Schmidt, and J.D. Stock (1996), Distribution of bedrock alluvial channels in forested mountain drainage basins. *Nature* 381, 587-589.
- Montgomery, D.R. and Gran, K.B., (2001). Downstream variation in channel width of bedrock channels. *Water Resources Research* 37, 1841-1846.
- O'Conner, J.E., Webb, R.H, and Baker, V.R., 1986. Paleohydrology of pool-riffle pattern development: Boulder Creek, Utah. *Geological Society of America Bulletin* 97, 410-420.
- Richardson, K., P.A. Carling (2005), A typology of sculpted forms in open bedrock channels. *GSA. Special Paper* 392. pp.108.
- Seidl M., W.E. Dietrich, J.W. Kirchner (1994), Longitudinal profile development into bedrock: an analysis of Hawaiian channels, *Journal of Geology* 102, 457-474.
- Shepherd RG, S.A. Schumm (1974), Experimental study of river incision. *Geological Society of America Bulletin* 85 257–268.
- Sklar, L. S., and W. E. Dietrich (1998), River longitudinal profiles and bedrock incision models: Stream power and the influence of sediment supply, in *River Over Rock: Fluvial Processes in Bedrock Channels, Rivers Over Rock, Geophys. Monogr. Ser.*, 107, edited by K. Tinkler and E. E. Wohl, pp. 237–260, AGU, Washington, D. C.
- Sklar, L., and W. E. Dietrich (2001), Sediment and rock strength controls on river incision into bedrock, *Geology*, 29, 1087– 1090, doi:10.1130/00917613
- Sklar, L., and W. E. Dietrich (2004), A mechanistic model for river incision into bedrock by saltating bed load, *Water Resources Research*, 40, W06301,doi:10.1029/2003WR002496.
- Snyder, N. P., K. X. Whipple, G. E. Tucker, and D. J. Merritts (2000), Landscape response to tectonic forcing: digital elevation model analysis of stream profiles in the Mendocino triple junction region, northern California, *Geological Society of America Bulletin* 112, 1250-1263.
- Snyder, N. P., K. X. Whipple, G. E. Tucker, and D. J. Merritts (2003), Channel response to tectonic forcing: Field analysis of stream morphology and hydrology in the Mendocino triple junction region, northern California, *Geomorphology*, 53, 97–127, doi:10.1016/S0169-555X(02)00349-5.
- Springer G.S., S. Tooth and E.E.Wohl (2005), Dynamics of pothole growth as defined by field data and geometrical description. *Journal of Geophysical Research-Earth Surface* 110, F04010. DOI: 10.1029/2005JF000321

- Stock, J.D. and D.R. Montgomery (1999), Geologic constraints on bedrock river incision using the stream power law, *Journal of Geophysical Research* 104, 4983-4993.
- Tinkler, K.J., (1993), Fluvially sculpted rock bedforms in Twenty Mile Creek, Niagara Peninsula, Ontario, *Canadian Journal of Earth Science* 30, 945-953.
- Tomkin J.H., M.T. Brandon, F.J. Pazzaglia, J.R. Barbour, S.D. Willett (2003). Quantitative testing of bedrock incision models, Clearwater River, NW Washington State. *Journal of Geophysical Research*, 108 (B6), 2308. doi: 10.1029/2001JB000862
- Tucker, G. E., and R. L. Slingerland (1994), Erosional dynamics, flexural isostasy, and long-lived escarpments: A numerical modeling study, *Journal of Geophysical Research*, 99, 12,229– 12,243.
- Turowski, J. M. (2009), Stochastic modeling of the cover effect and bedrock erosion, *Water Resources Research*, 45, W03422, doi:10.1029/2008WR007262.
- Turowski, J. M., D. Lague, and N. Hovius (2007), Cover effect in bedrock abrasion: A new derivation and its implications for the modeling of bedrock channel morphology, *J. of Geophys. Res., Earth Surf.*, 112, F04006, doi:10.1029/2006JF000697.
- Turowski, J. M., N. Hovius, Hsieh Meng-Long, D. Lague, and Chen Men-Chiang (2008a), Distribution of erosion across bedrock channels, *Earth Surf. Processes Landforms*, 33, 353-363.
- Turowski, L.M., N. Hovius, A. Wilson and M.J Horng, (2008b), Hydraulic geometry, river sediment and the definition of bedrock channels. *Geomorphology* 99, 26-38.
- van der Beek P. and P Bishop (2003), Cenozoic river profile development in the upper Lachlan catchment (SE Australia) as a test of quantitative fluvial incision models, *Journal of Geophysical Research* 108:2309, doi:10.1029/2002JB002125.
- Whipple, K. X. (2004), Bedrock rivers and the geomorphology of active orogens, *Annu. Rev. Earth Planet. Sci.*, 32, 151 – 185, doi:10.1146/annurev.earth.32.101802.120356.
- Whipple, K. X., and G. E. Tucker (1999), Dynamics of the stream-power river incision model: Implications for height limits of mountain ranges, landscape response timescales, and research needs, *Journal of Geophysical Research, Earth Surface*, 104, 17,661– 17,674.
- Whipple, K. X., and G. E. Tucker (2002), Implications of sediment-fluxdependent river incision models for landscape evolution, *Journal of Geophysical Research, Earth Surface*, 107(B2), 2039, doi:10.1029/2000JB000044.

- Whipple, K. X., G. S. Hancock, and R. S. Anderson (2000a), River incision into bedrock: Mechanics and relative efficacy of plucking, abrasion, and cavitation, *Geol. Soc. Am. Bull.*, 112, 490
- Whipple, K.X., N.P. Snyder, and K. Dollenmayer (2000b), Rates and processes of bedrock incision by the Upper Ukak River since the 1912 Novarupta ash flow in the Valley of Ten Thousand Smokes, Alaska, *Geology* 28(9), 835-838.
- Wobus, C. W., G. E. Tucker, and R. S. Anderson (2006), Self-formed bedrock channels, *Geophys. Res. Lett.*, 33, L18408, doi:10.1029/2006GL027182.
- Wohl, E. E. (1993), Bedrock channel incision along Piccaninny Creek, Australia, *Journal of Geology*, 101, 749– 761.
- Wohl, E.E. (1998), Bedrock channel morphology in relation to erosional processes, in *River Over Rock: Fluvial Processes in Bedrock Channels, Rivers Over Rock, Geophys. Monogr. Ser.*, 107, edited by K. Tinkler and E. E. Wohl, pp. 133-151, AGU, Washington, D. C.
- Wohl, E. (2004), Limits to downstream hydraulic geometry. *Geology* 32(10), 897-900.
- Wohl, E. E. and H. Ikeda (1997), Experimental simulation of channel incision into a cohesive substrate at varying gradients, *Geology*, 25, 295– 298.
- Wohl, E.E., D.M., Merritt (2001), Bedrock channel morphology, *Geol. Soc. Am. Bull.*, 113, 1205-1212.
- Wohl, E. and H. Achyuthan (2002), Substrate influences in incised-channel morphology, *Journal of Geology* 110, 115-120.
- Wohl, E.E. and Wilcox, A., 2005. Channel geometry of mountain streams in New Zealand. *Journal of Hydrology* 300, 252-266.
- Wohl, E., G.C.L. David (in press), Consistency of scaling relations among bedrock and alluvial channels. *Journal of Geophysical Research-Earth Surfaces* 113, F04013, doi:10.1029/2008JF000989
- Wohl, E.E., N. Greenbaum, A.P. Schick, V.R. Baker (1994), Controls on bedrock channel incision along Nahal Paran, Israel. *Earth Surface Processes and Landforms* 19, 1-13.
- Wohl, E.E., D.M. Thompson, A.J. Miller (1999), Canyons with undulating walls. *Geological Society of America Bulletin* 111(7), 949-459.
- Wohl, E.E., K.R. Vincent, D.J. Merritts (1993), Pool and riffle characteristics in relation to channel gradient. *Geomorphology* 6, 99–110.

Wohl, E.E., N. Greenbaum, A.P. Schick, V.R. Baker (1994), Controls on bedrock channel incision along Nahal Paran, Israel. *Earth Surface Processes and Landforms* 19, 1-13.

Wolman, M.G. and Miller, J.P., 1960, Magnitude and frequency of forces in geomorphic processes. *Journal of Geology* 68, 54-74.

Yang, C.T., 1971. Potential energy and stream morphology. *Water Resources Research* 7, 311-322.

Zen E.A., and K.L. Prestegard (1994), Possible hydraulic significance of 2 kinds of potholes – examples from the Paleo-Potomac River. *Geology* 22, 47-50.

CHAPTER 3. SUBSTRATE CONTROLS ON THE LONGITUDINAL PROFILE OF BEDROCK CHANNELS: IMPLICATIONS FOR REACH-SCALE ROUGHNESS

Abstract

This chapter examines the relationships among bedrock properties and hydraulics in shaping bedrock channel morphology at the reach-scale. The Ocoee River and four other bedrock streams in the Blue Ridge Province of the southeastern U.S., which have reach-scale differences in bedrock erodibility controlled by lithologic and structural variation, are the focus of this study. A simple conceptual model for concentrated erosion in bedrock channels is described and three hypotheses are tested in order to investigate the interactions among rock erodibility, characteristics of undulating rib-like bedforms, reach-scale gradient and hydraulic roughness and energy dissipation. Substrate differences correlate with variation in reach morphology (i.e., gradient, bedform orientation and amplitude), such that less erodible substrates are associated with steeper reach gradient and with transversely oriented ribs of greater amplitude. One-dimensional modeling in HEC-RAS indicated that in the reach with the least erodible substrate, and greatest bed slope and rib amplitude, the reach-averaged hydraulic roughness was the greatest. Increased hydraulic roughness in steeper reaches points to the importance of positive and negative feedbacks in these systems: Greater substrate erosional resistance limits profile lowering, which likely creates steeper bed slopes and greater stream power, creating a self-enhancing feedback. This local increase

in stream power is balanced by increased roughness resulting from the erosional processes that produce bedrock ribs, which represents a self-regulating feedback. The overall result reflects quantifiable adjustments between substrate resistance and hydraulic driving forces in bedrock channels.

3.1 Introduction

The morphology of bedrock channels typically displays high spatial variability. Bedrock channel morphology reflects hydraulic driving forces acting across different time scales (Baker, 1978, O'Connor et al., 1986) and substrate properties such as local lithologic and structural heterogeneity (Wohl and Achyuthan, 2002; Kobor and Roering, 2004; Frankel et al., 2007), jointing (Miller, 1991; Ehlen and Wohl, 2002), bedding, and base level history (Wohl et al., 1994 Lave and Avouac, 2002; Duvall et al., 2004)). The starting assumption for self-adjusted alluvial channels is that discharge exerts the dominant influence on channel form (Leopold and Maddock, 1953). Despite the high erosional thresholds and substrate heterogeneity in bedrock channels, some evidence exists that bedrock channel dimensions also scale with flow (Montgomery and Gran 2001; Wohl and David, 2008). However, local bedrock properties also influence channel morphology (Montgomery and Gran 2001). Therefore, feedbacks between hydraulic parameters and bedrock characteristics likely govern the balance between spatial variability of channel form and scaling of channel dimensions by flow.

In this chapter, I examine the effects of bedrock properties on the Ocoee River and other bedrock channels in the southeastern United States. These channels have downstream variations in lithology and structure that appear to correlate with variations in channel

morphology. Based on these observations, I develop a conceptual model for reach-scale variations in erosion along bedrock channels with high spatial variability in rock erodibility. This conceptual model is framed in the context of hydraulic driving forces relative to rock erodibility and explore how interactions among these two components govern reach-scale variations in channel geometry and hydraulics. Although not explicitly quantified as a component of these feedbacks in this chapter, sediment transport dynamics are recognized as an important control on the bedrock channel morphology in question and are explored in Chapter 4.

One end member of the conceptual model occurs when the substrate is homogenous and readily erodible by available energy. Under these conditions, the bed lowers uniformly, producing a relatively low gradient and an even bed with lower hydraulic roughness (Figure 3.1).

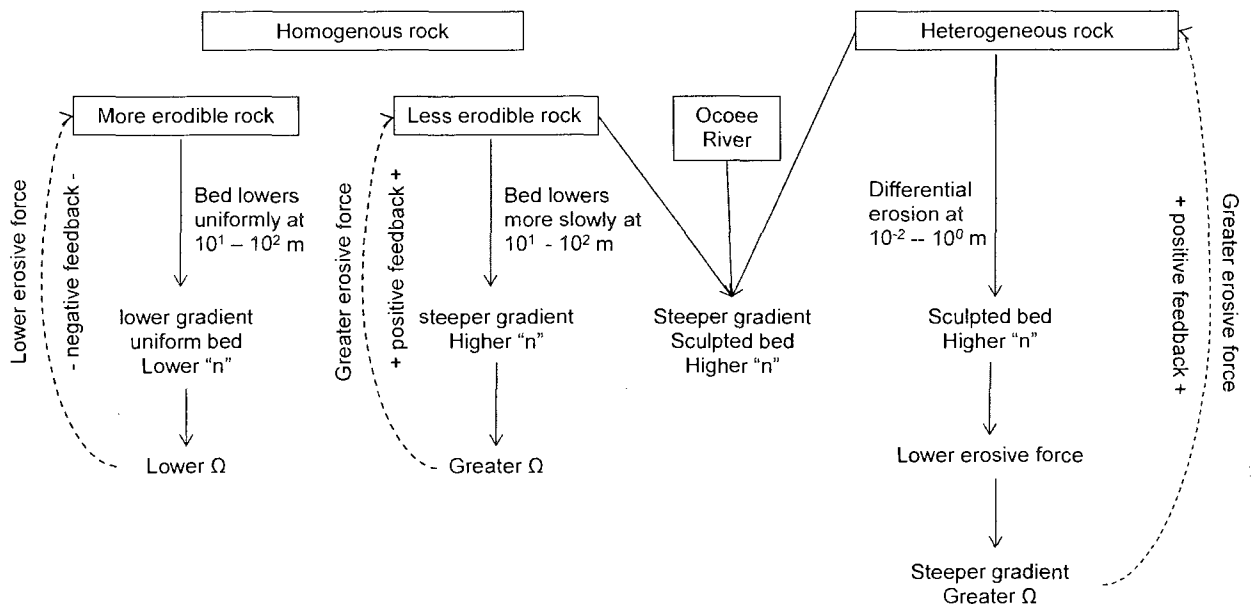


Figure 3.1. Conceptual model end members. Assuming constant discharge and channel width, the only change in total stream power ($\Omega = \gamma QS$) corresponds to a change in bed slope. The dashed arrows illustrate feedbacks. Spatial scales of erosion are represented for each end member.

In order to maintain simplicity, this model is considered at the reach scale for a channel of constant width and discharge. The only degrees of freedom are slope and boundary roughness. Rock erodibility is considered as an independent control. Alternative end members occur under conditions of less erodible rock, when the channel bed lowers less rapidly and reach-scale gradient steepens, or under conditions of heterogeneous substrate, when differential erosion can create a sculpted bed. In harder, more massive rock, sculpting is typical because wide joint spacing precludes plucking as an erosional process. In heterogeneous rock, structural and lithologic variation may influence the location of this sculpting such that weaker substrate is preferentially eroded or eroded more uniformly, whereas less erodible rock remains as topographically higher (meter scale) or steeper portions (reach scale) of the bed or has predominantly localized erosion. Localized erosion can result in knick points or knickzones along the profile (Gardner, 1983; Frankel et al., 2007), inner channels within the cross section (Baker, 1978; Shepherd and Schumm, 1974; Wohl and Ikeda, 1997; Johnson and Whipple, 2007), or sculpted abrasional forms such as potholes, flutes and grooves (Richardson and Carling, 2005). Another expression of focused erosion, which I explore for the first time in this chapter, is the formation of undulating, structurally-controlled bedrock ribs that are intermediate in scale between sculpted forms and either knickpoints or inner channels. When substrate is less erodible or more heterogeneous, steeper gradient and differential erosion increase hydraulic roughness (Figure 3.1).

Three sets of hypotheses arise from this conceptual model when applied to the Ocoee River and associated study reaches. (1) Rock erodibility varies with lithology and substrate

properties. (2) Differences in substrate properties correlate with differences in channel morphology, as reflected in gradient and bedform configuration. (3) Differences in substrate properties and channel morphology correspond to differences in hydraulic roughness. I test these hypotheses with the goal of better understanding the relative influence of different controls and processes shaping bedrock channel morphology.

3.2. Study Area

Substrate resistance, channel gradient and bedform configuration were studied on two sections of the Ocoee River, TN and four reaches along three other streams flowing through the Blue Ridge Province of the southern Appalachians: Tellico River, TN; Little River, TN; and Cheoah River, NC (Figure 3.2, Table 3.1).

Table 3.1. Blue Ridge Streams

	Stream Name (Reach)			
	Cheoah 1	Cheoah 2	Little	Tellico
Drainage Area (km ²)	460	460	275	300
Annual Peak Discharge (m ³ /s)	141	141	212	234
Reach Length (m)	170	144	145	192
Channel width (m)	47	55	28	59
Reach Gradient	0.0197	0.0093	0.0446	0.0418
Schmidt hammer	50 (5)	46 (5)	51 (6)	48 (4)
Selby	87	81	89	85
Rib orientation	transverse	transverse	transverse	oblique

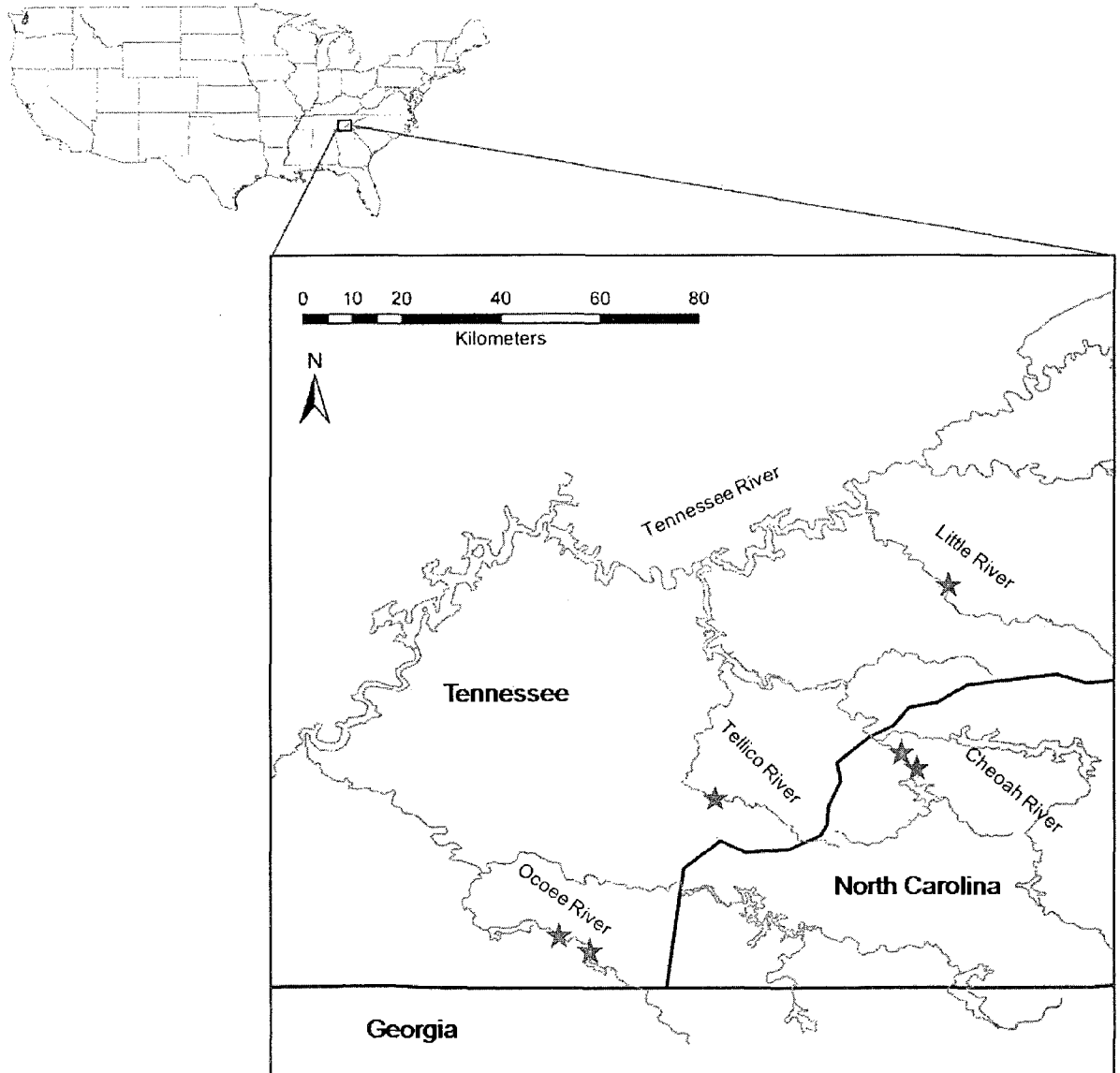


Figure 3.2. Study area site map. Study streams are labeled and site locations are indicated by stars. All streams are tributary to the Tennessee River. Only the major tributaries contributing to the study streams are shown.

These streams were selected for the presence of consistently oriented ribs, range of bed slopes, and proximity to the main study site on the Ocoee River. The channels are incised into deep gorges with steep valley walls, but bedrock exposure is low and hillslopes are densely vegetated and mantled with thick soils typical of humid temperate landscapes.

The region is tectonically quiescent, with homogenous denudation rates (25± 5 m/m.y.) over $10^4 - 10^5$ year time scales (Matmon et al., 2005).

The bedrock of all the study streams is composed of metasedimentary rocks (slates and metasandstones) that are a part of the Precambrian Ocoee Supergroup. Bedrock exposures in the main study area of the Ocoee River gorge are: the Precambrian-age Sandsuck Formation in the western gorge, which is composed of phyllites thinly interbedded with arkosic and calcareous quartzites; the Dean Formation, composed of thinly bedded quartzites and phyllites; and the Hothouse Formation, composed of metagreywacke and mica schist in the eastern gorge (Sutton, 1997). Metamorphic grade decreases in the downstream direction from garnet to below biotite. Through the gorge the rock units form a sequence of alternating resistant ledges of metagreywacke and quartzite and softer phyllite. All other Blue Ridge streams show exposures of metasandstones of the Ocoee Supergroup (e.g. Thunderhead Sandstone).

The two sections of the Ocoee River are impounded at the upstream boundaries by dams Ocoee No. 3 and Ocoee No. 2, respectively. The corresponding drainage areas for these study sections are 1200 km^2 and 1300 km^2 . These dams and their hydroelectric power facilities are operated by the Tennessee Valley Authority (TVA). The section below Ocoee No. 3 was chosen for detailed reach-scale measurements of hydraulic roughness. After the closure of the Ocoee No. 3 dam in 1942, the reach extending 8-km downstream to the No. 3 power station was completely dewatered, with the exception of winter storm flows that exceeded the hydropower capacity. Since the 1996 Olympics, the TVA has guaranteed flow on scheduled release days for the river section below the Ocoee No. 3 dam. The channel remains dry during much of the year except for scheduled releases. The scheduled releases

of roughly $45 \text{ m}^3/\text{s}$ occur for six hours on both Saturday and Sunday from Memorial Day weekend through Labor Day weekend. Winter and spring storms produce flows for which the daily average releases from the dam are typically in the range of 40 to $60 \text{ m}^3/\text{s}$, and peak flows can reach $800 \text{ m}^3/\text{s}$. In addition to this altered flow regime, the dam has also perturbed the sediment supply and capacity. Woody vegetation exists at many locations within the channel bed as a result of infrequent flow releases and dewatering of the channel under regulation by the TVA.

The features that I designate bedrock ribs are not unique to the Ocoee and other streams in the study area, but have not received much attention in the literature. Richardson and Carling (2005) describe structurally influenced, joint furrows and bedding plane furrows, which are concave sculpted features. Bedrock ribs are long, narrow portions of bedrock that protrude above the surrounding bed and are the opposing topographic expression of joint and bedding plane furrows (Richardson and Carling, 2005). Whether oriented transverse or parallel to flow, ribs are asymmetrical in cross section (Figure 3.3). Ribs are always oriented parallel to the metamorphic foliation in the rock (Figure 3.4), but in some cases the ribs also follow dominant joints. The orientation of the long axis of the ribs changes as the trend of the sinuous channel changes downstream, suggesting that rib orientation is controlled by structural features in the underlying folded metasedimentary units. Bedrock ribs appear to act as hydraulic controls when oriented at an angle that opposes the main flow direction. The occurrence of sculpted forms such as potholes and flutes along the boundaries of the ribs (e.g., along the upstream and downstream faces of transverse ribs, and in the troughs between longitudinal ribs) suggests that abrasion is the dominant mechanism of fluvial incision in this system.

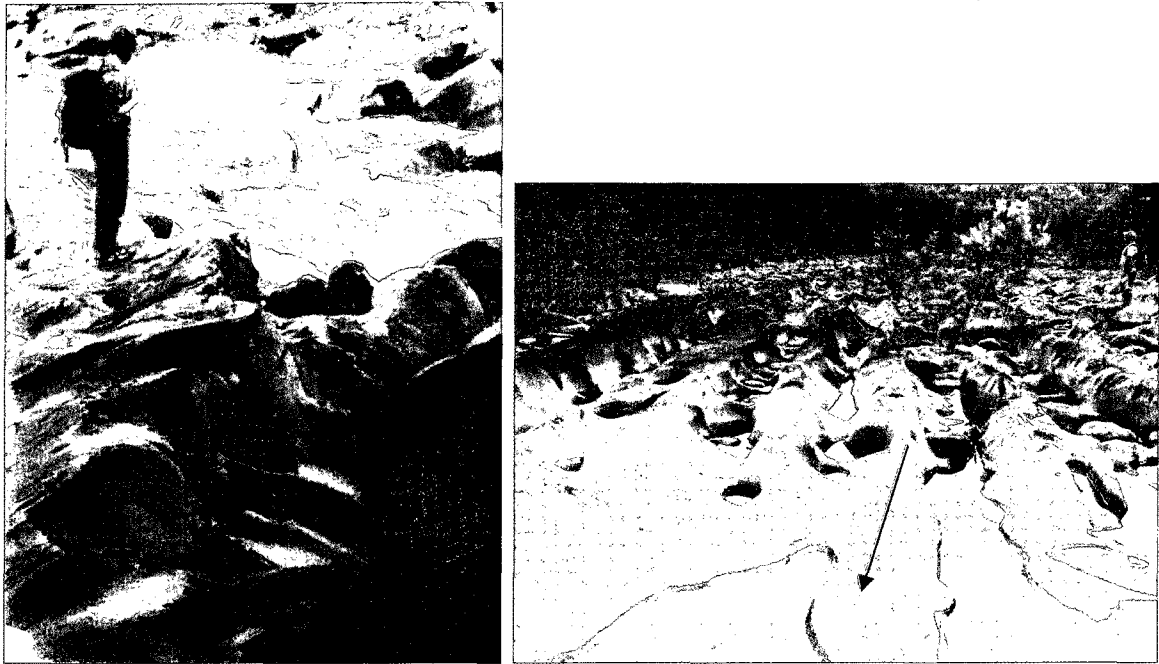


Figure 3.3. Photographs of bedrock ribs along the Upper Ocoee section. Arrows indicate the mean flow direction. A) Ribs are transverse to flow with apparent sculpting. B) Ribs are longitudinal to flow. The troughs between the ribs consist of coalesced potholes. Person in top right for scale.

Sediment in these streams consists of sand- to boulder-sized material that occurs in discontinuous patches, between ribs and within potholes (Figure 3.4). Isolated locations of this alluvial fill are armored by large cobbles and boulders. High concentrations of well sorted, gravel-sized material occur in the wake zones of the bedrock ribs. These deposits are loose and bed sediment tracer data from these patches in the Ocoee River subreaches indicate a high rate of exchange and flux within the deposit as a result of turbulent flow (Goode and Wohl, 2007). Results from this tracer study show that transport distances are greatest where ribs are of lowest amplitude, and are oriented parallel to flow. The angularity of the material ranges from very well rounded particles within potholes to more sub angular particles across the channel bed.



Figure 3.4. Photograph of longitudinal ribs in Upper Ocoee R2 showing alluvial patches in sculpted forms and between ribs. Flow is toward the viewer and there is a small tape for scale indicated in the circle.

This angularity difference appears to reflect not only the local hydraulic environment, but also the lithologic origin: phyllite produces more angular particles, whereas the metagreywacke corresponds to well-rounded particles. Also, sculpted features such as potholes tend to be larger and more numerous within reaches dominated by the metagreywacke.

3.3. Methods

3.3.1. Longitudinal variation in substrate and channel morphology

Longitudinal profiles were surveyed with a laser total station along two different sections of the Ocoee River and along three other streams in the region. The upper Ocoee section (UO) extends 4.5 km downstream of the Ocoee No. 3 dam to the 1996 Olympic whitewater course and includes four subreaches. The UO section is the primary field site for which I collected the most spatially detailed field data. To supplement the data from this site, and to demonstrate that this reach of the Ocoee is not regionally unique in having bedrock ribs, I added the middle Ocoee section (MO), which extends 3.5 km downstream from the Ocoee No.2 dam, as well as four reaches along the Tellico, Little, and Cheoah (2 reaches) Rivers.

The longitudinal profile for the UO site had points spaced at 1m intervals and was primarily designed to detect changes in bed gradient at the scale of tens to hundreds of meters. Rib geometry (amplitude and spacing) was measured via detailed transects parallel and transverse to flow within the four UO subreaches; transects documented the locations of rib crests and troughs as well as substrate type (alluvium or bedrock). Within these transects, rib orientation was characterized as either longitudinal, oblique or transverse to the downstream flow direction. These orientations were categorized according to the following criteria: longitudinal ribs varied $0^\circ \pm 10^\circ$ with respect to the main flow direction, transverse ribs were oriented $180^\circ \pm 10^\circ$ with respect to flow, and oblique ribs occurred at all other angles to flow.

At the other five sites, profile points were surveyed at ~3m intervals or less in order to document undulations in the bedrock streambed. Transitions in the orientation of bedrock ribs along each profile were noted. I also noted rib crests, troughs between ribs, and presence of either alluvium or bedrock. I visually identified rib crests during the survey, but determined the troughs from the minimum bed elevations upstream and downstream of the crest from the survey data. Ribs adjacent to the thalweg were also surveyed at the crest and lowest upstream and downstream points to document rib amplitude. Rib crest spacing was computed from the displacement between rib crests along the thalweg profile survey (Crickmore, 1970) or along transects surveyed orthogonal to the rib orientation when the ribs were longitudinal or oblique. Rib amplitude was calculated from the elevation difference between the average of the upstream and downstream trough elevations and the rib crest.

Two parameters were used to semi-quantitatively constrain rock erodibility; Selby rock mass strength (RMS) classification (Selby, 1980) and Schmidt hammer measurements (Duvall et al., 2004). Selby RMS classifications are based on numerical ratings assigned to: intact rock strength as measured using an N-type Schmidt hammer; joint spacing, width, orientation and continuity; rock weathering; and groundwater outflow. The Selby RMS classification scheme, intended initially for rock hillslopes, provides a semi-quantitative measure of bedrock strength over length scales that include heterogeneities such as joints and fractures. Schmidt hammer numbers scale empirically with compressive rock strength. In bedrock abrasion mill experiments Sklar and Dietrich (2001) demonstrated an inverse relation between abrasional resistance and tensile strength squared. Assuming that Schmidt hammer numbers are proportional to the tensile strength, greater Schmidt hammer numbers

will indicate less erodible bedrock. Although the Selby RMS partially relies on the Schmidt hammer numbers, the Selby RMS incorporates the joint characteristics that may influence the rib orientation and spacing, whereas, the Schmidt measure is purely a measure of the intact strength as resistance against abrasional impacts. Selby rock mass strengths were recorded at 21 evenly spaced locations within each subreach on the Upper Ocoee. A total of 210 Schmidt hammer measurements were taken within each subreach; an average of 10 measurements was incorporated in each Selby RMS. Selby RMSs were recorded at 10 locations within each of the other five reaches.

3.3.2. *Hydraulic modeling of reach-scale roughness*

Direct measurement of flow hydraulics in high-energy bedrock streams is difficult for practical reasons. The Ocoee River is not measurable by either wading or boat at normal flows because flow is too fast and turbulent. Direct measurements are possible only along the margins. There are also no bridges along the study area from which hydraulic measurements can be obtained. In this study I used the U.S. Army Corps of Engineers (USACE) one-dimensional flow model HEC-RAS (*U.S. Army Corps of Engineers (USACE), 2002*) to examine differences in Manning's roughness, n , between the four subreaches of the UO. Based on a given discharge, n and form energy losses (set to the default contraction and expansion coefficients), HEC-RAS uses the step-backwater method to iteratively calculate energy-balanced water-surface elevations between successive surveyed cross sections assuming steady gradually varied flow. The upstream and downstream boundary conditions were set to the known water-surface elevations for the bounding cross sections and subcritical flow conditions were assumed in all modeling runs. The four UO subreaches were selected according to rib orientation. I selected unvegetated,

straight reaches with consistent rib orientation to eliminate any other important sources of roughness such as woody bed vegetation or split channel flow. Roughly 10 cross sections (Table 3.2) were surveyed in each reach at a downstream spacing of approximately 15 m. Along each cross section, points were sampled at 1-m intervals to capture the highly variable bed topography. Figure 3.5 shows the 3-dimensional topography of the four modeled subreaches.

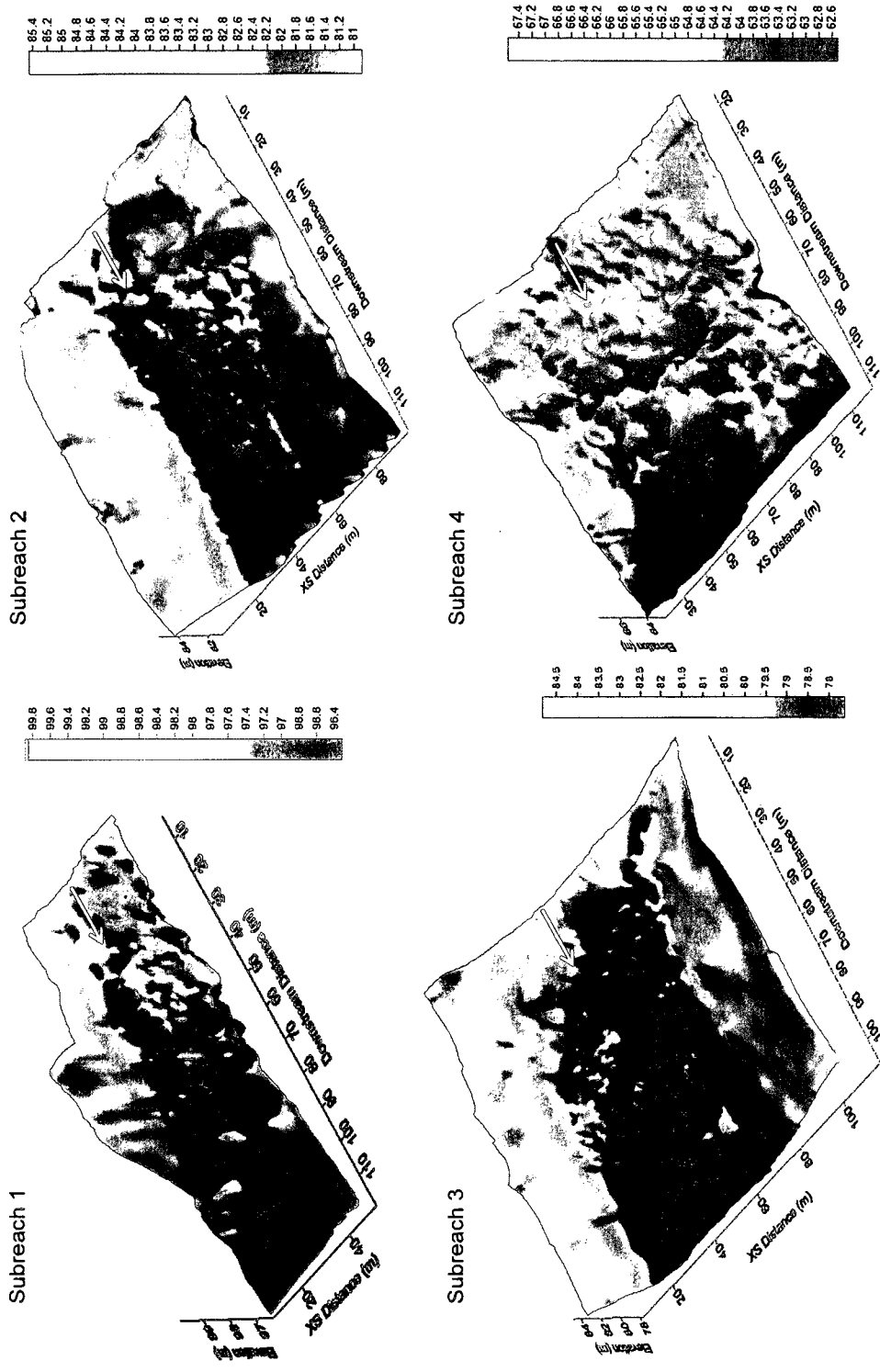


Figure 3.5. Three-dimensional plots of the four Upper Ocoee subreaches. The surfaces were created in Surfer from detailed topographic hand-surveyed data that was collected for other study components. These data were collected at roughly 1-m resolution.

Table 3.2. HEC-RAS one-dimensional modeling results and summary data for Upper Ocoee subreaches

Reach	UO1	UO2	UO3	UO4
Cross sections (n)	9	12	9	10
Rib orientation	longitudinal	longitudinal	oblique	transverse
Bed Slope (m/m)	0.0075	0.0088	0.0106	0.0197
Reach length (m)	178	198	89	76
Reach average <i>n</i>	0.059	0.075	0.092	0.107
W/D	49.99	96.84	75.04	103.15
Stdev bed elev (m)	0.36	0.40	0.43	0.51
Energy Slope (m/m)	0.011	0.013	0.007	0.022
Velocity (m/s)	1.43	1.10	0.89	0.93
Froude Number	0.50	0.42	0.30	0.35
Total Shear (N/m ²)	76.34	80.25	54.67	128.36
Total Stream Power (W)	4850	5900	3280	9890
Unit Stream Power (W/m ²)	118.74	91.17	49.66	133.08
Schmidt reading	34 (7)	40 (6)	40 (5)	46 (6)
Selby Score	65	72	75	77
Rib amplitude (m)	0.435	0.470	0.785	0.793
Rib spacing (m)	3.529	3.611	4.490	5.467
D50 (mm)	115	100	150	145
D84 (mm)	240	230	252	235

Water-surface elevations at each cross section within the subreach were surveyed during one known recreational flow discharge of 45 m³/s. HEC-RAS was used to iteratively determine *n* for each cross section; values for *n* were varied until the computed and observed maximum flow depth in the cross section converged to +/- 5 cm. In other words, these iterations were performed until the surveyed water surface profile along the channel margin matched the modeled water surface profile. The initial *n* for the downstream bounding cross section in each reach was set at the average *n* of all cross sections from the subsequent model run. I did not vary *n* across the cross section to maintain simplicity. The Ocoee does not have a pronounced thalweg, and the relatively minor variation in bed topography across each cross section justifies the use of cross-sectional average values of roughness.

To assess uncertainty in the actual discharge in the downstream subreaches (2, 3 and 4) as a result of discharge input from one small tributary draining roughly 15 km² and several small groundwater seeps between subreaches 1 and 2, I examined the sensitivity of the computed water-surface elevation by varying discharge at a constant n . In all three subreaches, I varied the discharge by 3 m³/s, which I estimated as the maximum input from the tributary and groundwater sources between the dam and these subreaches. In subreach 4, an increase in discharge of 3 m³/s led to a difference in the computed water surface of only 1-3 cm, which was within the level of detection. Computed water-surface elevations in upstream cross sections were not sensitive to the assumed n for the downstream boundary.

3.4. Results

3.4.1. Reach-scale differences in erodibility

Inter-reach differences in rock erodibility occur in the study streams. This was assessed by both Schmidt hammer readings and Selby rock mass strength classifications, which vary along the profiles of both sections of the Ocoee River. Of the 26 different reaches, differentiated along the profile according to rib orientation to flow, 19 were dominated by metagreywacke and 7 were dominated by softer and more densely foliated phyllite. Because the lithology is mixed within each reach, it is worth noting that rock erodibility, both in reality and in the measurements of it, may primarily reflect the relative proportions of weak and resistant bedrock. Although there was some variation in lithology within each reach, all reaches showed a strong dominance in bed substrate lithology (>80%). The Schmidt hammer readings of the dominant lithology in all reaches (phyllite or metagreywacke) were significantly different (Figure 3.6a; $p=0.02$). Significantly different

Selby RMS values (Figure 6b; $p < 0.01$) between these substrates also indicated contrasting rock erodibility. Based on the previously explained assumption that Schmidt hammer and Selby RMS measures are inversely related to erosional resistance, these results support the first hypothesis by indicating that reach-scale differences in rock erodibility are present.

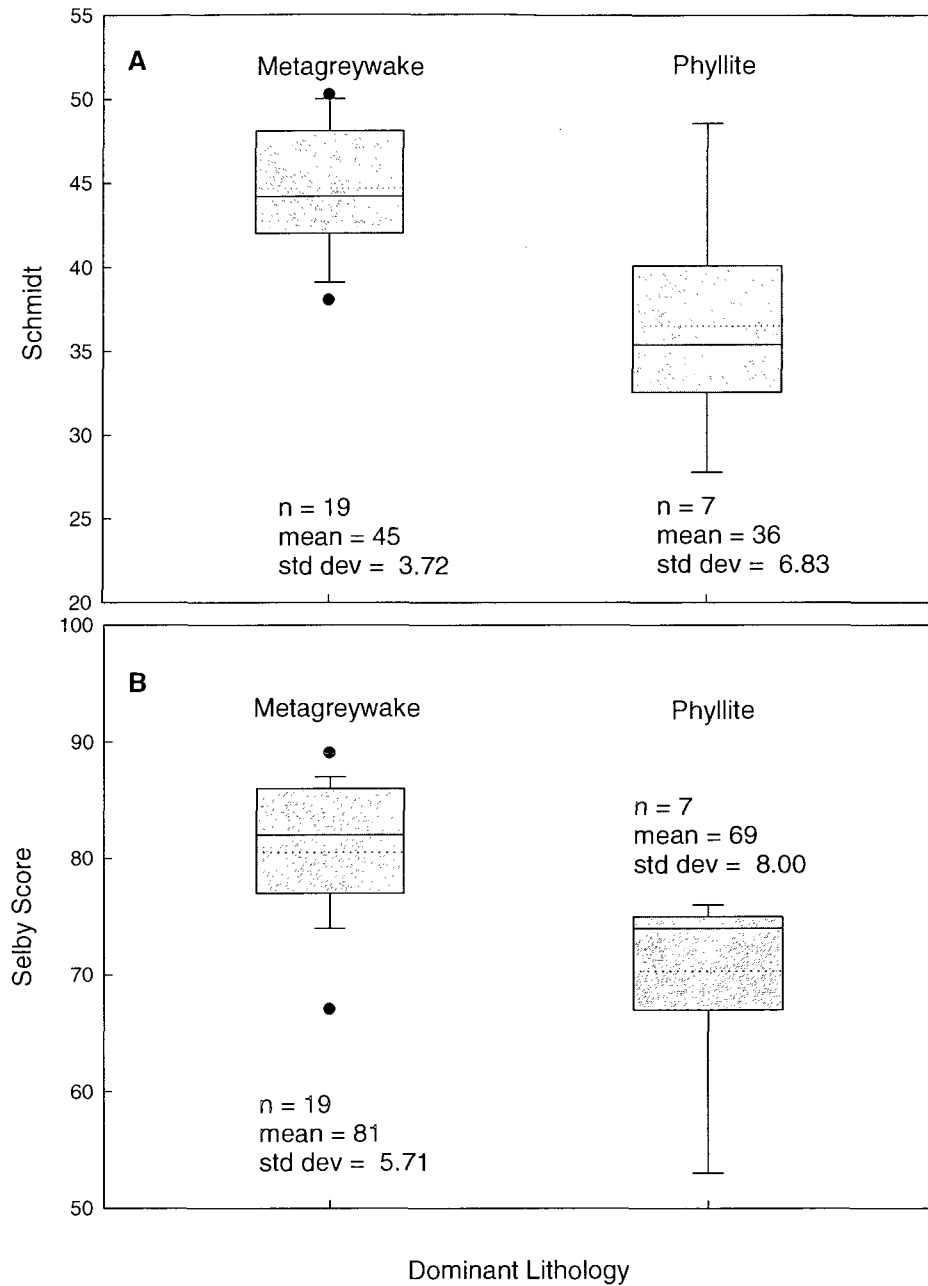


Figure 3.6. Comparison of substrate resistance (A. Schmidt hammer reading; B. Selby Score) among reaches along the Upper and Middle Ocoee sections. Reaches were distinguished based on rib orientation to flow. Within the box plots, the solid line represents median bed gradient and the dashed line indicates the mean. The box ends indicate the upper and lower quartile, and whiskers are the 10th and 90th percentiles. The solid dots represent outliers.

3.4.2. Substrate properties in relation to channel morphology

Simple regression analyses indicated that reach gradient, when adjusted by drainage area, varied as a significant positive power function of rock erodibility ($R^2 = 0.57$ and 0.42 , for Selby RMS and Schmidt reading, respectively) (Figure 3.7). In this relationship I multiplied reach gradient by drainage area to control for differences in channel scale. This new response variable is physically meaningful, as it represents a surrogate form of total stream power. The other Blue Ridge streams had the largest measures of rock strength because they exist farther to the east of the Ocoee River, where metamorphic grade is higher. Figure 3.7 also shows that in addition to reach gradient, both rock erodibility parameters tend to be larger in reaches with transverse ribs than in reaches with longitudinal ribs.

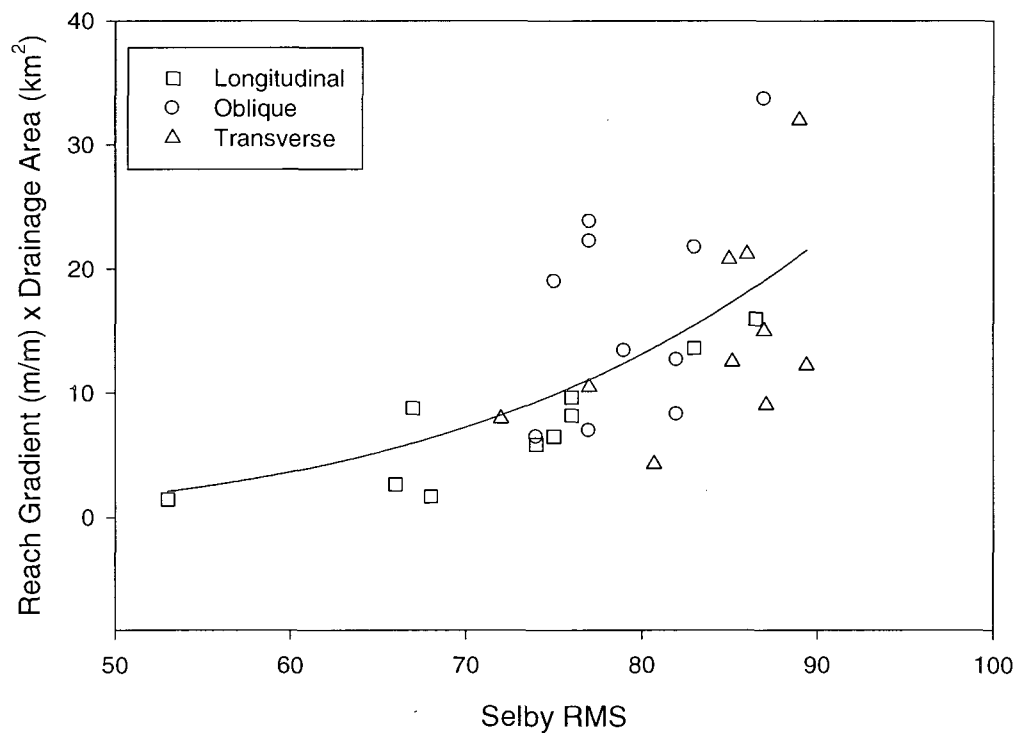
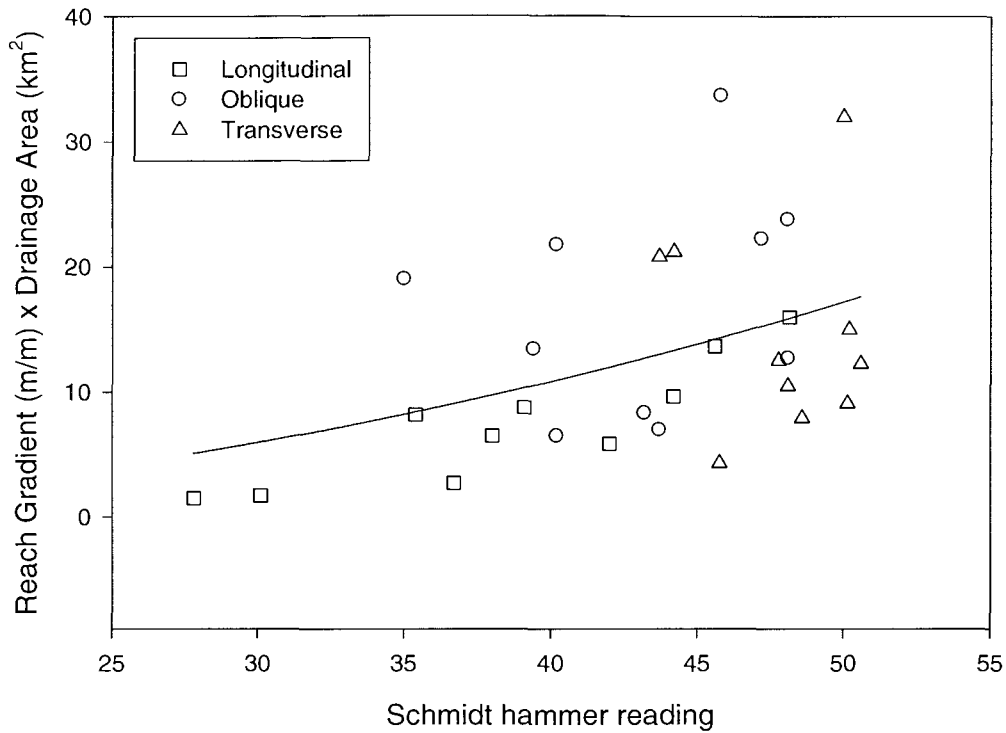
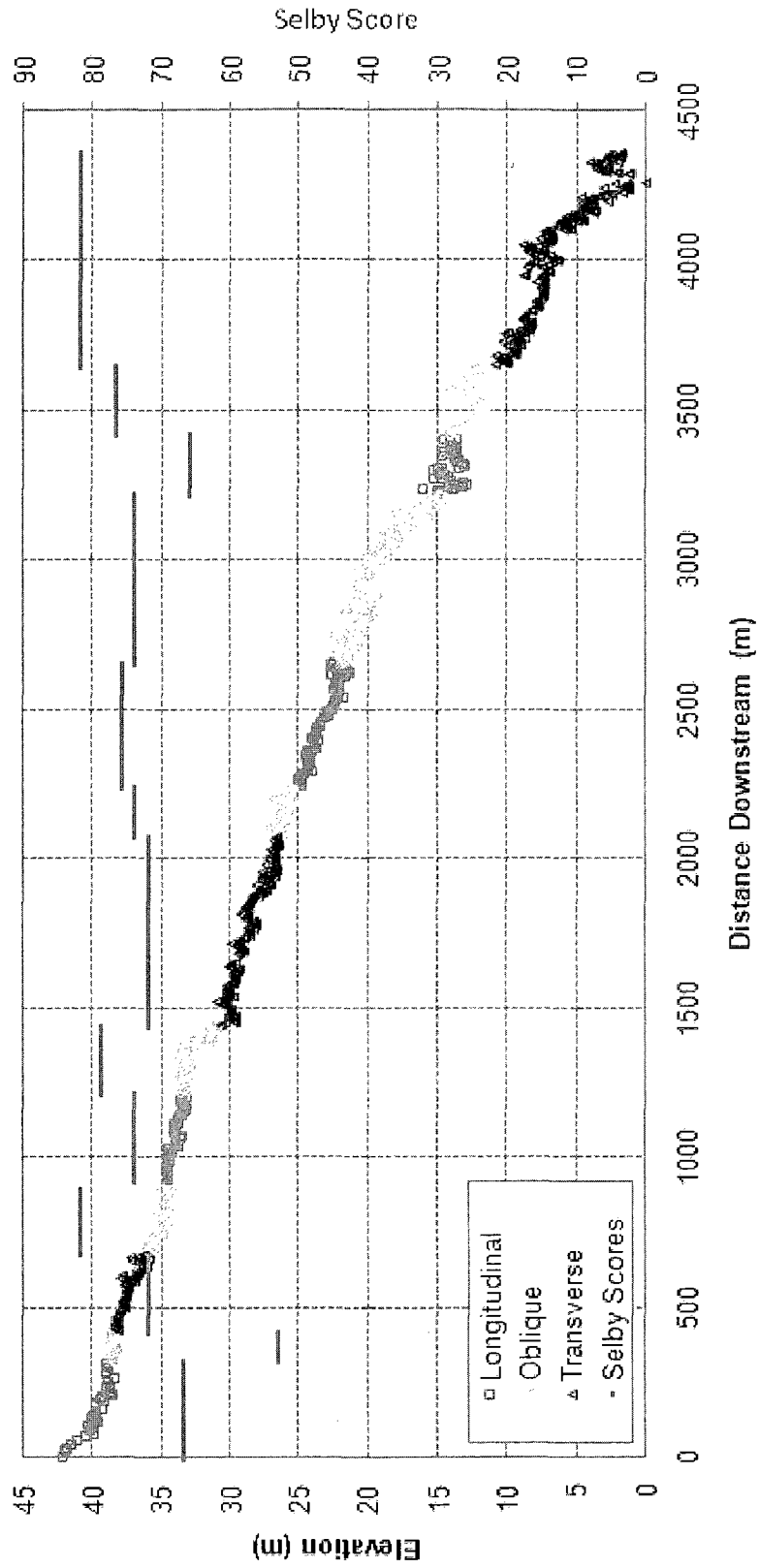


Figure 3.7. Reach gradient adjusted by drainage area as a function of rock erodibility. A) Schmidt reading, $R^2 = 0.42$; B) Selby Score, $R^2 = 0.57$. Both power functions are significant at $p < 0.05$. Data include reaches with varying rib orientation from all study streams (n=30).

Localized steep zones in the longitudinal profiles of both the upper and middle Ocoee correspond to bedrock ribs with a transverse orientation to flow, whereas longitudinally oriented ribs occur at lower gradient sections of the longitudinal profile (Figure 3.8). These profile plots also illustrate that steeper zones occur where the substrate resistance is greater. Comparison to the other three streams in the region corroborates these findings (Figure 3.9). Reach gradient was not adjusted by drainage area in this comparison because a large portion of the reaches correspond to the same drainage area, despite differences in rib orientation. The mean bed slope for reaches with bedrock ribs oriented transverse to flow is 0.020, compared to a bed gradient of 0.006 in reaches with longitudinally oriented bedrock ribs. A comparison of means with unequal variance indicated that the bed slopes for these different rib orientations were statistically different ($p < 0.01$). When the main flow direction is at an angle normal to the strike of the bedding and foliation of the substrate, the resulting bedrock ribs exert another level of resistance that correlates with an increase in channel slope.



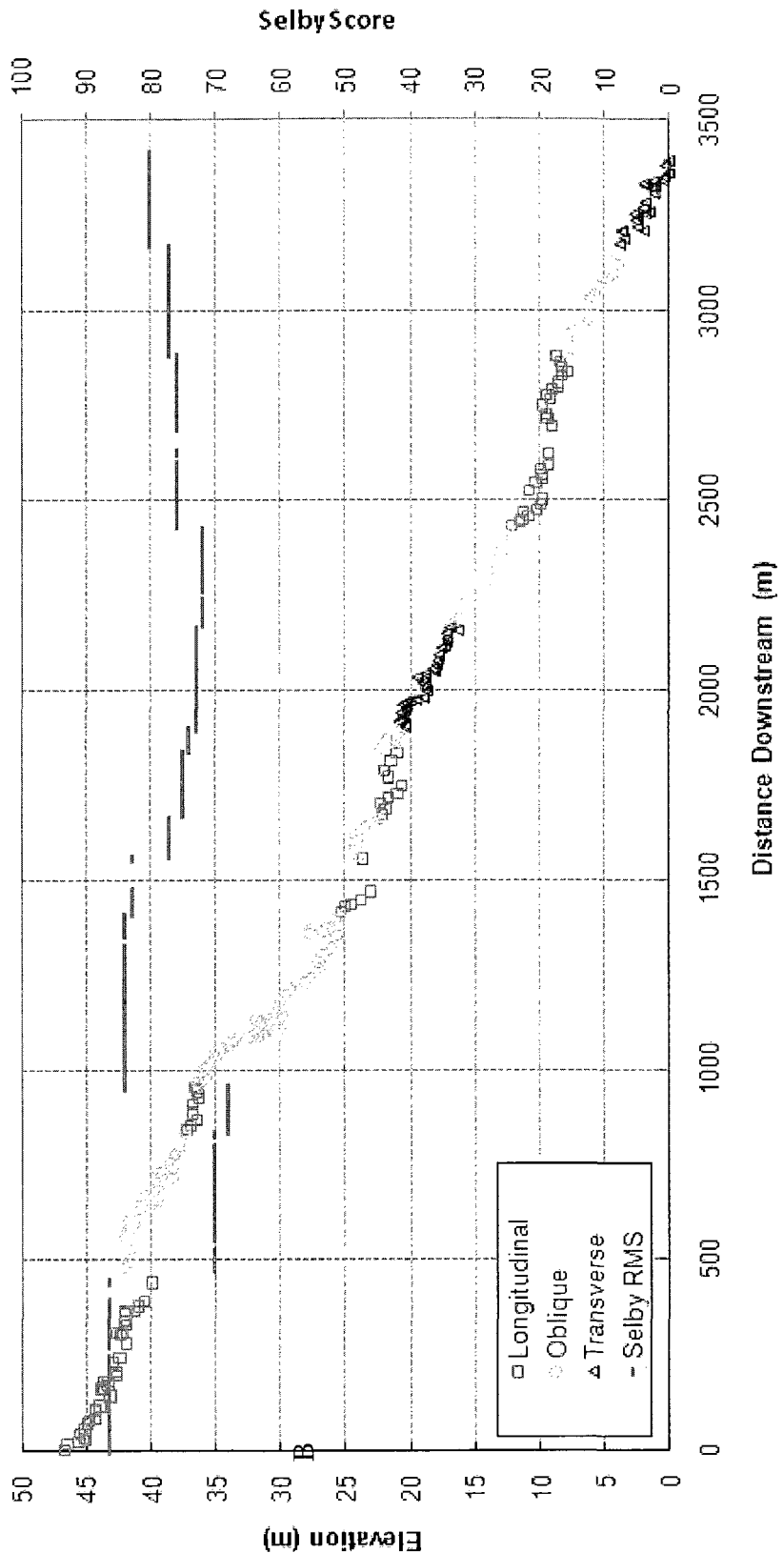


Figure 3.8. Longitudinal profile plots showing bed elevation variation according to rib orientation. Mean Selby Scores are indicated by the solid lines for each reach. A) Upper Ocoee; B) Middle Ocoee. Steep zones correspond to transverse ribs and greater Selby rock mass strength.

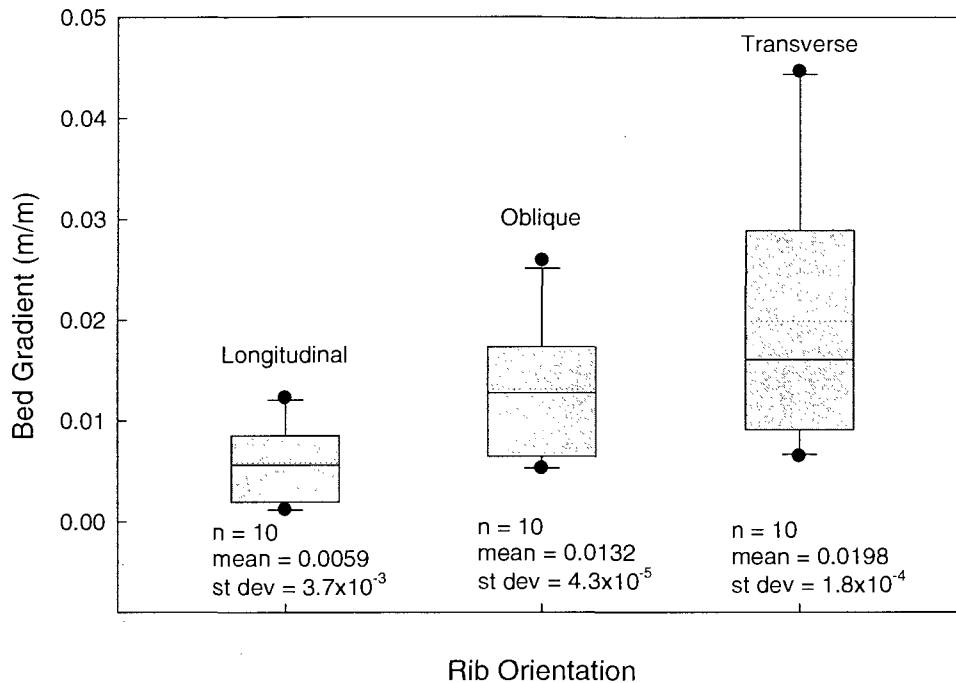


Figure 3.9. Comparison of bed slope among reaches with different rib orientations. Data include all surveyed reaches (Upper Ocoee, n=13; Middle Ocoee, n=13; Cheoah, n=2; Tellico, n=1; Little, n=1). Within the box plots, the solid line represents median bed gradient and the dashed line indicates the mean. The box ends indicate the upper and lower quartile, and whiskers are the 10th and 90th percentiles. The solid dots represent outliers.

Profile plots from three other streams in the region (Figure 3.10) illustrate that localized steep zones (10^1 -m scale) correspond to ribs of large amplitude. Rib amplitude data from these four reaches, in addition to the four subreaches on the UO, showed a significant logarithmic relationship between reach gradient and rib amplitude (Figure 3.11). Rib amplitude is also larger in reaches with higher substrate resistance (Figure 3.12a,b). These results support the second hypothesis that bedrock properties correlate with differences in channel morphology. Although rib amplitude and spacing are

positively correlated ($R^2 = 0.63$), rib spacing was not correlated with either reach-gradient or substrate resistance.

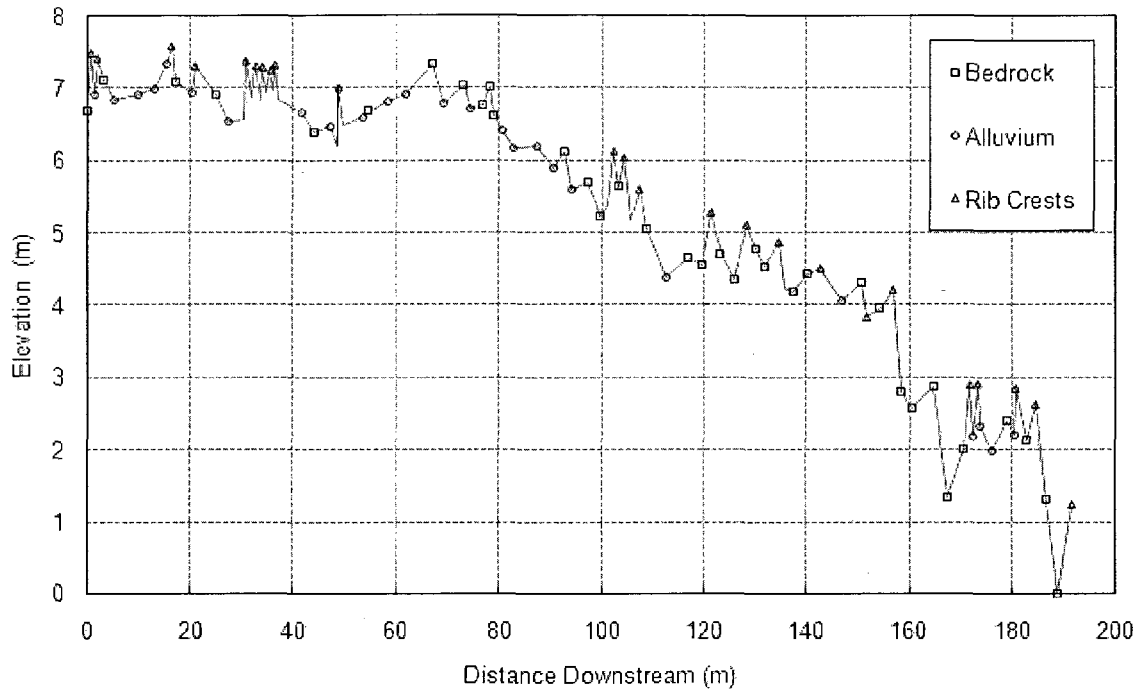


Figure 3.10. Detailed longitudinal profile plot of the Little River reach illustrating rib amplitude and spacing. The relationship between local gradient (10^1 -m scale) and rib amplitude is clearly seen in this plot. Points along the profile were identified as bedrock, alluvium or rib crests. Values of reach gradient, and rib amplitude and spacing for all four Blue Ridge stream reaches are presented in Table 3.1.

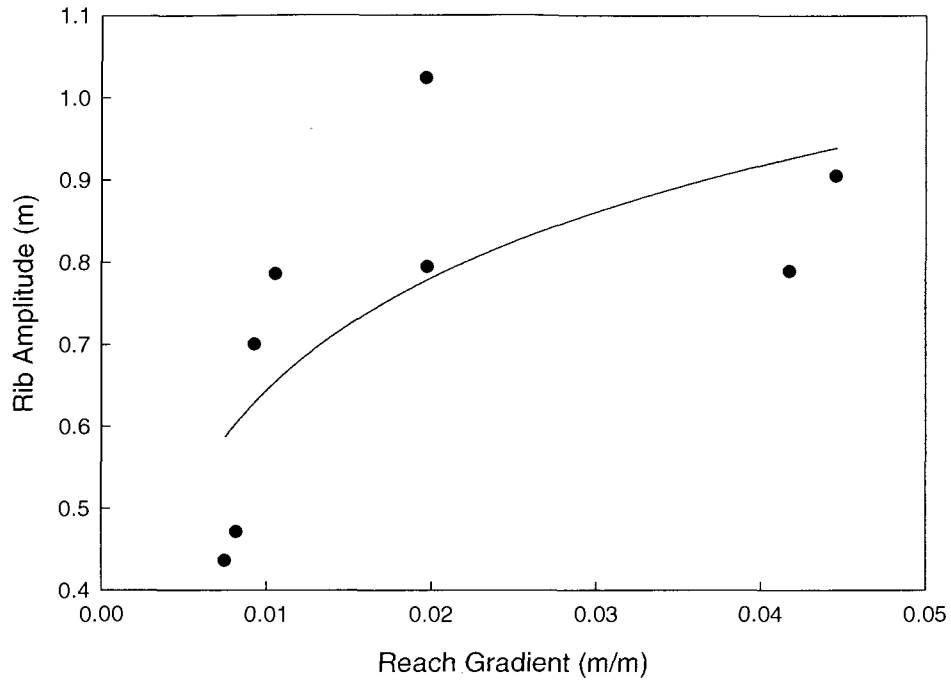


Figure 3.11. Positive logarithmic relationship between reach gradient and rib amplitude ($R^2=0.49$; $p=0.05$). Data points represent the four Upper Ocoee subreaches and the four reaches from other southeastern streams.

3.4.3. Substrate controls on reach-scale roughness

One-dimensional flow modeling results from HEC-RAS are summarized in Table 2. These results indicate that reach-scale roughness associated with ribs longitudinally oriented to flow is different from reach-scale roughness for ribs oriented transverse to flow (Figure 3.12).

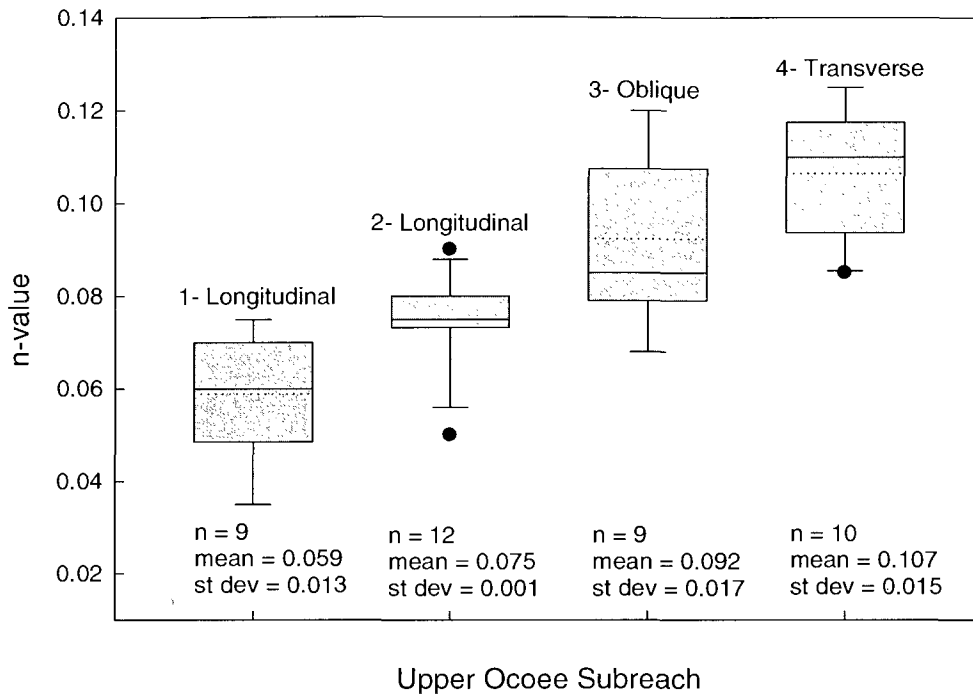


Figure 3.12. Comparison of calculated n-values from the upper Ocoee subreaches. Rib orientations are indicated above each plot. Samples represent each cross section from the HEC-RAS modeling. Within the box plots, the solid line represents median bed gradient and the dashed line indicates the mean. The box ends indicate the upper and lower quartile, and whiskers are the 10th and 90th percentiles. The solid dots represent outliers.

This result is consistent when UO1 and UO2 (longitudinal ribs) are compared separately to UO4 (transverse ribs) ($p < 0.01$). Comparison of mean Selby RMS between UO1 and UO4 shows that substrate resistance is significantly greater in the steeper reach with transverse ribs ($p < 0.01$). Selby scores in UO1 and UO2 were significantly different ($p < 0.01$), despite similar rib orientation, with UO1 showing lower Selby RMS than UO2. The substrate in UO1 is dominated by the more densely foliated phyllite, whereas UO2 shows a greater proportion of metagreywacke in the exposed bedrock. The metagreywacke and phyllite had significantly different Schmidt readings and Selby RMS ($p = 0.02$ and $p = 0.01$, respectively). These lithologic differences also produced ribs of

different amplitude. Rib amplitude was greater in the steeper reaches, UO3 and UO4, with oblique and transverse ribs, respectively. These substrate characteristics also correlate with reach-scale hydraulic roughness (Figure 3.13a,b).

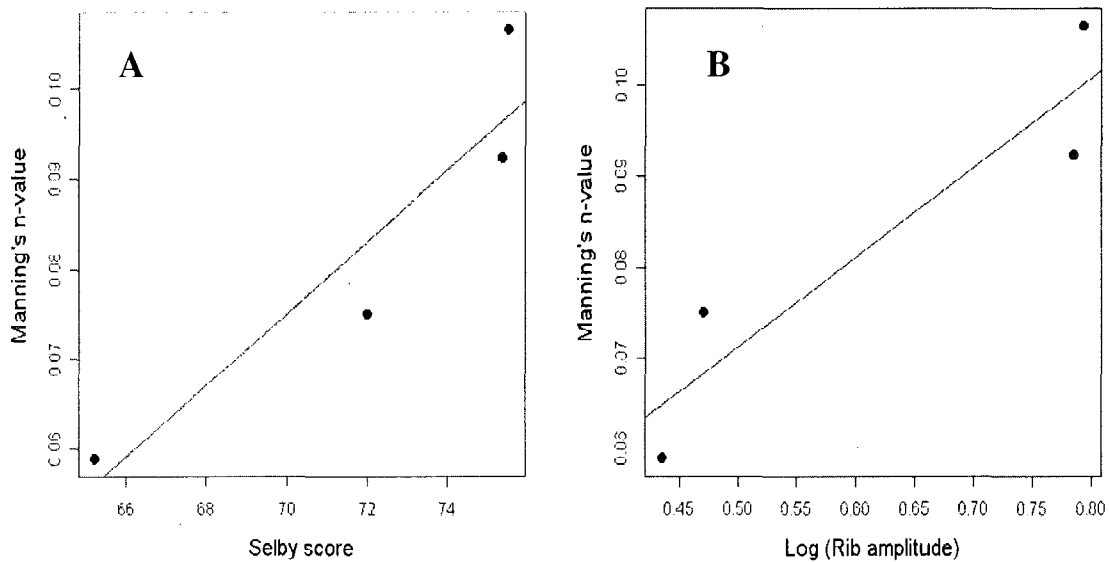


Figure 3.13. Substrate controls on reach-scale roughness. (a. $R^2 = 0.86$; b. $R^2 = 0.87$). Selby scores for each of the four Upper Ocoee reaches represent an average of 21 points in each reach. Average n-value in each reach is from all cross sections. Rib amplitudes are averaged from each reach (R1, n= 58, R2 n=99, R3 n=68, R4 n=70).

Although the small sample size ($n=4$) limits statistical conclusions, the finding that n is directly proportional to both Selby scores and rib amplitude suggests that the underlying bedrock substrate has an important influence on reach-scale hydraulics. These results support the third hypothesis that differences in substrate properties and morphology correspond to differences in hydraulic roughness. The results of these analyses indicate that bedrock bedforms correlate strongly with reach-scale hydraulic roughness and energy dissipation. Feedbacks among substrate characteristics and flow hydraulics are thus likely to be important in this system.

3.5 Discussion

Interpreted in the context of the conceptual model described previously, the results of this study show that reach-scale differences in rock erodibility strongly correlate with channel geometry and hydraulics. These results are interpreted to support the feedbacks illustrated in the conceptual model (Figure 3.1): lower rock erodibility limits bed incision, resulting in increased slope relative to segments of channel bed with less resistant substrate. Local steepening of the profile effectively increases total stream power, thus enhancing hydraulic driving forces. Although the Ocoee also widens in the steeper subreaches, the change is not sufficient to produce lower values of unit stream power (Table 3.2). The orientation of the bedrock ribs relative to flow direction in the study reaches appears to be an independent parameter that reflects the underlying bedrock structure. Steeper bed slopes also correlate with transversely oriented bedrock ribs of greater amplitude, which increase reach-scale hydraulic roughness. Increased hydraulic roughness presumably mediates the local increase in stream power along steeper reaches, providing a self-regulating feedback. Correlations in rock erodibility and rib orientation that appear in the data limit separation of these two variables. This precludes determining which of the two is a more important independent control on reach-scale geometry and hydraulics.

An interesting illustration of the adjustments among substrate resistance and channel geometry comes from one notable meander along the MO. The local strike and lithology of the ribs remains constant through the bend, but change in flow direction results in variation of rib orientation to flow; ribs transition from longitudinal to oblique and close to transverse. A corresponding transition in slope occurs through the bend and

gradient increases as rib orientation changes from longitudinal to transverse. The relationships between rib orientation, the dominant joint and foliation orientation, and the channel gradient suggest that the channel bed morphology reflects the underlying substrate. Also, the orientation of the ribs exerts another level of flow resistance to which the channel must respond in order to maintain vertical incision. The amplitude of these ribs also appears to increase slightly as the ribs change in orientation. This potential correlation in rib amplitude and orientation suggests that the morphology adjusts in response to independent substrate controls. If the transversely oriented ribs of greater amplitude create greater hydraulic roughness, then greater reach gradient where the ribs are transverse suggests that the stream adjusts to locally increase reach-averaged stream power and localize erosion in response to this independent substrate characteristic.

The interactions between hydraulics and substrate that are inferred for the Ocoee River can be compared to those proposed to act along alluvial channels. Bedforms in alluvial systems range from dunes and ripples in sand bed streams to steps and pools in gravel-bed streams. The geometry and characteristics of alluvial bedforms are often interpreted in the context of extremal hypotheses (Davies and Southerland, 1980; Richards, 1976; Grant, 1997; Wohl and Merritt, 2008). The fundamental assumption behind extremal hypotheses which posit minimization of variance in hydraulic variables along a channel is that sites of greater energy expenditure, such as lateral constrictions or local steepening, will erode to a channel configuration with lower energy expenditure (e.g., Kieffer, 1989). This assumption only holds if the boundary is readily deformable such that channel cross-sectional geometry can change substantially in response to increased energy expenditure. As boundary erodibility decreases, other mechanisms such

as increased boundary roughness become more important. In coarse alluvial systems, for example, the geometry of step-pool sequences adjusts in a manner that enhances flow resistance when the channel is supply-limited (Davies and Sutherland, 1980; Abrahams et al., 1995). The presence of bedrock bedforms (Wohl and Grodek, 1994; Duckson and Duckson, 2001) suggest that interactions between hydraulic energy and bedforms in bedrock streams might also regulate energy dissipation in these systems.

Wohl and Merritt (2001) discriminated bedrock-channel geometry according to gradient, substrate heterogeneity, and Selby rock mass strength. They interpreted correlations between channel morphology and substrate characteristics to indicate that, similar to alluvial streams, bedrock channel morphology reflects adjustments between hydraulic driving forces and substrate erodibility. The presence of spatial variations in substrate erodibility presumably creates spatial differences in these adjustments along bedrock channels that may limit the minimization of variance. Hartshorn et al. (2002) found greater variability and more irregular erosion in the quartzites. They attributed differences in channel morphology to differences in the intact rock strength and joint spacing. Similarly, intact rock strength, Selby RMS, and orientation of bedrock structures that can be differentially sculpted to produce bedrock ribs vary significantly among the four subreaches of the upper Ocoee and strongly influence reach-scale geometry and hydraulics.

The longitudinal variation in substrate characteristics along the rivers described here likely limits the degree to which these channels develop uniform energy expenditure, as reflected in reach-average values of stream power that vary by a factor of ~3. However, the heterogeneities in resistance may also set up mechanisms to locally

enhance energy dissipation, resulting in feedbacks between hydraulics and substrate that tend to reduce longitudinal variation in energy expenditure in a manner similar that hypothesized for alluvial streams.

Wohl et al. (1999) showed that periodicity in the flow structure, created by bed or bank forms, perpetuates bedrock bedforms in the downstream direction, which leads to a feedback between forms and hydraulics such that flow conditions oscillate around critical flow, as explained for alluvial channels by Grant (1997). If flow oscillates around critical, then the effect is to minimize downstream variation in energy expenditure. Both alluvial and bedrock channels adjust roughness, albeit in different ways, to minimize inter-reach variability in energy expenditure.

We have neglected bedload effects in this discussion, in part because upstream sediment supply to the Ocoee study reaches is altered by the presence of a dam. Sediment transport likely plays an important role, however, in the adjustments between hydraulics, boundary configuration and incision of bedrock channels. Recent flume studies document how bedrock roughness influences incision patterns through its effect on local bed sediment transport (Johnson and Whipple, 2007; Finnegan et al., 2007). Also, Chatanantavet and Parker (2008) experimentally showed that the hydraulic roughness provided by the bedrock surface is an important factor in controlling the degree of alluviation. Their results agreed with those of Demeter et al. (2005), who showed that bedrock beds with greater roughness required a lower sediment supply rate before alluvial patches formed. All four of these studies point to the influence of bedrock roughness on localized bed sediment transport, which ultimately controls the incision rate (Sklar and Dietrich, 1998, 2004). Although I did not examine bed sediment transport in

this study, these results indicate that hydraulic roughness is enhanced through the development of larger bedrock bedforms in reaches of steeper gradient and greater substrate resistance. This not only illustrates focused erosion as predicted by the conceptual model, but also points to the importance of positive and negative feedbacks in development of bedrock channel morphology. In Chapter 4 I investigate how bedrock channel morphology influences bed sediment transport. Overall, the results here provide another example where, as in alluvial streams, bedrock channel morphology reflects a quantifiable balance between hydraulic driving forces and substrate resistance (Wohl and Merritt, 2001).

3.6. Conclusions

Lithologic and structural variation along the profiles of the streams examined in this study creates differences in the substrate erodibility. These substrate heterogeneities lead to localized concentration of hydraulic energy, which is reflected by the positive correlation between rock erodibility and reach gradient. Bedrock ribs of greater amplitude are also consistent with steeper reach gradients. In reaches with transverse ribs, the gradient is steeper than segments with longitudinal ribs. These results suggest that reach gradient is largely a function of independent lithologic and structural controls. First-order assessment of reach-scale roughness in this bedrock channel indicates that the orientation of bedrock ribs also controls roughness and energy dissipation. Comparison of Manning's n between the reaches suggests that roughness increases with rib amplitude and as the orientation of bedrock ribs changes from longitudinal to transverse. Although increased

reach gradient occurs where rock erodibility is lower, which suggests locally greater potential for erosion through increased stream power, these steeper reaches are also associated with greater bedform amplitude and increased hydraulic roughness and energy dissipation, and this may counteract increases in stream power. These linkages demonstrate that there are complex feedbacks that operate between the underlying substrate, channel morphology and hydraulics, which reflect a balance between the hydraulic driving forces and substrate erodibility of bedrock streams.

References

- Abrahams, A.D., G. Li, J.F. Atkinson (1995), Step-pool streams: adjustment to maximum flow resistance, *Water Resources Research* 31(10), 2593-2602.
- Chatanantavet, P., G. Parker (2008), Experimental study of bedrock channel alleviation under varied sediment supply and hydraulic conditions, *Water Resources Research* 44, W12446, doi:10.1029/2007WR006581.
- Crickmore, M. J. (1970), Effect of flume width on bedform characteristics, *J. Hydraul. Eng. Div.*, 96(HY2), 473–496.
- Baker, V.R., (1977), Stream-channel response to floods, with examples from central Texas. *Bulletin of the Geological Society of America*, 88, 1057-1071.
- Davies, T.R., A.J. Southerland (1980), Resistance to flow past deformable boundaries. *Earth Surface Processes* 5, 175-179.
- Demeter, G.I., L.S. Sklar, J.R. Davis (2005), The influence of variable sediment supply and bed roughness on the spatial distribution of incision in a laboratory bedrock channel, *EOS Trans AGU*, Fall Meet Suppl., Abstract H53D-0519.
- Duckson, D.W., L.J. Duckson (2001), Channel bed steps and pool shapes along Soda Creek, Three Sisters Wilderness, Oregon, *Geomorphology*, 38, 267-279.
- Duvall, A., E. Kirkby, D.W. Burbank (2004), Tectonic and lithologic controls on channel profiles and processes in coastal California. *Journal of Geophysical Research* 109:
- Finnegan, N.L., L.S. Sklar, T.K. Fuller (2007), Interplay of sediment supply, river incision, and channel morphology revealed by transient evolution of an experimental bedrock channel, *J. Geophys. Res.*, 112, F03S11.
- Frankel, K.L., F.J. Pazzaglia, J.D. Vaughn (2007), Knickpoint evolution in a vertically bedded substrate, upstream-dipping terraces, and Atlantic slope bedrock channels. *Geological Society of America Bulletin* 119 (1-3), 476-486.
- Ehlen, J., E.E. Wohl (2002), Joints and landform evolution in bedrock canyons, *Transactions, Japanese Geomorphological Union* 23(2), 237-255.
- Goode, J.R. and E. Wohl (2007), Coarse sediment transport dynamics at three spatial scales of bedrock channel bed complexity, *EOS Trans AGU*. 88(52), Fall Meet Suppl., Abstract H51E-0794.

- Gardner, T.W. (1983), Experimental study of knickpoint and longitudinal profile evolution in cohesive, homogeneous material. *Geological Society of America Bulletin*, 94, 664–672.
- Grant, G.E. (1997), Critical flow constrains flow hydraulics in mobile-bed streams: A new hypothesis, *Water Resources Research* 33, 349-358.
- Hartshorn, K., N. Hovius, W.B. Dade, R.L. Slingerland (2002), Climate-driven bedrock incision in an active mountain belt. *Science* 297, 2036-2038.
- Johnson, J.P., K.X. Whipple (2007), Feedbacks between erosion and sediment transport in experimental bedrock channels, *Earth Surf. Proc. Landforms*, 32, 1048-1062.
- Kieffer, S.W. (1989), Geologic nozzles, *Reviews of Geophysics*, 27, 3-38.
- Kobor, J.S., J.R. Roering (2004), Systematic variation of bedrock channel gradients in the central Oregon Coast Range: implications for rock uplift and shallow landsliding *Geomorphology* 62, 239-256.
- Lave, L., J.P. Avouac (2001), Fluvial incision and tectonic uplift across the Himalayas of central Nepal, *Journal of Geophysical Research* 106, 26,561-26,591.
- Langbein, W.B. (1964), Profiles of rivers of uniform discharge. *United States Geological Survey Professional Paper* 501B, 119-122.
- Leopold, L.B., T. Maddock, (1953), The hydraulic geometry of stream channels and physiographic implications. U.S. Geological Survey Professional Paper 252, pp. 57.
- Matmon, A., P.R., Bierman, J. Larsen, S. Southworth, M. Pavich, M. Caffee, (2005), Temporally and spatially uniform rates of erosion in the southern Appalachian Great Smoky Mountains, *Geology* 31, 155-158.
- Miller, J.R., (1991), The influence of bedrock geology on knickpoint development and channel bed configuration along downcutting streams in south-central India, *Journal of Geology* 99, 591-605.
- Montgomery, D.R., K.B. Gran (2001), Downstream variations in the width of bedrock channels. *Water Resources Research* 37(6), 1841-1846.
- O’Conner, J.E., R.H. Webb, V.R Baker (1986), Paleohydrology of pool-riffle pattern development: Boulder Creek, Utah. *Geological Society of America Bulletin* 97, 410-420.
- Richards, K.S. (1976), The morphology of riffle-pool sequences. *Earth Surface Processes* 1, 71–88.

- Richardson, K., P.A. Carling (2005), A typology of sculpted forms in open bedrock channels. *GSA. Special Paper 392*. pp.108.
- Shepherd RG, S.A. Schumm (1974), Experimental study of river incision. *Geological Society of America Bulletin* 85 257–268.
- Selby, M.J. (1980), A rock mass strength classification for geomorphic purposes: with tests from Antarctica and New Zealand. *Zeit. Geomorph* 24, 31-51.
- Sutton, S.J. (1991), Development of domainal slaty cleavage fabric at Ocoee Gorge, Tennessee. *Journal of Geology* 99 (6) 789-800.
- U. S. Army Corps of Engineers (USACE) (2002), HEC-RAS river analysis system user's manual, version 3.1, Inst. for Water Resour., Hydrol. Eng. Cent., Davis, Calif.
- Wohl, E.E., T. Grodek (1994), Channel bed-steps along Nahal Yael, Negev desert, Isreal, *Geomorphology*, 9, 117-126.
- Wohl, E.E., H. Ikeda (1997), Experimental simulation of channel incision into a cohesive substrate at varying gradients. *Geology* 25, 295-298.
- Wohl, E.E., D.M., Merritt (2001), Bedrock channel morphology, *Geol. Soc. Am. Bull.*, 113, 1205-1212.
- Wohl, E., H. Achyuthan (2002), Substrate influences in incised-channel morphology, *Journal of Geology* 110, 115-120.
- Wohl, E., G.C.L. David (in press), Consistency of scaling relations among bedrock and alluvial channels. *Journal of Geophysical Research-Earth Surfaces*.
- Wohl, E. D.M. Merritt (2008), Reach-scale geometry of mountain streams, *Geomorphology* 93, 168-185.
- Wohl, E.E., D.M. Thompson, A.J. Miller (1999), Canyons with undulating walls. *Geological Society of America Bulletin* 111(7), 949-459.
- Wohl, E.E., N. Greenbaum, A.P. Schick, V.R. Baker (1994), Controls on bedrock channel incision along Nahal Paran, Israel. *Earth Surface Processes and Landforms* 19, 1-13.

CHAPTER 4: COARSE SEDIMENT TRANSPORT DYNAMICS AT THREE SPATIAL SCALES OF BEDROCK CHANNEL BED COMPLEXITY

Abstract

Independent lithologic and structural controls in bedrock systems interact with coarse sediment transport to play a key role in bedrock incision processes such as abrasion. This field study was conducted the Ocoee River in the Blue Ridge Province of the southern Appalachians, USA, where the fold-dominated terrain is revealed in the channel bed as linear bedrock ribs that vary in orientation to flow at the reach scale. Painted tracer clasts were used to measure coarse sediment transport dynamics over several flow events (3-year temporal scale). I designated 4 reaches with internally consistent channel geometry within the study area, and also examined differences in patterns of coarse clast movement between reaches and across three progressively smaller spatial scales within each reach. These data were used to test three hypotheses designed to enhance our understanding of coarse sediment transport dynamics in bedrock channels. Results indicated that transport distance was not a significant function of grain size, as has been reported for alluvial channels. Reach-scale differences in channel morphology (rib orientation and amplitude) correlate with transport distance. At different intra-reach scales, the smallest spatial resolution was the best predictor of transport distance. The highly complex bed topography in this system leads to widely varying coarse sediment transport dynamics. Complex interactions among gradient and bed roughness appear to govern reach-scale differences in the degree of alluvial cover.

4.1. Introduction

Recent research has focused on understanding reach-scale processes involved in bedrock channel incision (e.g. Johnson and Whipple, 2007; Finnegan et al., 2007; Chatanantavet and Parker, 2008) in order to better constrain parameters and assumptions required for landscape evolution models (e.g., Howard, 1994; Whipple and Tucker, 2002; Sklar and Dietrich, 2004; Turowski et al., 2007; Lamb et al., 2008). Particular interest has focused on the important role of bedload material in controlling incision via abrasion in bedrock systems (Sklar and Dietrich, 1998; 2001; Hartshorn et al., 2002). Abrasion occurs as saltating bedload translates the kinetic energy of the mobile particle into removal of bedrock material; abrasion can be a dominant erosional mechanism in bedrock-dominated channels, especially in massive bedrock and where there is an intermediate supply of coarse bedload material. Given the importance of alluvial material in bedrock channel systems, the mechanics of bedload transport processes exert a strong influence on the rate and style of bedrock channel incision.

Despite constant hydraulic conditions, several flume (e.g., Hassan and Church, 2001; Singh et al., 2009) and field studies (e.g., Gomez and Church, 1989; Hoey, 1992; McNamara and Borden, 2004) have observed strong spatial and temporal variability in bedload transport rates within alluvial channels. Although several explanations have been proposed for these fluctuations, including variability in transport over bedforms (Schmidt and Ginz, 1995; Thompson et al., 1996; Cudden and Hoey, 2003), temporal variability in sediment supply (Beschta, 1987), and variation in armoring and sorting (Whiting et al.,

1988), bedload transport has also been described as a stochastic process both in early work (Einstein, 1937; 1950) and contemporary studies of alluvial (Hassan and Church, 1992; Pyrcce and Ashmore, 2003a,b; McNamara and Borden, 2004), and bedrock (Turowski, 2009) channels. Given the high level of variability in natural systems, a stochastic component will always need to be incorporated into any explanation or prediction of fluvial processes and is essential to understanding the dynamics of natural channels (Snyder et al., 2003; Tucker, 2004; Lague, et al., 2005; Turowski, 2009). Nonetheless, constraining the components of the variability in sediment transport allows for better understanding of these systems. In this study I examine the role that spatial variability plays in controlling coarse sediment transport in a bedrock channel with lithologically and structurally induced channel bed complexity.

Sediment transport and deposition in bedrock channels differ from alluvial systems in that sediment loads are relatively low, highly turbulent flows are capable of transporting up to boulder-sized particles for large distances, and coarse sediment is directly supplied from the adjacent hillslopes through landslides, rock fall, or debris flows (Wohl, 1999; Whipple, 2004). Bedrock channels also differ from alluvial counterparts because of the influence of bedrock characteristics (i.e., lithology and structure) on channel boundary configuration.

Under conditions of low bedload supply relative to transport capacity, sediment in transport acts to abrade the bedrock channel surfaces and the tools effect dominates. Conversely, when bedload supply increases, particle collisions and interactions favor deposition into alluvial patches, eventually covering the bedrock. In this case the bedload material inhibits bedrock incision and the cover effect dominates. At intermediate

sediment supply rates, there are enough tools for abrasion, but not enough for alluvial cover to form. This conceptual model was initially proposed by Gilbert (1877), and more recently quantified by Sklar and Dietrich (1998). Although this threshold model is fairly simple conceptually, there are many nuances and details that arise when it is further examined experimentally (Johnson and Whipple, 2007; Finnegan et al., 2007; Chatanantavet and Parker, 2008) and in the field, as I do in this study.

The saltation abrasion model (Sklar and Dietrich, 1998; 2004) incorporates bedload supply and transport, for example, but does not incorporate morphology as a degree of freedom and instead assumes a planar bed surface. Bedrock channels commonly display complex bed topography as a result of sculpting and rock characteristics (Richardson and Carling, 2005). This complex bed topography, in alluvial or bedrock systems, largely influences the local flow field (Furbish, 1993; Nelson et al., 1995; Papanicolaou et al., 2001), the dynamics of sediment transport (Yager et al., 2007; Thompson, 2007), local erosion rate (Hancock et al., 1998; Johnson and Whipple, 2007), and spatial variation in the surface texture of bed sediments (Dietrich, et al., 1989), such that sediment supply, grain size, and bedrock detachment are all interrelated variables that tend to offset variation in one another (Sklar and Dietrich, 2008). Roughness supplied from sculpted forms in bedrock systems increases form drag, which likely reduces the local shear stress in zones of active sediment transport and erosion (Shepherd and Schumm, 1974; Wohl and Ikeda, 1997; Wohl, 1998; Wohl et al., 1999; Johnson and Whipple, 2007; Finnegan et al., 2007; Turowski et al., 2007; Chatanantavet and Parker, 2008). Therefore, roughness is likely to locally reduce sediment transport capacity and the topography controls the spatial distribution of sediment transport.

As a result of these complex interactions, understanding how variable bed topography in bedrock systems influences sediment transport processes will enhance bedrock incision models. In considering the processes of coarse sediment transport in a bedrock channel with a high level of spatial variability in channel form, I acknowledge that it is the sediments considered that are likely the tools for creating the bed topography analyzed. Understanding the spatial variation in sediment transport within this topographic setting permits insight into the feedbacks between channel form and shaping processes. The time scale for which the channel-shaping processes operate is much larger than the three-year time scale over which this study was conducted.

The primary objective of this study is to examine the spatial and temporal controls on the variability of coarse sediment transport in a bedrock channel. To address this objective, I structure data analysis and interpretation around testing three hypotheses: (1) Transport distance correlates with grain size. This hypothesis reflects the results of bedload transport studies in alluvial channels, many of which demonstrate a correlation between grain size and transport distance. I tested whether this hypothesis adequately summarizes observed movement of marked tracer clasts during summer low flows, annual peak flows and cumulatively over three years of study in a bedrock channel. (2) Differences in distance of coarse sediment transport exist between study reaches and can be explained in relation to inter-reach differences in hydraulics and channel geometry. This hypothesis is designed to test the idea that, if transport distance is not a simple function of grain size, then observed differences in the distances which clasts move can be explained by other factors that govern transport and deposition. (3) Transport distance varies with spatial resolution and the local-scale variability in channel bed topography

has the strongest correlation with coarse sediment transport distance. This hypothesis is designed to test the relative strength of correlations between potential control variables and clast transport distance over three different spatial scales within each study reach. It is also designed to examine how the interpretation of processes influencing coarse sediment transport differs as a result of examining these processes at varying spatial scales. I use the term coarse sediment transport rather than bedload transport because the nature of this study precludes determination of the mode of transport.

4.2. Study Area

The study area is located in the Ocoee River gorge, Tennessee between the Tennessee Valley Authority (TVA) Ocoee No. 3 dam and the 1996 Olympic whitewater course (Figure 4.1). The Ocoee here flows through the Blue Ridge Province of the Southern Appalachians, with a drainage area of approximately 1300 km². Although the channel flows through a deeply incised gorge with steep valley walls, hillslopes exhibit limited bedrock exposure and are densely vegetated and mantled with thick soils typical of humid temperate landscapes. Homogenous denudation rates (25± 5 m/m.y.) over 10⁴ – 10⁵ year time scales (Matmon et al., 2005) characterize this tectonically quiescent region. Bedrock in this region consists of metasedimentary rocks (slates and metasandstones) contained within the Precambrian Ocoee Supergroup. Specifically, bedrock exposures through the Ocoee River gorge are: the Precambrian-age Sandsuck Formation in the western gorge, which is composed of phyllites thinly interbedded with arkosic and calcareous quartzites; the Dean Formation, composed of thinly bedded quartzites and phyllites; and the Hothouse Formation, composed of metagreywacke and mica schist in the eastern gorge (Sutton, 1997). Through the gorge the rock units alternate

between resistant ledges of metagreywacke and quartzite and softer phyllite sequences. As the channel in the study area meanders across folded metamorphic units, the orientation of flow relative to the dip and lithology of the bedrock varies.



Figure 4.1. Digital Orthophoto of the Ocoee River study area (USGS, 1997). Reach boundaries are indicated by the solid white lines. Note the downstream variation of rib orientation. The location of Reach 4 is indicated although it was not included in this study for reasons explained.

The bed topography consists of undulating rib-like bedrock forms that I refer to as bedrock ribs. These features are not unique to the Ocoee River, but occur in other streams throughout the Blue Ridge Province (Chapter 3) and have not received much attention in the literature. Similar structurally influenced features such as concave sculpted joint furrows and bedding plane furrows are described by Richardson and Carling (2005) in their comprehensive report on sculpted forms in bedrock channels. Bedrock ribs differ from these features as opposing topographic features; they are long, narrow portions of bedrock that protrude above the surrounding bed. Ribs are asymmetrical in cross section regardless of planform orientation, consistently oriented parallel to the metamorphic foliation in the rock, and occasionally follow dominant joints. The strike of the ribs varies as the trend of the sinuous channel changes downstream, which suggests that rib orientation is controlled by structural features in the underlying folded metasedimentary units. The occurrence of sculpted forms such as potholes and flutes along the boundaries of the ribs (e.g., along the upstream and downstream faces of transverse ribs, and in the troughs between longitudinal ribs) suggests that abrasion is the dominant mechanism of fluvial incision in this system. A detailed explanation of the rib features and the interactions between hydraulics and rock erodibility associated with these forms is outlined in Chapter 3.

These bedrock forms are associated with locally similar zones of coarse material deposits. Alluvial material in this system consists of sand- to boulder-sized sediment that occurs in discontinuous patches, in the intervening lows between ribs and within potholes. Isolated locations of this alluvial fill are armored by large cobbles and boulders. High concentrations of well sorted, gravel-sized material occur in the wake zones of the

bedrock ribs (**Error! Reference source not found.a**). The angularity of the material ranges from very well rounded particles within potholes to more sub angular particles across the channel bed. This difference in angularity appears to reflect not only the local hydraulic environment, but also the lithologic origin: phyllite produces more angular particles, whereas the metagreywacke corresponds to well-rounded particles.

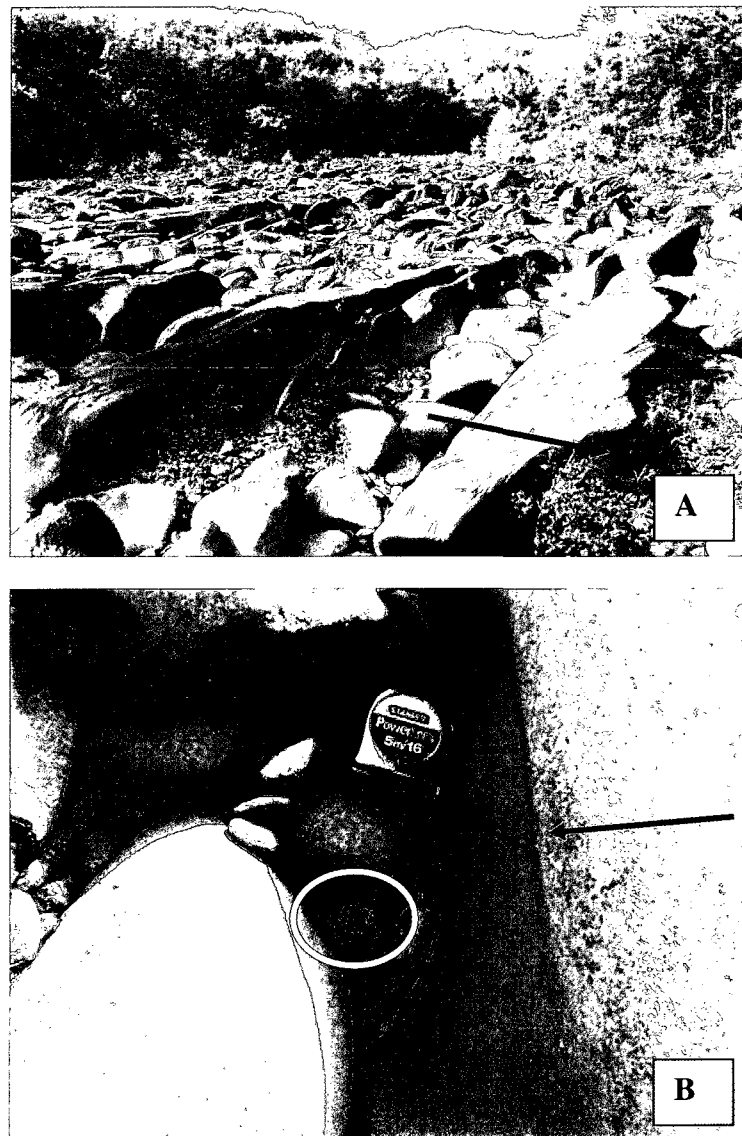


Figure 4.2. a) Photograph illustrating the coarse sediment deposition in between ribs in Reach 3. b) Tracer clast (circled) downstream of a bedrock rib in a local hydraulic environment classified as shielded. Tape measure for scale. Arrows indicate flow direction.

The upstream boundary of the study section is impounded by the Ocoee No. 3 dam, which is operated by the TVA. The reach extending 8-km downstream to the No. 3 power station was left completely dewatered after the closure of the Ocoee No. 3 dam in 1942. Only exceptional winter storm flows that exceed the hydropower capacity are routed through the natural channel. Since the 1996 Olympics, the TVA has guaranteed recreational flows of roughly 45 m³/s for six hours on both Saturday and Sunday from Memorial Day weekend through Labor Day weekend in the river section below the Ocoee No. 3 dam. Winter and spring storms produce flows for which the daily average releases from the dam range from 40 to 60 m³/s, and peak flows can reach 800 m³/s. Infrequent flow releases and dewatering of the channel under regulation by the TVA has led to woody vegetation establishment in many locations of the channel bed.

4.3. Methods

Four study reaches within the 4-km-long study area were selected according to the orientation to flow of the bedrock ribs: longitudinal; transverse; and oblique. The length of each surveyed reach was controlled by the persistence of the rib morphology. In other words, reaches continued for as long as the rib orientation and dominant lithology remained constant and the channel remained a straight, single flow channel. Tracer clasts were sampled in all but the downstream-most reach (Reach 4; Figure 4.1). This reach is frequented by recreational swimmers during the weekdays between summer releases. My initial installation of painted tracers in this reach failed within the first day, when I found

the tracers removed from the channel bed and placed in cairns on bedrock surfaces. Therefore, anthropogenic interference precluded experimental tracers in Reach 4.

Within the first three reaches (Figure 4.1), tracer clasts were selected from the bed material via a random walk. The high degree of spatial variation in bed topography and alluvial cover in the study area precluded following the procedure of tracer installation outlined by Wilcock (1997). In order to capture the spatial variability of depositional environments associated with the complex bed topography, tracers were selected from the channel bed via random walk. This random selection procedure allowed us to span the channel width several times and capture a representative distribution of particles. A few of the largest grains in each reach were visually identified and included in the sample so that in the instance of a very large flood, I would have well-constrained competence estimates. This transect method of sampling captured the wide range of depositional zones associated with the complex bedrock channel bed topography (i.e., grains were located up- and downstream of ribs, in the thalweg, or in pools).

The size, measured along the intermediate axis, and angularity were recorded for each tracer. I applied a roughly 5-cm square patch of yellow concrete paint to each clast, and wrote the tracer number on the paint patch with a black permanent marker. Care was taken not to disrupt the bed material when clasts were tagged with paint. If the tracer was not incorporated in the armor layer, a paint patch and number were applied to a second side to increase the likelihood of finding the tracer if it flipped over after transport. The initial survey of tracer locations was followed by six repeat surveys for each reach after four summer recreational flow releases ($Q_{\text{peak}} = 46.75 \text{ m}^3/\text{s}$) and two yearly flows (Q_{peak}

= 80.68 m³/s and 87.87 m³/s). Discharge records were obtained from the TVA and included hourly flow data for the three years of this study (Figure 4.3).

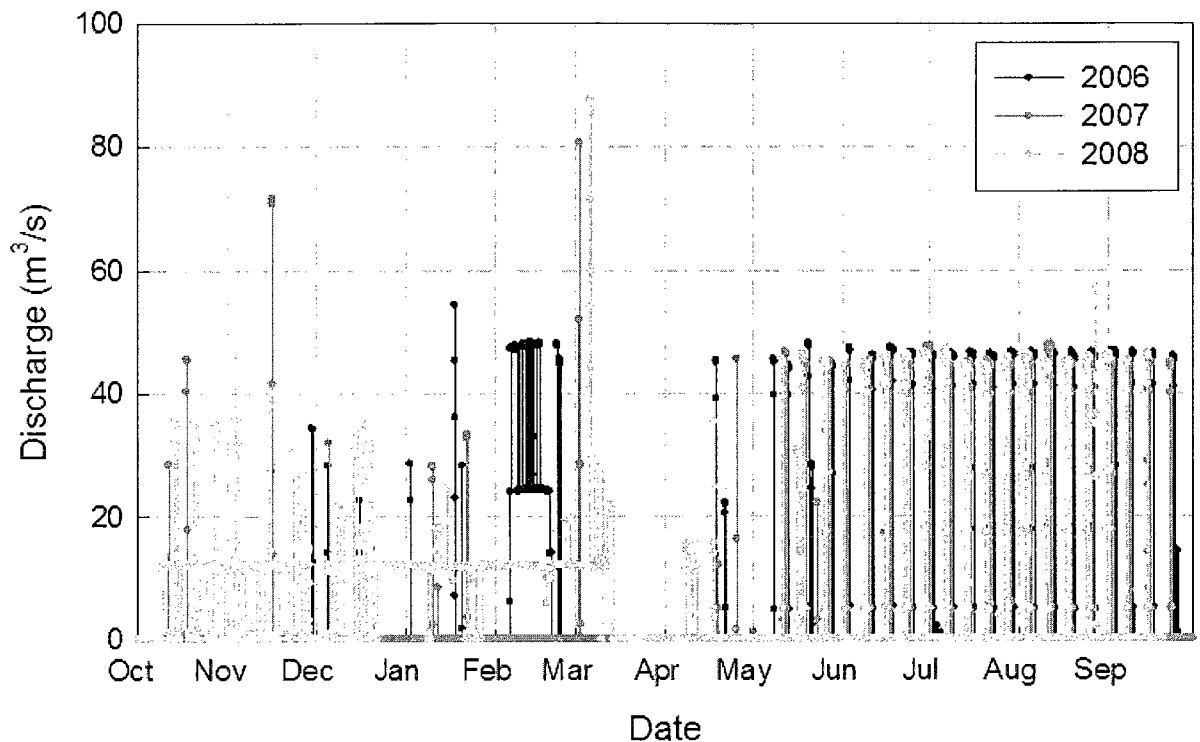


Figure 4.3. Annual hydrograph for Ocoee No. 3 for three years of study. Note the systematic fluctuations in summer recreational release flows. Hourly data obtained from the TVA.

Tracers were considered mobile if the calculated transport distance between surveys was greater than the particle diameter. This accommodated for any error inherent to repeat surveys. Instrument locations were consistently reoccupied so that the back-sight error to the benchmark was less than 5 mm in distance and elevation. Because each clast was tagged with a 5-cm square of paint, I was confident that repeat surveys represented the same location on each clast every survey. Transport distances were calculated by differencing the surveyed coordinates between re-surveys. Following

Church and Hassan (1992), the grain size of the tracer clasts was divided by the median size of the sediment mobilized in a given flow. They adjusted the grain sizes by the characteristic size of the bed material based on the expectation that the transport distance of the tracers is influenced by its size relative to the median grain size of the bed material. Although I recognize that many other variables in bedrock systems influence transport, as is assessed in this study, I applied a similar standardization method to report results in a format similar to other studies.

The overall structure of the data included six repeat surveys to examine the temporal variability in coarse sediment transport and four spatial resolutions (1 inter-reach, 3 intra-reach). Scales of intra-reach comparisons were: cross-sectional (cross section morphology and average hydraulics), zonal (morphologic bed region), and local (grain-scale topography). Tracers were referenced to the nearest cross-section after each re-survey. Each reach included between 9 and 10 cross sections at a spacing of roughly 10- to 15-m downstream. Tracers were located in the upstream section of all reaches. Cross-sectional averaged hydraulics were determined from HEC-RAS one-dimensional modeling (Chapter 3). Each peak discharge that occurred between tracer resurveys was modeled in HEC-RAS using the Manning's roughness coefficients determined in the earlier study. Without known water-surface elevations at the upstream and downstream reach boundaries for these peak flows, the downstream boundary condition was set to critical flow. Accuracy in assuming critical flow conditions has been supported in other studies of bedrock channels (Tinkler, 1997; Wohl and Ikeda, 1997). Although supercritical flow likely occurs locally within each reach, model runs were performed assuming subcritical flow and typical step-backwater calculations were performed. The

substantial protrusion of the bedrock ribs from the channel bed, which exerts a downstream hydraulic control, and the relatively shallow bed slopes, support this assumption of subcritical flow. The hydraulic variables obtained from this modeling for both cross section and reach-averaged scale analysis included: velocity, v , total boundary shear stress, τ , and unit stream power, ω .

The bed within each reach was divided into zones of contiguous and internally consistent morphology (e.g., zone of alluvial patch with limited rib exposure versus zone with highly variable rib topography and substantial bedrock exposure). These zones were visually delineated in the field and each reach was divided into between 4 and 6 different zones. These areas were assigned in the field and each tracer was categorized into a given zone after plotting the tracer locations and morphological zones. Morphological zones covered bed areas of roughly 20 x 50 m. All survey points were used to calculate the standard deviation of the bed elevation with a given zone. These values provided a quantitative metric for comparing the meso-scale variability in morphology and corresponding hydraulics. In addition, orthogonal transect surveys of bedrock ribs in each morphological zone were used to calculate the mean amplitude of bedrock ribs. Because protrusion of these ribs likely influences the local-scale hydraulics and may interfere in downstream transport of bedload, the amplitude of ribs within each region was used as a quantitative metric for the analysis at this intermediate spatial scale.

The local, grain-scale for each tracer was visually characterized during each re-survey. The area within one grain diameter was visually assessed for its potential influence on the transport of a given tracer (Figure 4.2b). These categorical variables included: free (no surrounding particles or ribs protruded above the tracer), shielded

(surrounding particles or ribs protruded above the tracer and appeared to alter the local hydraulic environment of the tracer), imbricated, buried (required removing sediment in order to recover the tracer), embedded in the armor layer, and/or within a pothole.

4.4. Results

The summary statistics for the tracer transport determined after each recovery are presented in Table 4.1. The recovery rate was nearly 100% in all three reaches during the recoveries between summer flows in the first year (2006). The recovery rate was lowest in the last resurvey (2008), but remained above 60% in all three reaches (61%, 63%, and 70%, respectively).

Table 4.1. Summary of transport distances and tracer sizes transported

Year	Q_{peak} (m)	L_{mean} (m)	St Dev	L_{50} (m)	LD_{50} (m)	$D_{50\text{mobile}}$ (mm)	L_{max} (m)	$D_{L\text{max}}$ (mm)	n_{mobile}	Recovered %
2006 (1)	47.5	0.38	0.54	0.16	0.40	70	2.42	50	81	99.6
2006 (2)	46.5	0.27	0.64	0.13	0.23	60	6.36	110	166	99.2
2006 (3)	47.5	0.16	0.17	0.10	0.10	50	1.22	75	129	99.2
2006 (4)	46.4	0.22	0.37	0.13	0.58	55	3.69	55	110	99.0
2006 (mean)	47.0	0.30	0.43	0.10	0.328	59	3.40	73	122	99.2
2007	80.7	3.49	4.66	1.84	2.69	80	26.97	50	142	77.0
2008	88.9	4.70	5.85	2.62	4.21	75	28.92	45	68	61.0
Cumulative	4.19	1.619	6.55	4.65	266	75	40.27	35	266	
2006 (1)	47.5	0.20	0.20	0.13	0.23	60	1.10	65	117	99.7
2006 (2)	46.5	0.27	0.90	0.11	0.18	55	8.03	20	86	99.7
2006 (3)	47.5	0.20	0.37	0.10	0.08	45	2.73	65	73	99.7
2006 (4)	46.4	0.16	0.24	0.09	0.14	85	1.26	25	94	99.3
2006 (mean)	47.0	0.20	0.43	0.10	0.156	61	3.30	44	93	99.6
2007	80.7	0.87	1.36	0.29	0.81	70	7.35	25	112	82.7
2008	88.9	2.82	6.02	0.69	2.45	70	25.53	105	55	62.5
Cumulative	2.52	3.89	2.52	1.26	2.52	80	28.52	20	232	
2006 (1)	47.5	0.45	0.65	0.20	0.38	55	4.02	90	127	99.7
2006 (2)	46.5	0.35	0.64	0.14	0.32	50	5.19	85	105	99.7
2006 (3)	47.5	0.34	0.49	0.20	0.28	75	4.19	20	179	99.7
2006 (4)	46.4	0.36	0.39	0.21	0.40	70	3.09	50	168	99.7
2006 (mean)	47.0	0.40	0.54	0.20	0.34	63	4.10	61	145	99.6
2007	80.7	1.15	1.84	0.53	0.36	80	11.86	30	130	73.3
2008	88.9	1.90	2.62	0.96	2.55	80	13.96	30	69	70.0
Cumulative	2.29	3.08	1.10	1.10	1.83	90	27.05	30	227	

The results are presented in a progression of the three key hypotheses. In natural systems the spatial and temporal components to the dynamics of any process are highly intertwined. To separate these two components, the results are outlined in a progression of decreasing spatial scale as the first tier of analysis. The temporal variability (i.e., variation in discharge magnitude and duration) is examined within each spatial scale.

The size distributions of tracers from each reach are relatively consistent (**Error! Reference source not found., Error! Reference source not found.**), with median sizes D_{50} of 115 mm, 100 mm, and 110 mm, respectively. This consistency allows inter-reach comparisons of transport dynamics without differences in the bed material size distribution as a confounding effect that needs to be adjusted for. Nonetheless, a modified version of the scaling convention applied by Church and Hassan (1992) is used so that variables are reported in nondimensional terms, which both tightens the comparison of transport dynamics at different spatial and temporal scales and enhances the potential to compare these results to other field studies or apply relationships to other experimental and theoretical studies. The absolute transport distances are used in comparison between reaches because standardizing these distances by a reach-dependent variable would limit the ability to detect variability among reaches. Examination of transport at smaller scales in each reach used the nondimensional transport distance to isolate comparisons as a function of scale.

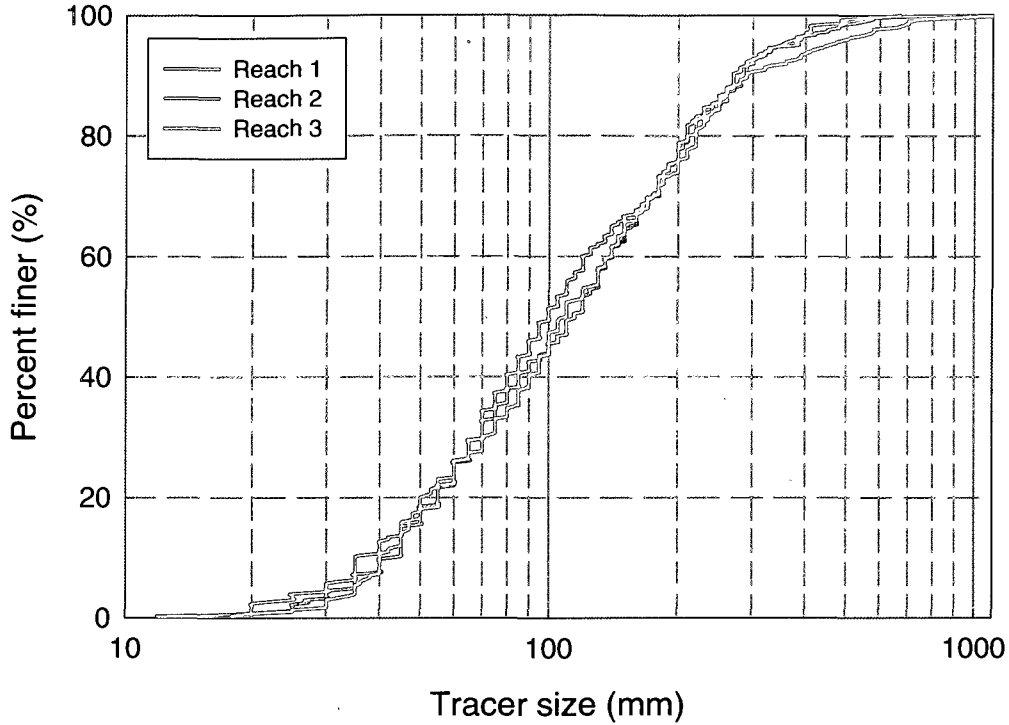


Figure 4.4. Size distribution of tracer clasts sampled from the existing bed material in each reach

Table 4.2. Summary of reach differences including percent cover

	Reach 1	Reach 2	Reach 3	Reach 4
Rib orientation to flow	Longitudinal	Longitudinal	Oblique	Transverse
Mean rib amplitude (m)	0.435	0.570	0.785	0.798
Reach gradient	0.0075	0.0082	0.0106	0.0198
Manning's n	0.059	0.075	0.094	0.107
D16 (mm)	50	46	48	na
D50 (mm)	115	100	150	na
D84 (mm)	240	230	252	na
	Percent cover by substrate type (%) [*]			
Bedrock	56.8	40.3	38.2	56.6
Boulders	23.7	23.5	23.7	20.0
Cobbles	10.6	21.0	20.0	11.7
Gravel	8.9	15.2	18.2	11.7

^{*}Percent cover was determined from surveyed grids of ~1 m spacing

Table 4.3. Hydraulic variables from HEC-RAS modeling of peak discharges in each reach between each recovery

Variable	Summer 2006: Mean of 4 Resurveys								
	Summer 2007 Resurvey			Summer 2008 Resurvey			Summer 2008 Resurvey		
	Reach 1	Reach 2	Reach 3	Reach 1	Reach 2	Reach 3	Reach 1	Reach 2	Reach 3
Q _{peak} (m ² /s)	46.75	46.75	46.75	80.68	80.68	80.68	87.87	87.87	87.87
Manning's n	0.06	0.08	0.09	0.06	0.08	0.09	0.06	0.08	0.09
Mean flow depth (m)	0.79	0.67	0.81	1.05	0.87	1.02	1.09	0.91	1.07
Width (m)	42.57	67.00	62.65	44.90	70.62	70.75	45.30	71.19	72.60
Velocity (m/s)	1.47	1.05	1.00	1.79	1.37	1.20	1.86	1.41	1.22
Total boundary shear stress (N/m ²)	87.05	74.98	107.88	114.85	123.00	140.26	123.28	128.78	146.48
Max Flow depth (m)	1.55	1.37	1.58	1.86	1.61	1.90	1.91	1.66	1.97
Width/Depth	54.07	99.38	77.32	42.85	81.01	69.51	41.52	77.87	68.06
Friction Slope (m/m)	0.0093	0.0105	0.0120	0.0095	0.0129	0.0130	0.0097	0.0130	0.0134
Unit Stream Power (W/m ²)	99.72	71.87	88.13	168.29	144.57	145.54	183.65	156.87	159.62

4.4.1. Transport distance and tracer size (H1)

There is no clearly defined relationship between tracer size and transport distance (Figure 4.5), which does not support the first hypothesis. The average transport distances, mobile tracer sizes, and hydraulic data from the four summer flow periods in 2006 were used in all analyses of 2006 flows. Data from these summer tracer recoveries corresponded to the smallest magnitude and duration flows (Table 4.2; Figure 4.3), and showed no relationship between transport distance and particle size in all reaches. The cloud of data indicates a large amount of variability unexplained by this simple relationship. After the winter flows during the next two years, the relationship improves slightly (2007), but the lack of a correlation between particle size and transport distance is maintained (Figure 4.5c). Examining this relationship integrated over the three-year period and increasing the temporal scale, variability in transport distance remains unexplained by differences in tracer size (Figure 4.5d).

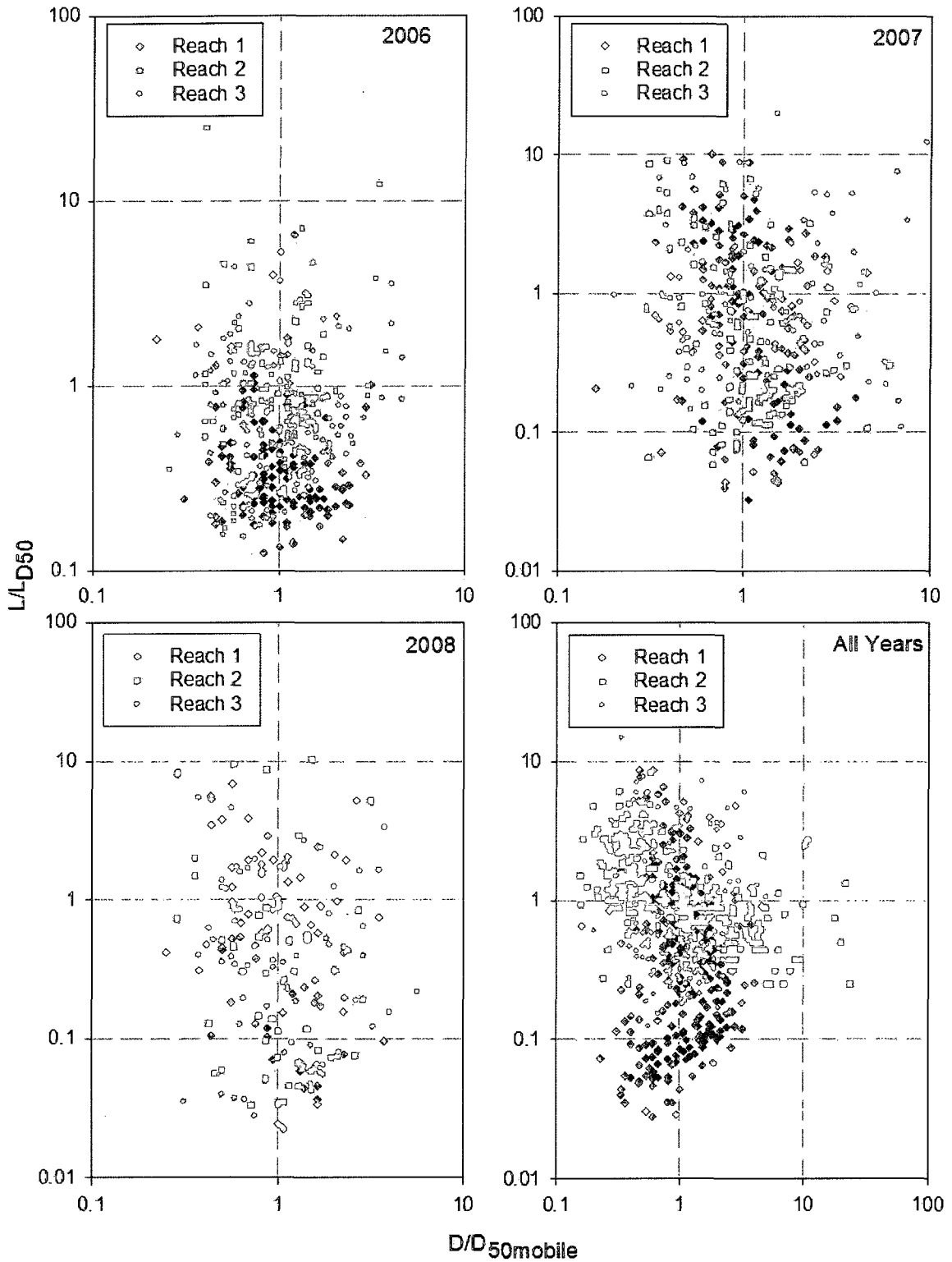


Figure 4.5. Transport distance (normalized by the transport distance of the $D_{50\text{ mobile}}$ tracer for that flow period) versus the tracer size (standardized by the $D_{50\text{ mobile}}$). a) Averages for all four resurveys during summer release flows. b) 2007, c) 2008, d) Total transport over entire study period.

4.4.2. Inter-reach variability in transport distance (H2)

The size distributions of tracers mobilized during the entire study period in all three reaches are fairly consistent (Figure 4.6). After all re-surveys the $D_{50\text{mobile}}$ in each reach did not vary greatly, but the transport distance of that size tracer varied among reaches (Table 4.3). For example, in the 2008 re-survey after the year of the largest peak flow (87.87 m³/s) and the longest duration of flows (Figure 4.3), the mean transport distance of the $D_{50\text{mobile}}$ in Reach 1 was roughly two times the distance in Reaches 2 and 3 (4.65 m, 2.52 m and 2.55, respectively for $D_{50\text{mobile}} = 75\text{mm}$, 70mm and 80 mm, respectively).

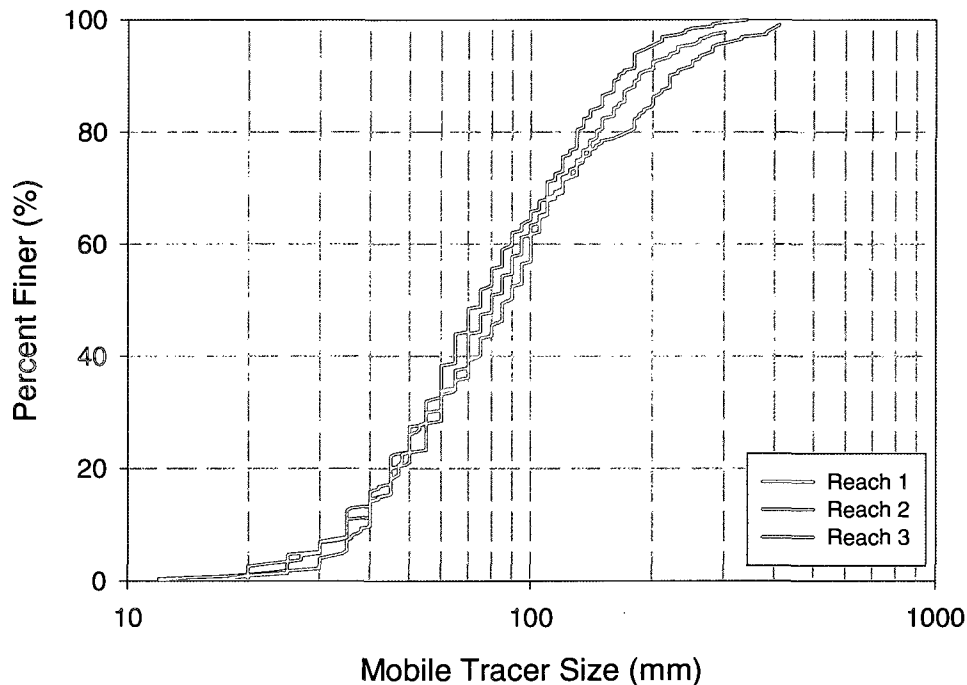


Figure 4.6. Size distribution of mobile tracers from each reach. Data include tracers that showed transport distances greater than one particle diameter in at least one re-survey period.

Comparison of the cumulative distributions of transport distance for all six recoveries and three reaches (Figure 4.7) indicates that more tracers were transported longer distances in Reach 1. More tracers were transported shorter distances in Reach 3, whereas Reach 2 yielded an intermediate distribution of transport distances. Figure 4.7 also illustrates that in all reaches, more tracers were transported longer distances during the 2008 flows of greater duration and higher peak discharge than any other flow period. According to the Tukey HSD multiple comparison tests on the log-transformed mean transport distance between reaches, Reach 1 was consistently associated with significantly greater transport distances than the other two reaches (Figure 4.8). Transport distances in Reach 2 and 3 were statistically similar after 2007, 2008 and the full study period, but different during the summer flows documented in the 2006 resurveys.

The sediment sizes and transport distances integrated over the entire three-year study period are presented in Table 4.2. The median grain size mobilized over all six recovery periods varied slightly between the three reaches (75 mm, 80 mm and 90 mm, respectively). Although reach 1 had the greatest D_{50} of the tracers, it had the smallest $D_{50\text{mobile}}$ over the entire study. Reach-averaged hydraulic data from HEC-RAS modeling of all peak flows are presented in Table 4.3. These modeling results indicated that the reach-averaged velocities and unit stream power in Reach 1 were the largest, which should lead to transport of larger bed material. However, the trends in total boundary shear stress in each reach are consistent with the $D_{50\text{mobile}}$ in each reach (i.e., Reach 3 was associated with the largest $D_{50\text{mobile}}$, as well as the greatest total boundary shear stress). I state these trends in reach-averaged sediment transport while recognizing the limited sample for rigorous statistical analyses in these trends. Also, despite this slight trend, the

sediment sizes are not substantially different. Even with these caveats, the consistent and statistically significant reach-scale differences in coarse sediment transport distances support hypothesis 2.

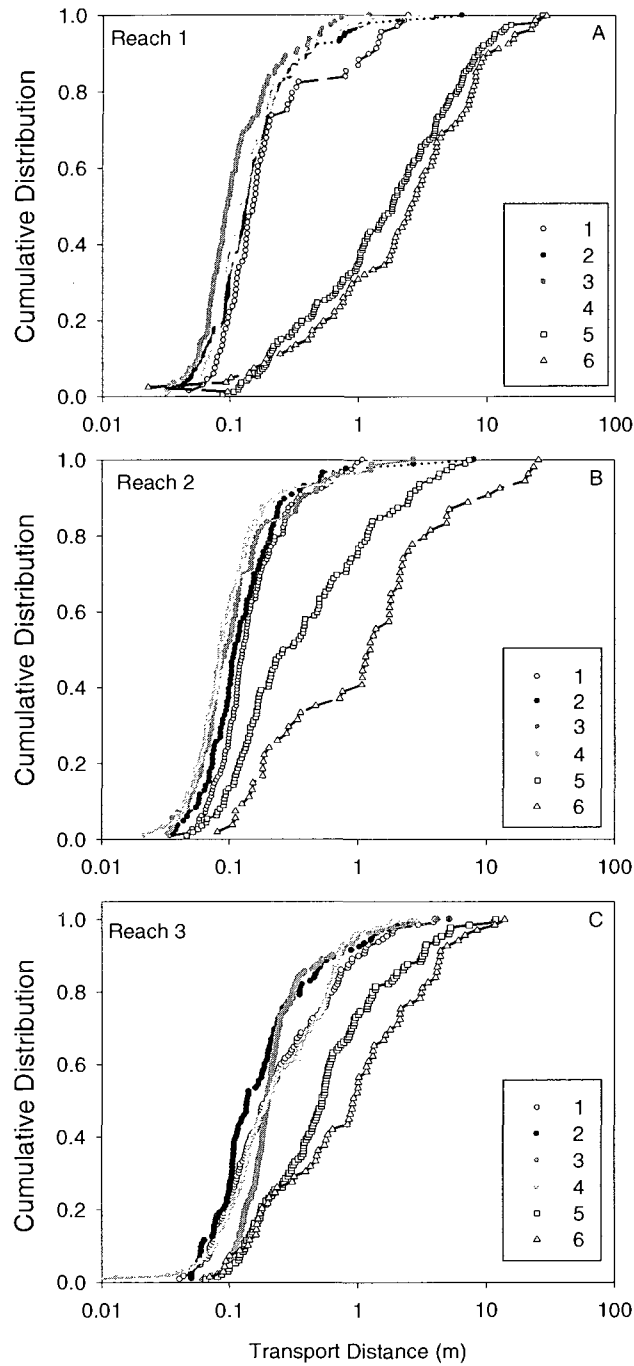


Figure 4.7. Cumulative distributions of transport distances after six re-surveys for all three reaches (a, b and c, respectively). Numbers indicate the recovery stage. Corresponding flows are reported in Table 4.2.

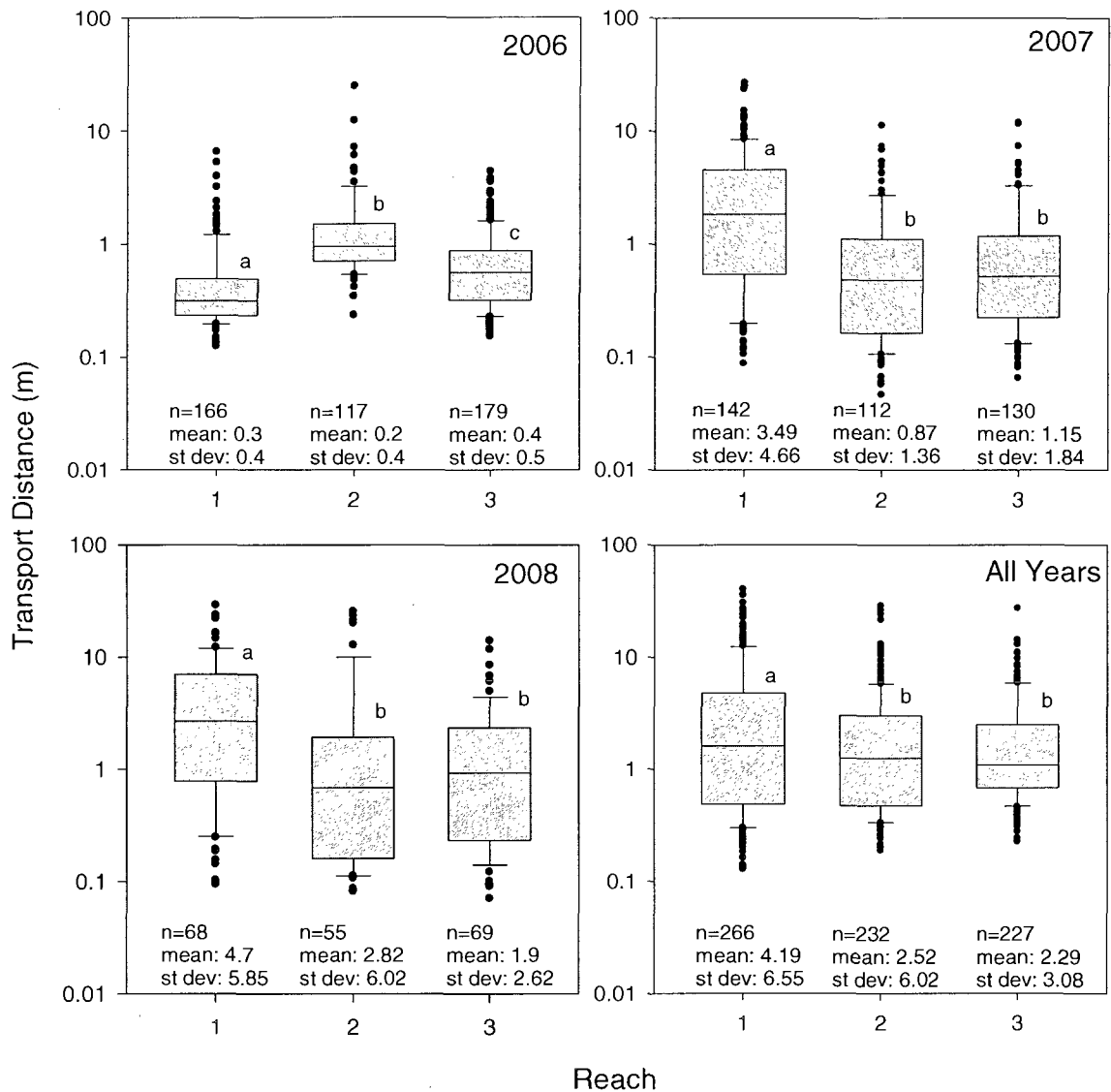


Figure 4.8. Reach-scale variation in transport distances. Years indicate the re-survey period. The box-plots indicate upper and lower quartiles as box ends, 10th and 90th percentiles as whiskers, and median values as the line within each box. Dots indicate values outside the 10th and 90th percentiles. Transport distances were log transformed for normality. Significant differences are indicated by contrasting letters above each box (Tukey's HSD following ANOVA on log transformed data).

4.4.3 *Intra-reach variability in transport distance (H3)*

Within each reach, transport distance was examined at three spatial scales: (1) cross sectional, with tracers linked to the nearest cross section and hydraulic parameters modeled for that cross section; (2) zonal scale, with tracers linked to geomorphically similar bed regions and analyzed in relation to both the standard deviation of bed elevations as well as mean amplitude of bedrock ribs within that zone; and (3) local scale, with tracers classified according to the local hydraulic environment.

ANOVA of transport distance by cross section was not significant in either the 2007 or 2008 recovery period in any of the reaches (Table 4.4). Figure 4.9 illustrates these results from Reach 1 as an example. That transport distances were similar among cross sections, suggests that transport distance does not vary with differences in cross-sectionally averaged hydraulics. In Reach 1, despite a nearly two fold difference in unit stream power between two cross sections, mean transport distances were not significantly different (Figure 4.9).

Table 4.3. Summary of ANOVA analysis of transport distance by intra-reach spatial scale

2007						
	XS		ZONE		LOCAL	
	F value	p-value	F value	p-value	F value	p-value
Reach 1	1.77	0.14	3.46	0.005	19.2	<0.0001
Reach 2	0.52	0.47	0.76	0.47	8.9	<0.0001
Reach 3	1.44	0.23	3.79	0.006	36.1	<0.0001

2008						
	XS		ZONE		LOCAL	
	F value	p-value	F value	p-value	F value	p-value
Reach 1	1.15	0.34	1.56	0.19	26.3	<0.0001
Reach 2	0.22	0.64	0.93	0.40	19.3	<0.0001
Reach 3	0.48	0.70	1.59	0.21	6.8	<0.0001

*Bolded values indicate significance (p<0.05).

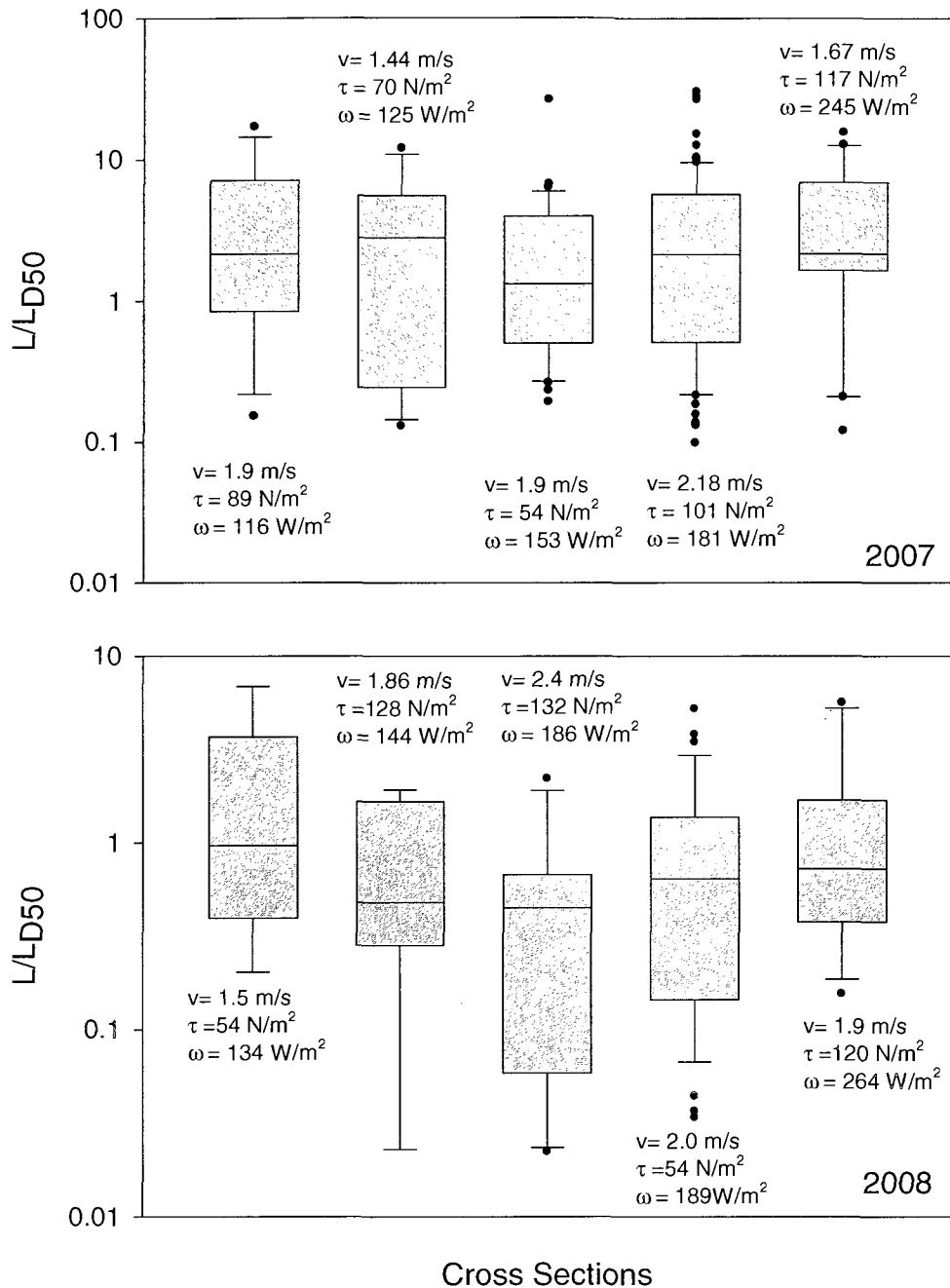


Figure 4.9. Box plot comparing the transport distance of tracers by cross section hydraulics in Reach 1. a) Transport distance (2007) by cross section (ANOVA, $F=1.77$, $p=0.14$). b) Transport distance (2008) by cross section (ANOVA, $F=1.15$; $p=0.34$), so comparison of means was not appropriate. The box-plots indicate upper and lower quartiles as box ends, 10th and 90th percentiles as whiskers, and median values as the line within each box. Dots indicate values outside the 10th and 90th percentiles. The velocity, v , total boundary shear stress, t , and unit stream power, w , obtained from HEC-RAS modeling of the peak discharge between recoveries are indicated for each cross section.

Variability in transport distance is enhanced at the scale of morphologically similar bed zones within a given reach (Figure 4.10). For the 2007 tracer recovery, the significant ANOVA results indicate zone-scale differences in transport distance in Reaches 1 and 3 (Table 4.4). This relationship was not significant in Reach 2, or in any reach for the 2008 recovery. Transport distances do not appear larger in bed regions where the rib amplitude A and standard deviation of the bed topography Z_{stdev} are relatively low, as one would expect. Also, in Reach 3, pairwise comparisons indicated that the only zones with significantly different mean transport distances had similar mean rib amplitudes ($A= 0.65$ m and 0.69 m, respectively) and standard deviations of the bed elevation ($Z_{stdev} = 0.33$ m and 0.36 m, respectively) within each zone. Therefore, neither rib amplitude nor topographic variability appear to control transport distance.

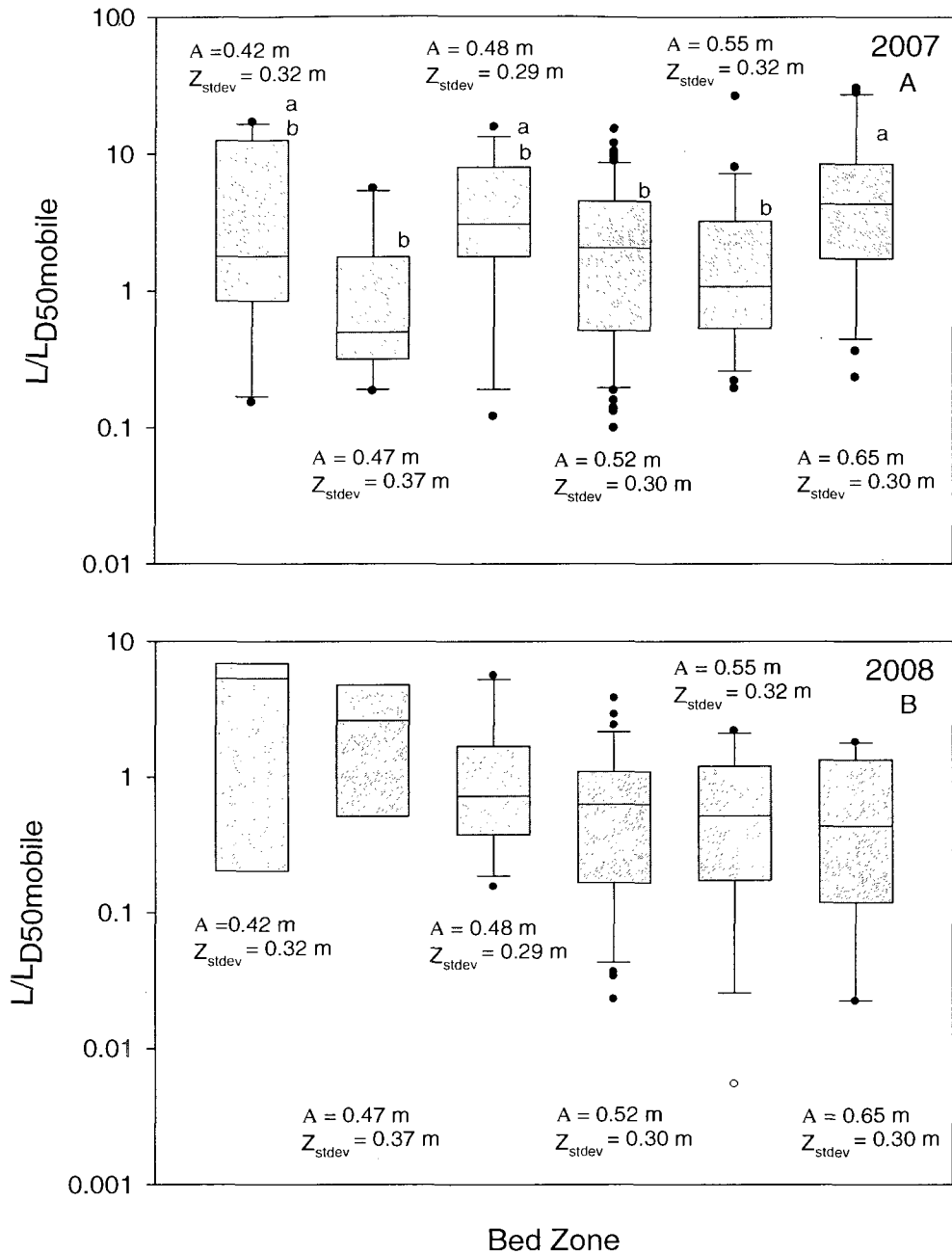


Figure 4.10. Box plot comparing tracer transport distance by zone topographic metrics in Reach 1. a) Transport distance (2007) by zone (ANOVA, $F=3.46$, $p=0.005$). Significant pairwise differences in means ($p < 0.05$) are indicated by contrasting letters above each box (Tukey's HSD following ANOVA on log transformed data). b. Transport distance (2008) by zone was not significant (ANOVA, $F=1.56$; $p=0.19$), so comparison of means was not appropriate. The box-plots indicate upper and lower quartiles as box ends, 10th and 90th percentiles as whiskers, and median values as the line within each box. Dots indicate values outside the 10th and 90th percentiles. Z_{stdev} is the standard deviation of the bed elevation within the bed zone, and A is the mean amplitude of bedrock ribs within that area. Boxes are in order of increasing A from left to right.

In all three reaches and for both recovery periods, there was a strong relationship between transport distance and the local hydraulic environment descriptor (Table 4.4). In reach 1 for example, particles that were unaffected by surrounding grains or bedrock ribs (*free*) were transported the greatest distances (Figure 4.11). In some cases, shielded particles were transported relatively long distances, which could be explained by local turbulence fluctuations in wake zones. Pairwise comparisons using the Tukey HSD following ANOVA, in all three reaches and for both years, consistently showed that the transport distance of tracers classified as *free* was significantly different ($p < 0.05$) from imbricated, shielded or buried particles. The significant difference in transport distance according to local-scale distinctions provides support for hypothesis 3, but this is more rigorously tested through multiple regression analysis.

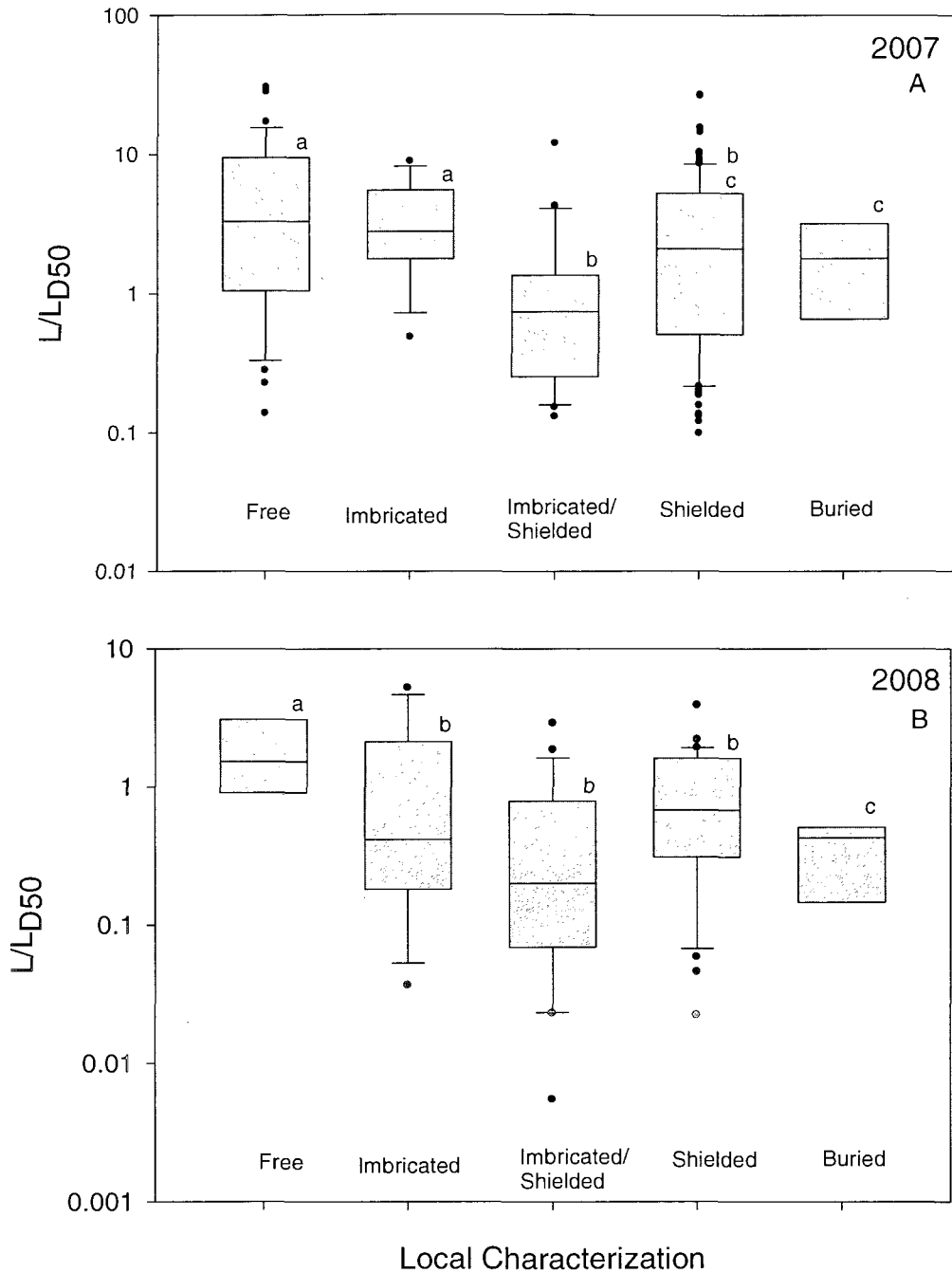


Figure 4.11. Box plot comparing tracer transport distance by local hydraulic environment classification in Reach 1. a) Transport distance (2007) by local classification (ANOVA, $F=19.17$, $p<0.0001$). b) Transport distance (2008) by local classification (ANOVA, $F=26.26$; $p<0.0001$). Significant pairwise differences in means ($p<0.05$) are indicated by contrasting letters above each box (Tukey's HSD following ANOVA on log transformed data). The box-plots indicate upper and lower quartiles as box ends, 10th and 90th percentiles as whiskers, and median values as the line within each box. Dots indicate values outside the 10th and 90th percentiles.

Multiple linear regression was applied to both inter-reach and intra-reach scale variables. Model selection based on the AIC and adjusted R^2 indicated that of the three intra-reach scales, the local classification explained the greatest variability in transport distance, thereby further supporting hypothesis 3. The parameters tested in these models included: tracer size, reach, cross section unit stream power, mean rib amplitude within the bed zone and local characterization. These model results were consistent for 2007 and 2008 analyzed separately. The best one-parameter model included only local scale classification ($p < 0.0001$ in both years; adjusted $R^2 = 0.45$ and 0.20 for 2007 and 2008, respectively). The best two-parameter model included the reach and local scale ($p < 0.0001$ in both years; adjusted $R^2 = 0.48$ and 0.32 for 2007 and 2008, respectively). Both parameters in these models were also significant at $p < 0.0001$. Although none of the models tested explained more than 50 % of the variability in transport distance, multiple linear regression was still a useful method to more rigorously address the question of which scale is the most appropriate for predicting coarse sediment transport in bedrock systems when grain size may not be as good a predictor as in alluvial systems. Also, the fact that only 50 % of the variability in transport distance could be explained by these models suggests a component of unexplained variability which supports the stochastic nature of sediment transport in these systems.

4.5. Discussion

4.5.1. *Controls on transport distance*

Transport distance was not dependent on tracer size as has been reported in alluvial studies (Church and Hassan, 1992). This suggests that in a bedrock channel with complex bed topography, other factors are more important in controlling coarse sediment transport. In order to examine these other possible controls, the second and third hypotheses tested for differences according to inter-reach (hypothesis 1) and intra-reach (hypothesis 2) spatial scales. The most consistent significant differences occurred between reaches and with local hydraulic environment. Reach-scale differences suggest that reach-scale variation in morphology and hydraulics are important controls on coarse sediment transport. Reaches in this study varied mostly in the orientation and amplitude of bedrock ribs, which influences hydraulics. The finest spatial resolution of intra-reach variability was the best predictor of coarse sediment transport distance. This suggests that the complex bed topography of bedrock channels controls bedload transport differences at scales potentially smaller than bedform scales of alluvial channels (Schmidt and Ginz, 1995; Thompson et al., 1996; Cudden and Hoey, 2003).

4.5.2. *Limitations and uncertainties*

There are several potential limitations to the study design discussed here that create uncertainties when extrapolating from the results described above. Although transport distance was not related to grain size in any of the reaches over the study period, it is possible that at longer time scales transport distance varies more closely with grain size because local-scale controls that influence transport distance during single

flows might become less important when averaged over longer timespans that include multiple transport events.

The D_{50} of the unrecovered tracers was similar to the D_{50} of the mobile tracers in the last resurvey. This suggests that unrecovered particles were transported, despite unknown transport distances. It is uncertain whether these particles were transported beyond the reach or moved to obscure locations within the highly variable alluvial deposits and bedrock channel bed topography (i.e., within potholes or between ribs). Although the recovery rates were relatively large between surveys, there are inherent difficulties in using visually identified tracers. It was necessary to re-paint and number most tracers each year because sun bleaching and algal growth obscured the tracer number. There were several cases in the 2007 and 2008 resurveys where the tracer number was indistinguishable. Re-numbering and measurement, along with spatial comparison to the previous year's location, allowed for these tracers to be accurately matched to the original number and included in the recovery.

Because bed regions were not determined prior to the sediment sampling, I did not sample an equal number of tracers from each region, making it difficult to accurately compare coarse sediment transport between bed regions. The initial overall intent of this tracer study was to examine reach-scale coarse sediment transport; it was after the initial tracer installation that I decided to assess the spatial controls on sediment transport at different scales. Alternatively, I could have installed an equal number of tracers of uniform size in morphologically similar patches to constrain the variability and correlate coarse sediment transport with bedrock channel bed topography, as others have done in alluvial channels (Wilcock, 1997). However, the main goal in selecting tracers from the

existing bed material was to ensure that the conditions were as natural as possible.

Studies that use imposed tracers tend to show higher transport rates and distances (Pyrce and Ashmore, 2003; Sear et al., 2000) because particles are not in natural locations such as incorporated into the armor layer.

During high flow conditions when the transport capacity is so high that the total shear stress is much greater than the critical shear stress, particle hop lengths increase more rapidly with increasing shear stress than particle impact velocities (Sklar and Dietrich, 1998; 2004). In this study I measured the total transport distance of particles or the path length (Einstein, 1937), which integrates all the lengths of individual saltation hops. I cannot determine the difference between particle path lengths and hop lengths. However, the observation that the transport distances in all three reaches were shortest for the weekly summer recoveries with lower magnitude and shorter duration discharges, suggests that the transport distances associated with the larger yearly flows were an integration of several saltation hop lengths.

The shorter transport distances recorded after the four summer weekend flows peaking at $40 \text{ m}^3/\text{s}$ may reflect the shorter temporal resolution, which facilitates documenting transport distances that may be closer to the hop length of single transport events. However, these flows were also half the magnitude of the yearly peak, after which larger transport distances were measured. It is not clear how the magnitude of individual flow peaks affects the integration of all flow events. Complexity in coarse sediment transport in this system is also demonstrated by some clasts being transported upstream. These few upstream transport events always occurred in sites of complex bed

topography and hydraulics. The local hydraulic environment set up by the bedrock rib forms likely plays a strong role in determining sediment transport dynamics.

Spatial variations in turbulence structure, and thereby sediment flux, which are not describable in terms of local bed shear stress, are likely to be of fundamental significance to almost all aspects of coarse sediment transport (Nelson et al., 1995; Papanicolaou et al., 2001). I consistently observed redistribution of gravel located in the lee of bedrock ribs. The gravel-sized tracers in this hydraulic environment showed measurable transport distances in each re-survey, but overall these particles typically remained within the same lee deposit. Tracer particles were commonly buried within these deposits and recovery required sorting through the deposit.

4.5.3. Consideration of dam effects on sediment supply and alluvial cover

There are a few reasons why well-developed alluvial patches occur in this bedrock system despite the location downstream from a dam. Greater bed roughness may lead to a higher likelihood of forming alluvial patches at lower sediment supply rates. Davis et al. (2005) documented similar results in a flume study examining the influence of channel bed topography on partial alluviation. To address this question further, I compared the degree of alluvial cover in the four reaches, which varied in channel slope and roughness of the bedrock channel bed topography. If the dam exerts a dominant effect on the coarse sediment supply, then alluvial cover should be lower in the upstream reaches. Reach 1 did show the least degree of alluviation, which would suggest that the dam had reduced the sediment supply in this system. However, Reach 1 also showed the lowest hydraulic roughness and rib amplitude (Table 4.1), as well as the largest reach-averaged velocity and unit stream power (Table 4.3). Because roughness has been shown

to control the degree of alluvial cover, as I describe further below, there are competing arguments for why this reach would show the lowest alluviation (roughness vs. downstream dam effects).

Another effect of the dam is the alterations to the flow regime. Ocoee No. 3 is unique because the channel downstream remains dry much of the time, with the exception of regularly scheduled summer recreational releases and large floods that cannot be stored in the upstream reservoir. The majority of the flow is diverted by the TVA to a power station 8 km downstream. The result is that without regularly occurring flows in this portion of the channel, and with continuing limited sediment input from lateral sources such as valley walls, banks, and tributaries, the sediment supply within the channel bed may have changed relatively little under the existing, severely limited regime of flow and sediment transport. In the absence of large, prolonged flows to transport sediment downstream of the dam, the typically documented downstream effects that dams have on sediment supply would be minimized in this system. Other investigators working in regulated rivers have also inferred that armoring, degradation, and morphologic change or textural response below dams can be negligible in cases of low sediment supply and transport rates (Fassnacht et al., 2003). For a given reduction in the sediment supply, if the flows are correspondingly reduced to produce no change in the ratio of supply to transport capacity, then it is not likely that changes in the alluvial cover downstream from the dam will occur.

4.5.4. Factors influencing alluvial cover in bedrock channels

Beyond the effects of the dam on sediment supply and transport, inter-reach variations in gradient might also influence the degree of alluvial cover. Reach gradient

increases downstream among the four study reaches examined here. Gradient, as a component of shear stress and stream power, can be used as an indirect measure of reach-averaged sediment transport when discharge does not vary between reaches. Therefore, assuming a relatively constant sediment supply in all four reaches, the fourth reach farthest downstream should display the lowest degree of alluviation because the relative transport capacity is greatest. Under this assumption, reach-averaged transport distances should also be positively correlated with gradient. Reach 4 did display the lowest percentage of alluvial cover (Table 4.1). Reach 1 (shallowest gradient) also had the lowest proportion of alluvial cover, however, and consistently had the largest coarse sediment transport distances. Less alluvial cover and greater sediment transport distances in Reach 1 could be explained by reach-averaged velocity and unit stream power being largest in this reach; these hydraulics appeared to be controlled by the relatively narrow channel width and high velocity associated with lower hydraulic roughness supplied by smaller, longitudinal ribs.

According to flume studies (Davis, et al., 2005; Finnegan et al., 2007; Johnson and Whipple, 2007; Chatanantavet and Parker, 2008), if the roughness of the channel bed topography is the dominant control on the degree of alluviation, then Reach 4, having the greatest variation in bed topography and the highest roughness values from the hydraulic modeling (Chapter 3), should show the largest proportion of alluvial cover. The fact that both Reach 1 (lowest roughness) and Reach 4 (highest roughness) showed the largest proportion of bedrock exposure (both with 57% bedrock exposed) (Table 4.1) suggests that factors other than bed roughness influence alluviation in the study area. The junction of a tributary channel between reaches 1 and 2 suggests that lower alluvial cover in reach

1 might represent primarily dam influences, whereas lower alluvial cover in reach 4 might reflect the influence of gradient, but I cannot rigorously test this interpretation.

Chatanantavet and Parker (2008) examined the relationship between sediment ratio, channel slope and proportion of bedrock exposure and found a rationale for two scenarios of alluviation. In steep bedrock channels with large immobile boulders, a negative linear relationship exists between the proportion of bedrock exposure and the sediment ratio (supply/capacity). On the other hand, where bedrock channels lack large boulders, there is a threshold value of the sediment ratio at which bedrock exposure decreases and the channel transitions from fully exposed to fully alluviated. The value of the sediment ratio at which this progressive alluviation occurs is dependent on slope. At higher slopes, the bedrock remains exposed for larger sediment ratios. In cases where progressive alluviation occurs, a positive feedback is set up between increasing hydraulic roughness of the channel bed and enhanced deposition. This decreased transport capacity then leads to continued deposition (Chatanantavet and Parker, 2008). In a similar but opposite scenario where bedrock exposure is maintained, a positive feedback exists to promote exposure: Greater bedrock exposure reduces the hydraulic roughness, which increases the transport capacity and leads to clearing the bedrock surface.

A major assumption of the experiments of Chatanantavet and Parker (2008) is that the hydraulic roughness associated with grain roughness and alluvial bedforms superimposed on a bedrock surface is greater than hydraulic resistance supplied by the bedrock. They clearly state that their experiments focus on plane-bed bedrock channel beds. Considering the two positive feedbacks that they used to summarize their experimental results in the context of the Ocoee and other streams in the Blue Ridge with

bedrock ribs, the same assumption regarding the relative hydraulic resistance associated with the alluvium versus bedrock cannot be made. In the reaches examined in this study, bedrock topography has larger dimensions than the alluvial material. The bedrock ribs have a lower relative submergence than even the D_{84} in most cases. The only patches of alluvium that exist in these streams occur in topographic lows between ribs and within sculpted features such as potholes. The Ocoee thus best fits Chatanantavet and Parker's (2008) first scenario, of large immobile obstacles to flow that promote a negative linear relation between bedrock exposure and sediment supply/capacity. Assuming that sediment supply is similar in the three reaches downstream from the tributary junction, the lack of any consistent trend in bedrock exposure with respect to either gradient or bedrock rib amplitude suggests that multiple processes govern alluviation. Complex interactions among the three potential controls of distance from the dam, gradient, and bed roughness on alluvial cover limit us from separating their relative importance between reaches.

This study is a snapshot in time and although many interesting questions arise, an understanding of the sediment transport regime and dynamics that have led to the exposed bedrock topography seen along the Ocoee is not explicitly developed. However, two other streams studied in this region not affected by a dam upstream showed similar topography. I did not measure sediment transport along these streams or bedrock exposure, because without regulation I did not have proper constraints on discharge. The experimental set up along the Ocoee River, using the dam to control the flows at which I documented sediment movement, provided the best control for testing questions related to bedload transport in this large and complicated fluvial system.

4.6. Conclusion

This study demonstrates that complex-bed topography in a bedrock channel exerts a major control on the transport dynamics of coarse material over at least relatively short temporal (circa 3 yr) and small spatial (10^2 m) scales. Complex bed topography in a bedrock channel appears to preclude size-dependent transport distance by creating extreme spatial variability in the magnitude of hydraulic forces that influence sediment entrainment and transport. A comparison of three reaches with different bedrock rib orientation and amplitude indicates that where ribs are longitudinal to flow and of lower amplitude transport is less obstructed, which leads to greater transport distances than in reaches where the ribs are oblique to flow and of larger amplitude. At the reach-scale, oblique or transverse ribs increase the reach-scale roughness and reduce reach-averaged velocity, which corresponds to lower transport distances. Because local scale bedrock channel morphology correlates most strongly with transport distance, it likely plays a dominant role in the transport of coarse sediment. Ribs of greater amplitude create more localized zones of low velocity to shield clasts from entrainment. The importance of local-scale controls and the lack of size dependence on coarse-sediment transport distance may limit the use of reach-scale sediment transport functions in bedrock channels with similar morphologic complexity.

References

- Beschta, R.L., (1987), Conceptual models of sediment transport in streams, in *Sediment transport in gravel-bed rivers*, edited by C.R. Thorne, J.C. Bathurst, and R.D. Hey, pp. 387-419, John Wiley and Sons, Chichester.
- Chatanantavet, P., G. Parker (2008), Experimental study of bedrock channel alleviation under varied sediment supply and hydraulic conditions, *Water Resour. Res.*, 44, W12446, doi:10.1029/2007WR006581.
- Church, M. and M.A. Hassan (1992), Size and distance of travel of unconstrained clasts on a streambed, *Water Resour. Res.*, 28(1), 299-303.
- Cudden, J.R. and T.B. Hoey (2003), The causes of bedload pulses in a gravel channel: the implications of bedload grain- size distributions, *Earth Surf. Proc. Landforms*, 28, 1411-1428.
- Davis, J. R., L. S. Sklar, G. I. Demeter, J. P. Johnson, and K. X. Whipple (2005), The influence of bed roughness on partial alluviation in an experimental bedrock channel, *Eos Trans. AGU*, 86(52), Fall Meet. Suppl., Abstract H53D-0508.
- Dietrich, W. E., J. W. Kirchner, H. Ikeda, and F. Iseya (1989), Sediment supply and the development of the coarse surface layer in gravel-bedded rivers, *Nature*, 340, 215– 217.
- Einstein, H. A. (1937), Bedload transport as a probability problem. Ph.D. Dissertation (English translation, in *Sedimentation, Water Resources Publications* edited by H.W. Shen, Appendix C, pp. 105, Fort Collins, CO.
- Einstein, H. A. (1950), The bed-load function for sediment transportation in open channel flows, *Tech. Bull.*, 1026, Soil Conserv. Serv., U.S. Dep. of Agric, Washington, D. C.
- Fassnacht, H., E.M. McClure, G.E. Grant, P.C. Klingman (2003), Downstream effects of the Pelton-Round Butte hydroelectric project on bedload transport, channel morphology, and channel-bed texture, Lower Deschutes River, Oregon, In: *A Peculiar River: Geology Geomorphology, and Hydrology of the Deschutes River, Oregon, Water Science and Application*, 7, edited by G. E. Grant and J.E. O'Connor, pp. 169-201, AGU, Washington, D. C.
- Finnegan, N. J., L. S. Sklar, and T. K. Fuller (2007), Interplay of sediment supply, river incision, and channel morphology revealed by the transient evolution of an experimental bedrock channel, *J. of Geophys. Res., Earth Surf.*, 112, F03S11, doi:10.1029/2006JF000569.
- Furbish, D.J. (1993), Flow structure in a boulder mountain stream with complex bed topography, *Water Resour. Res.*, 29(7), 2249-2263.

- Gomez, B. and M. Church (1989), An assessment of bed load sediment transport formulae for gravel bed rivers, *Water Resour. Res.*, 25(6), 1161-1186.
- Hancock G.S., Anderson R.S., and Whipple KX. 1998. Beyond power: bedrock river incision process and form. in *River Over Rock: Fluvial Processes in Bedrock Channels, Rivers Over Rock, Geophys. Monogr. Ser.*, 107, edited by K. Tinkler and E. E. Wohl, pp. 35-60, AGU, Washington, D. C.
- Hartshorn, K., N. Hovius, W.B. Dade, R.L. Slingerland (2002), Climate-driven bedrock incision in an active mountain belt. *Science* 297, 2036-2038.
- Hassan, M.A. and M. Church. (1992), The movement of individual grains on the streambed, in *Dynamics of gravel-bed rivers*, edited by P. Billi, R.D. Hey, C.R. Thorne and P. Tacconi, pp. 159-175, John Wiley and Sons, Chichester.
- Hassan, M. A., and M. Church (2001), Sensitivity of bed load transport in Harris Creek: Seasonal and spatial variation over a cobble-gravel bar, *Water Resour. Res.*, 37(3), 813– 825, doi:10.1029/2000WR900346.
- Hoey, T., (1992), Temporal variations in bedload transport rates and sediment storage in gravel-bed rivers, *Progress in Physical Geography*, 16, 319-338.
- Howard, A. D. (1994), A detachment-limited model of drainage basin evolution, *Water Resour. Res.*, 30, 2261– 2285.
- Johnson, J. P., and K. X. Whipple (2007), Feedbacks between erosion and sediment transport in experimental bedrock channels, *Earth Surf. Proc. Landforms*, 32, 1048–1062.
- Kirchner, J. W., W. E. Dietrich, F. Iseya, and H. Ikeda (1990), The variability of critical shear stress, friction angle, and grain protrusion in waterworked sediments, *Sedimentology*, 37, 647– 672.
- Lague, D., N. Hovius, and P. Davy (2005), Discharge, discharge variability, and the bedrock channel profile, *J. of Geophys. Res., Earth Surf.*, 110, F04006, doi:10.1029/2004JF000259.
- Lamb, M. P., W. E. Dietrich, and L. S. Sklar (2008), A model for fluvial bedrock incision by impacting suspended and bedload sediment, *J. of Geophys. Res., Earth Surf.*, 113, F03025, doi:10.1029/2007JF000915.
- Matmon, A., P.R., Bierman, J. Larsen, S. Southworth, M. Pavich, M. Caffee, (2005), Temporally and spatially uniform rates of erosion in the southern Appalachian Great Smoky Mountains, *Geology* 31, 155-158.

- McNamara, J.P. and C. Borden, (2004), Observations on the movement of coarse gravel using implanted motion-sensing radio transmitters, *Hydrological Processes*, 18, 1871-1884.
- Nelson, J., Shreve, R. L., McLean, S. R., and Drake, T. G. (1995). "Role of near-bed turbulence structure in bed-load transport and bed-form mechanics." *Water Resour. Res.*, 31(8), 2071–2086.
- Papanicolaou, A.N., P. Diplas, C.L. Dancy, M. Balakrishnan, (2001), Surface roughness effects in near-bed turbulence: Implications to sediment entrainment, *J.l of Eng. Mechanics*, 127, 211-218.
- Pyrce, R.S. and P.E. Ashmore (2003a), Particle path length distributions in meandering gravel-bed streams: results from physical models, *Earth Surf. Proc. Landforms*, 28, 951-966.
- Pyrce, R.S. and P.E. Ashmore (2003b), The relation between particle path length distributions and channel morphology in gravel-bed streams: a synthesis, *Geomorphology*, 56, 167-187.
- Richardson, K., P.A. Carling (2005), A typology of sculpted forms in open bedrock channels. *GSA. Special Paper 392*. pp.108.
- Schmidt, K.-H. and D. Gintz (1995), Results of bedload tracer experiments in a mountain river, in *River geomorphology*, edited by E.J. Hickin, pp. 37-54, John Wiley and Sons, Chichester.
- Sear, D.A., M.W.E. Lee, R.J. Oakey, P.A. Carling, and M.B. Collins (2000), Coarse sediment tracing technology in littoral and fluvial environments: A review, in *Tracers in Geomorphology*, edited by I. D. L. Foster, pp. 21-55, John Wiley and Sons, Chichester.
- Shepherd RG, S.A. Schumm (1974), Experimental study of river incision. *Geological Society of America Bulletin* 85 257–268.
- Singh, A., K. Fienberg, D.J. Jerolmack, J. Marr, and E. Foufoula-Georgiou (2009), Experimental evidence for statistical scaling and intermittency in sediment transport rates, *J. of Geophys. Res., Earth Surf.*, 114, F010125.
- Sklar, L. S., and W. E. Dietrich (1998), River longitudinal profiles and bedrock incision models: Stream power and the influence of sediment supply, in *River Over Rock: Fluvial Processes in Bedrock Channels, Rivers Over Rock, Geophys. Monogr. Ser.*, 107, edited by K. Tinkler and E. E. Wohl, pp. 237–260, AGU, Washington, D. C.
- Sklar, L., and W. E. Dietrich (2001), Sediment and rock strength controls on river incision into bedrock, *Geology*, 29, 1087– 1090, doi:10.1130/00917613

- Sklar, L., and W. E. Dietrich (2004), A mechanistic model for river incision into bedrock by saltating bed load, *Water Resour. Res.*, 40, W06301, doi:10.1029/2003WR002496.
- Snyder, N. P., K. X. Whipple, G. E. Tucker, and D. J. Merritts (2003), Importance of a stochastic distribution of floods and erosion thresholds in the bedrock river incision problem, *J. of Geophys. Res., Earth Surf.*, 108(B2), 2117, doi:10.1029/2001JB001655.
- Sutton, S.J. (1991), Development of domainal slaty cleavage fabric at Ocoee Gorge, Tennessee. *J. of Geology* 99 (6) 789-800.
- Thompson, D.M. (2007), The influence of lee sediment behind large bed elements on bedload transport rates in supply-limited channels, *Geomorphology*, 99, 420-432.
- Thompson, D.M., E.E. Wohl, and R.D. Jarrett (1996), A revised velocity-reversal and sediment-sorting model for a high-gradient, pool-riffle stream, *Physical Geography*, 17, 142-156.
- Tucker, G.E. (2004), Drainage basin sensitivity to tectonic and climatic forcing: Implications of a stochastic model for the role of entrainment and erosion thresholds, *Earth Surf. Proc. Landforms*, 29, 185-205.
- Turowski, J. M. (2009), Stochastic modeling of the cover effect and bedrock erosion, *Water Resour. Res.*, 45, W03422, doi:10.1029/2008WR007262.
- Turowski, J. M., D. Lague, and N. Hovius (2007), Cover effect in bedrock abrasion: A new derivation and its implications for the modeling of bedrock channel morphology, *J. of Geophys. Res., Earth Surf.*, 112, F04006, doi:10.1029/2006JF000697.
- U.S. Geological Survey (1997), Digital orthophoto quarter-quadrangles, Menlo Park, CA.
- Wilcock, P.R. (1997), Entrainment, displacement and transport of tracer gravels, *Earth Surf. Proc. Landforms* 22, 1125-1138.
- Whipple K.X. (2004), Bedrock rivers and the geomorphology of active orogens. *Annual Review of Earth and Planetary Sciences* 32, 151–185.
- Whipple, K. X., and G. E. Tucker (2002), Implications of sediment-flux dependent river incision models for landscape evolution, *J. of Geophys. Res., Earth Surf.*, 107(B2), 2039, doi:10.1029/2000JB000044.
- Whiting, P.J., W.E. Dietrich, L.B. Leopold, T.G. Drake, and R.L. Shreve (1988), Bedload sheets in heterogeneous sediment, *Geology*, 16, 105-108, 1988.
- Wohl, E. E. (1993), Bedrock channel incision along Piccaninny Creek, Australia, *J. Geol.*, 101, 749– 761.

- Wohl, E.E. (1998), Bedrock channel morphology in relation to erosional processes, in *River Over Rock: Fluvial Processes in Bedrock Channels, Rivers Over Rock, Geophys. Monogr. Ser.*, 107, edited by K. Tinkler and E. E. Wohl, pp. 133-151, AGU, Washington, D. C.
- Wohl, E.E. (1999), Incised bedrock channels, in *Incised River Channels: Processes, Forms, Engineering and Management*, edited by S. Darby and A. Simon, pp. 187-218, John Wiley and Sons, Chichester.
- Wohl, E.E., H. Ikeda (1997), Experimental simulation of channel incision into a cohesive substrate at varying gradients. *Geology* 25, 295-298.
- Wohl, E. E., D. M. Thompson, and A. J. Miller (1999), Canyons with undulating walls, *Geol. Soc. Am. Bull.*, 111, 949– 959.
- Yager, E. M., J. W. Kirchner, and W. E. Dietrich (2007), Calculating bedload transport in steep boulder bed channels, *Water Resour. Res.*, 43, W07418, doi:10.1029/2006WR005432.

CHAPTER 5. SUBSTRATE INFLUENCES ON THE SIZE AND SPATIAL PATTERNS OF STREAM POTHOLES: A FIELD EXAMPLE

Abstract

Adjustment to bedrock-channel form largely occurs via either abrasion or plucking, with abrasion being the dominant mechanism of erosion in massive substrate. Localized abrasion occurs as sculpted forms; at this field site, primarily potholes. I measured the dimensions and surveyed the locations of potholes in four reaches along the Ocoee River, Tennessee in the Blue Ridge Province of the Southern Appalachians. The goal was to assess the inter- and intra-reach spatial occurrence of potholes in a bedrock channel with no defined thalweg and heterogeneous substrate of varying erosional resistance. Inter-reach differences in lithology and channel morphology lead to differences in both the size and spatial patterns of potholes. In reaches with more resistant rock and heterogeneous bed topography, pothole dimensions (i.e., radius and depth) are larger and follow an aggregated spatial pattern. The likelihood of pothole formation tends to be greatest at intermediate relative bed elevations, suggesting that local hydraulics and tools versus cover relationships govern pothole formation and maintenance. The relative abrasion of experimental concrete grinders supports the interpretation that local hydraulic environment, as reflected by bed elevation, tends to be more important than pothole dimensions in controlling the erosional efficiency of potholes.

5.1. Introduction

Potholes are often cited as the most efficient mechanism of bedrock abrasion in massive lithologies (Hancock et al., 1998; Whipple et al., 2000a), thereby providing locally effective means of channel incision (Gilbert, 1906; Alexander, 1932; Kale and Shingade, 1987; Wohl, 1993). In their flume study of the interactions between bedload transport and bedrock channel morphology, Johnson and Whipple (2007) noted pothole erosion 50 times greater than the flume-averaged incision within a single time increment. In an experimental flume study, Carter and Anderson (2006) observed that potholes formed readily in all model geometries when sediment was supplied.

Complex topography is the rule rather than the exception for sculpted bedrock features, making characterizing their geometry very difficult. Quantitative studies of pothole geometries have focused on the relationship between depth and radius, because these variables influence the hydraulics within individual potholes (Alexander, 1932; Angeby, 1951). The geometry of individual potholes has been linked to formative mechanisms and internal hydraulics using simple power functions between pothole depth and aperture size (Kale and Shingade, 1987; Springer et al., 2005, 2006).

Many of the initial investigations stressed the importance of bedload material within potholes as the tools of pothole abrasion (Gilbert, 1877; Alexander, 1932; Angeby, 1951). Kale and Shingade (1987) documented a good correlation between the grinder particle size and pothole dimensions. The vortex-induced sediment transport associated with potholes produces significantly larger erosion via bedload than suspended load (Sklar and Dietrich, 2001). Although many studies have recognized the importance of

pothole erosion as a mechanism of bedrock channel incision, few have quantitatively documented pothole spatial occurrence and erosional effectiveness in field settings.

The spatial distribution and size of potholes have been qualitatively linked to inner channels and slot canyons (Shepherd and Schumm, 1974; Wohl and Ikeda, 1997; Springer et al., 2006; Johnson and Whipple, 2007), knickpoints (Kale and Shingade, 1987) and to distance from the channel center (Lorenc et al., 1994; Kale and Shingade, 1987). In slot canyons within the Navajo Sandstone, coalescence of potholes has been argued as a mechanism of channel formation, and the hydraulic variability between merging potholes has been shown to influence the distribution of energy between the channel bed and canyon walls (Wohl et al., 1999; Johnson et al., 2005). Lateral potholes on bedrock channel walls have also been suggested as an efficient mechanism of adjusting bedrock channel width (Zen and Prestegard, 1994). In their study of potholes associated with a large knick point, Kale and Shingade (1987) noted a disparity in the number of potholes occurring on each bank, which they attributed to variation in relative elevation of each bank and the consequences for flood inundation. They also reported a larger frequency of isolated potholes than coalesced potholes. Coalesced potholes tended to be concentrated in the channel center, where they expected abrasion processes to be more intense and prolonged, although they did not consider cover effects in these deeper channel sections. Hartshorn et al. (2002) reported the greatest erosion rates within a parabolic-shaped channel at intermediate elevations, which they attributed to variation in the caliber and frequency of impacting sediment at different elevations.

Recent studies have focused on lateral incision and adjustment in bedrock channel width and cross sectional form as an additional degree of freedom for bedrock channel

change (Finnegan et al., 2005; Stark, 2006; Wobus et al., 2006; Turowski et al., 2008). In massive substrates where abrasion dominates channel erosion and geometric adjustment, the distribution of potholes across the channel is likely related to bedrock channel width adjustment. In flume experiments aimed to investigate the collective adjustment of bedrock channel slope, width, roughness, alluvial cover and incision rate, Finnegan et al. (2007) observed that channels adjust their width through alterations in the location of vertical incision. The location within the channel and the width of the localized incision zone are directly related to the balance between bedload supply and transport capacity. The spatial distribution and dimension of potholes may therefore provide insight into width adjustment in bedrock channels.

In bedrock channels such as the one examined in this study, where lithologic and structural variation strongly influence channel form and cross-sectional geometry is broad and shallow, the spatial distribution of potholes may not be localized to the channel thalweg or the bedrock walls. In cases such as this, there may be other influences on the spatial distribution of potholes; understanding the potential controls on pothole locations will enhance our ability to predict lateral and vertical incision as related to the lithologic and structural setting. Here, I present the first quantitative evaluation of spatial patterns of pothole occurrence in a bedrock channel with a high width-to-depth ratio and undulating bedrock rib bedforms that are largely controlled by rock properties, and lacking steep bedrock banks or walls.

We quantify parameters that are integral to understanding the importance of potholes in bedrock channel incision. The field site is divided into four study reaches differentiated based on lithology and structural expression of bedrock ribs in the channel

bed (Chapter 3). If rock characteristics influence the dominant mechanism of bedrock erosion (plucking versus abrasion), then potholes, as indicators of abrasion, will be less developed in more densely jointed lithologies that facilitate plucking. This assumes that plucking of material around potholes will limit pothole growth in these reaches. A reach dominated by a more massive lithology will favor the formation of larger potholes. Consequently, I hypothesize that, at the inter-reach scale, pothole dimensions (depth and radius) will be significantly different between the four study reaches (H1). If we assume that potholes form preferentially where more variable bed topography creates more complicated hydraulics that facilitate flow separation and localized abrasion, then potholes will follow a more aggregated pattern in reaches with the greatest topographic variability. The second hypothesis is thus that the spatial patterns of potholes will differ between the four reaches (H2). At the intra-reach scale, I hypothesize that potholes that follow an aggregated spatial pattern will be segregated according to dimensions (H3). This hypothesis is based on the assumption that larger potholes will form in regions of the channel with higher local velocities and associated stronger vorticity, greater bedload transport, and larger supply of grinders to potholes. In a channel with a well-defined thalweg, the largest potholes would be expected to form in the channel center, which receives the most flow over more prolonged durations. Lacking a well-defined thalweg, I expect potholes at the study sites to form where local channel configuration enhances abrasion. Finally, I hypothesize that the spatial occurrence of potholes is correlated to the bed elevation relative to some arbitrary water-surface elevation, which relates the pothole to the local hydraulics (H4). Because the channel lacks a well-defined thalweg, inner channel and steep channel walls, I assume that the relative elevation of potholes

compared to a spatially variable and complex channel bed topography is a better descriptor of the local hydraulic environment than distance from the channel margin.

In addition to testing these hypotheses regarding the spatial distribution and dimensions of potholes, I examine the relative efficiency of pothole abrasion by testing for correlations between the relative abrasion of experimental grinders and pothole dimensions. I also compare the relationships between pothole depth and radius in this study to the results of Springer et al. (2006). Potholes are defined following Richardson and Carling (2005) (p.14), as “essentially round (in plan view), deep depressions, which are, or can be expected to be, eroded by vortices with approximately vertical axes by mechanisms other than plucking.”

5.2. Study Area

This study was conducted along the Ocoee River gorge, Tennessee, which flows through the Blue Ridge Province of the Southern Appalachians, and drains an area of approximately 1300 km². Four study reaches were located between the Tennessee Valley Authority (TVA) Ocoee No. 3 dam and the 1996 Olympic whitewater course (Figure 5.1). The channel flows through a deeply incised gorge with steep valley walls, but hillslopes exhibit limited bedrock exposure and are densely vegetated and mantled with thick soils typical of humid temperate landscapes. This tectonically quiescent region has homogenous denudation rates (25± 5 m/m.y.) over 10⁴ – 10⁵ year time scales (Matmon et al., 2005). The regional lithology consists of metasedimentary rocks (slates and metasandstones) contained within the Precambrian Ocoee Supergroup. Specifically, bedrock exposures through the Ocoee River gorge are: the Precambrian-age Sandsuck

Formation in the western gorge, which is composed of phyllites thinly interbedded with arkosic and calcareous quartzites; the Dean Formation, composed of thinly bedded quartzites and phyllites; and the Hothouse Formation, composed of metagreywacke and mica schist in the eastern gorge (Sutton, 1997). Through the gorge the rock units alternate between resistant ledges of metagreywacke and quartzite and softer phyllite sequences. As the channel in the study area meanders across folded metamorphic units, the orientation of flow relative to the dip and lithology of the bedrock varies.

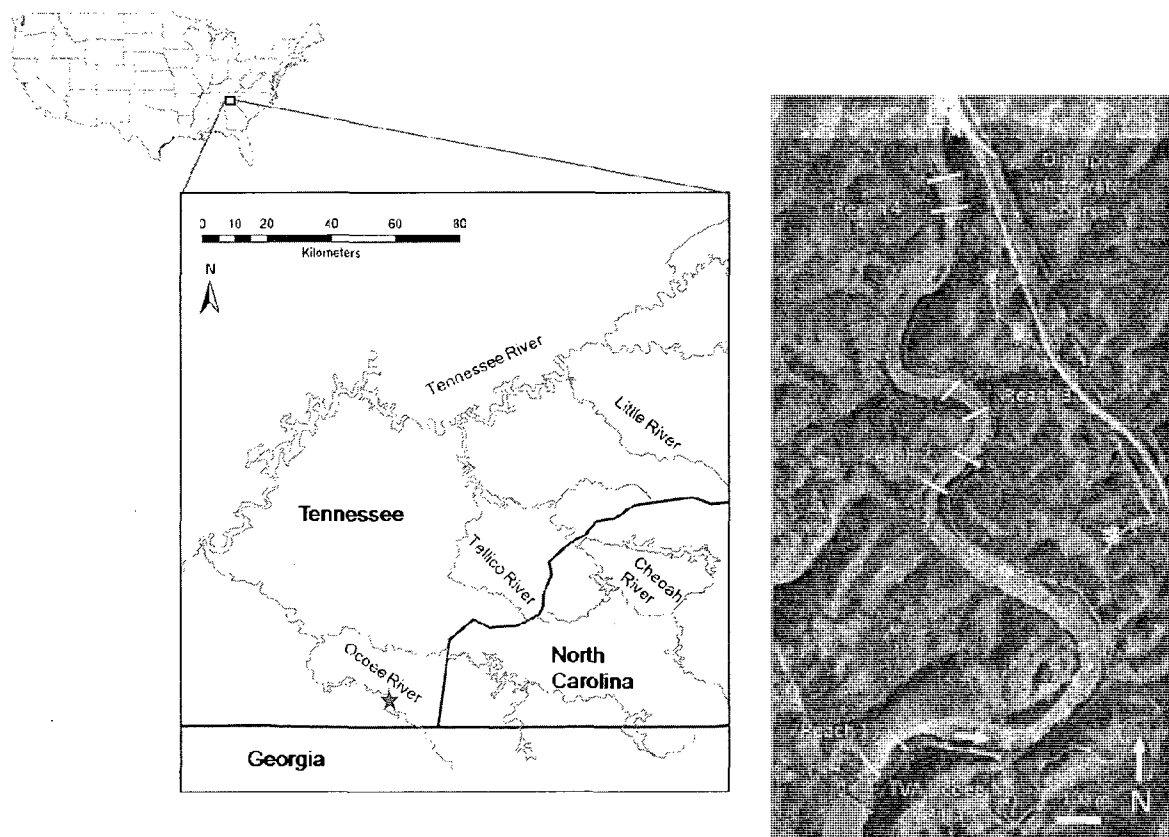


Figure 5.1. Study area. Location of study section on the Ocoee River is indicated by the star, and the reach locations are shown on the Digital Orthophoto of the Ocoee River study area (USGS, 1997). Reach boundaries are indicated by the solid white lines.

The bed topography consists of long, narrow portions of bedrock that protrude above the surrounding bed; I refer to these as bedrock ribs (Chapter 3). Ribs are asymmetrical in cross section regardless of planform orientation, consistently oriented parallel to the metamorphic foliation in the rock, and occasionally follow dominant joints. The strike of the ribs varies as the trend of the sinuous channel changes downstream. A detailed explanation of the rib features and the interactions between hydraulics and rock erodibility associated with these forms is outlined in Chapter 3.

Bedrock ribs are associated with locally similar zones of coarse material deposits. Alluvial material in this system consists of sand- to boulder-sized sediment that occurs in discontinuous patches, in the intervening lows between ribs and within potholes. The angularity of the material ranges from very well rounded particles within potholes to more sub angular particles across the channel bed. This difference in angularity appears to reflect not only the local hydraulic environment, but also the lithologic origin: phyllite produces more angular particles, whereas the metagreywacke corresponds to well-rounded particles.

The upstream boundary of the study section is impounded by the Ocoee No. 3 dam, which is operated by the TVA (Figure 5.1). The segment extending 8-km downstream to the No. 3 power station was left completely dewatered after the closure of the Ocoee No. 3 dam in 1942. Only exceptional winter storm flows that exceed the hydropower capacity are routed through the natural channel. Since the 1996 Olympics, the TVA has guaranteed recreational flows of roughly $45 \text{ m}^3/\text{s}$ for six hours on both Saturday and Sunday from Memorial Day weekend through Labor Day weekend in the river section below the Ocoee No. 3 dam. Winter and spring storms produce flows for

which the daily average releases from the dam range from 40 to 60 m³/s, and peak flows can reach 800 m³/s.

5.3. Methods

5.3.1. Field Methods

Four study reaches within the 4-km-long study area were selected according to the orientation to flow of the bedrock ribs: longitudinal; oblique and transverse (Figure 5.1). Longitudinal ribs occurred in the first two reaches, but differed in amplitudes and dominant lithology (Table 5.1).

Table 5.1. Reach variable summary

	Reach 1	Reach 2	Reach 3	Reach 4
Rib orientation to flow	Longitudinal	Longitudinal	Oblique	Transverse
Mean rib amplitude (m)	0.43	0.57	0.78	0.80
Reach gradient (m/m)	0.0075	0.0082	0.0106	0.0198
Manning's n	0.059	0.075	0.092	0.107
MSE from planar regressions	0.065	0.1091	0.153	0.255
Mean Schmidt reading	34	40	40	45
Mean Selby Score	65	72	75	77
Number of potholes surveyed	105	296	176	146
Area of pothole survey (m ²)	3885	5130	5695	9898
Mean pothole density	0.027	0.058	0.031	0.015
Mean Pothole Radius (cm)	15.5	20.5	24.6	21.5
Mean Pothole Depth (cm)	17.1	21.8	27.9	36.8
Mean Pothole Max Depth (cm)	23.2	29.9	39.7	49.7

Oblique ribs and transverse ribs occurred in reaches 3 and 4, respectively. The spatial locations of all potholes were surveyed within a sub area of each reach, where I also had highly detailed bed topography surveys. Pothole dimensions (depth and radius) were determined from five survey points; one at the base and four along the rim (Figure 5.2). Grinders were excavated from filled potholes in order to get the most accurate depth

measurements. The mean depth was calculated as the difference between the mean rim elevation and the pothole center elevation. Because the rim elevations tended to vary widely, I also calculated the maximum depth based on the highest rim elevation. Pothole rims were defined in the field as being where the perimeter had substantial curvature, which likely reflects the extent of the vortex associated with the pothole.



Figure 5.2. Photograph of pothole in Reach 4 on the downstream side of a massive rib. Note the variability in the rim elevation that is typical of potholes cut into rib perimeters.

In the three upstream-most reaches, a randomly selected subset of 25 potholes was selected for detailed measurements. All grinders were removed from these potholes and grain sizes (3 axes) were measured from a random subsample. Experimental concrete grinders of similar dimension to the D_{50} excavated from the potholes were installed in the cleared potholes. Repeat measurements of the grinder size were performed for each reach on grinders that remained in the original pothole after each of four summer recreational flow releases ($Q_{\text{peak}} = 46.8$ cms), and one survey was performed the

following summer after winter flows ($Q_{\text{peak}} = 80.7$ cms). Between flows the grinders were recovered and the three axes were measured to determine the change in grinder diameter between flows.

5.3.2. *Statistical Analyses*

Ripley's K-function, a cumulative distribution function of distances between points within a set area, was used to graphically determine the spatial pattern of potholes at different locations within each reach (Ripley, 1977) and thereby test (H2). The K-function is a second-order statistic that can be used to test the null hypothesis of spatial randomness according to a Poisson distribution. This statistic examines the proportion of the total possible points within a rectangular area that are within a specified distance of each other. The range of pothole sizes was grouped into three equal sample size classes of radius and depth and the largest and smallest of the three groups were tested for spatial relationships in pothole size using both Pielou's index of segregation and the Multi-Response Permutation Procedure for Association (MRPPA). These statistics were used to test (H3). Pielou's index tests the null hypothesis of spatial independence (i.e., no segregation) based on a Chi-square distribution (Pielou, 1961). This statistic is calculated by taking an individual pothole, locating its nearest neighbor, and recording the size class of both potholes. This procedure is repeated n times. A positive test statistic indicates positive segregation (i.e., similarly sized potholes are located near each other), whereas a negative test statistic indicates that differently sized potholes tend to occur together. The distance-based MRPPA statistic is calculated as a weighted average (over groups) of the within group distances and computes all pairwise distances (Mielke, 1986). If the within-

group distances are smaller, then the groups are clustered. This statistic is used to test the null hypothesis of no segregation.

5.3.3. *Modeling the probability of pothole formation*

Topographic data within the active channel from different surveys (~ 1-m sampling frequency) within each reach were used to define a mean surface through the reach. These surfaces were determined through planar regressions. All reaches have relatively high width-to-depth ratios and no well-defined thalweg, which justifies the use of a planar surface. The predicted values of this mean bed surface were increased by 2 m. Subtracting the actual elevation of the pothole center and adding the mean pothole depth yielded the depth below this assumed water-surface slope, $Z_{relative}$ (Figure 5.3).

$$Z_{relative} = (Z_{predicted} + 2m - depth_{ph}) - Z_{actual} \quad (1)$$

Although water surface slopes in these reaches are not uniform, this metric provides the best descriptor of the pothole's local hydraulic environment (i.e., flow depth above the pothole center), given the lack of true water-surface elevations, but wealth of bed topography data.

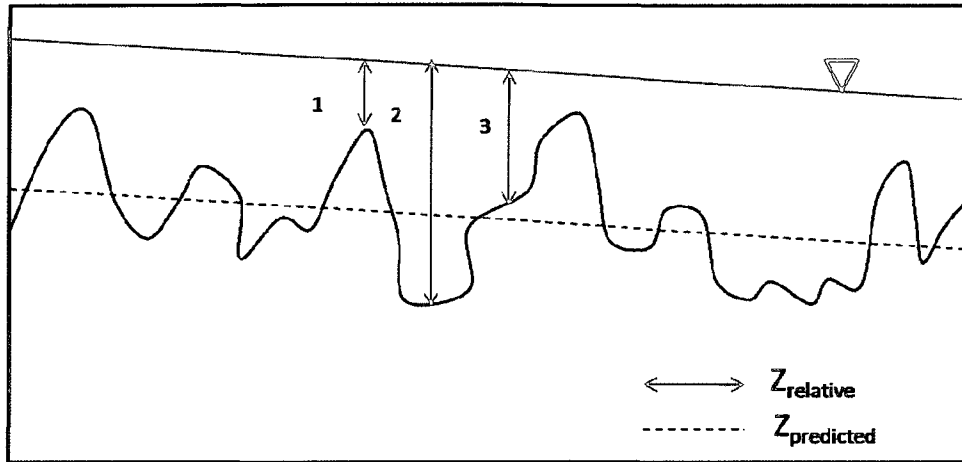


Figure 5.3. Schematic showing how pothole elevations relative to some arbitrary flow depth were calculated. Flow is from left to right in this longitudinal view of the surveyed channel bed and hypothetical water surface. The water surface was assumed to mirror the mean bed elevations for simplicity.

If the location of potholes is related to the local hydraulic environment, then whether a pothole can form and be maintained should relate to the elevation of the bedrock surface relative to some water surface elevation, $Z_{relative}$. This assumption is rooted in the concept of tools versus cover effects (Sklar and Dietrich, 1998; 2004), as applied to potholes. The formation and maintenance of stream potholes via abrasion requires a constant flux of tools delivered as bedload. For larger $Z_{relative}$, it is more likely that the deep trough is filled with alluvial material of limited mobility (cover effect), thereby limiting pothole formation. Lower values of $Z_{relative}$ likely correspond to the crests of ribs, or bedrock elevations that are inaccessible by bedload under most flows and subject to abrasion only by suspended sediment. Therefore, it is expected that bed location at an intermediate depth will have the greatest probability of forming a pothole, because the hydraulics favor the supply and transport of coarse material that can act as grinders and facilitate pothole abrasion.

Let $Y_i = 1$ if a pothole exists at relative elevation X_i , and $Y_i = 0$ at relative elevations where there are no potholes, where E_i is the expected value of relative elevations:

$$\begin{aligned} Y_i &= 1 && \text{when } E_i \leq X_i \\ Y_i &= 0 && \text{when } E_i > X_i \end{aligned}$$

For a given relative elevation X_i selected at random,

$$P(Y_i = 1 | X_i) = P(E_i \leq X_i) \quad (2).$$

The probability $P(E_i \leq X_i)$ is the cumulative probability distribution (cdf) of potholes of all relative elevations within each individual reach. Assuming a logistic expression of the cdf of pothole locations, then

$$P(E_i \leq X_i) = \frac{\exp(\beta_0 + \beta_1 X_i + \dots + \beta_k X_i^k)}{1 + \exp(\beta_0 + \beta_1 X_i + \dots + \beta_k X_i^k)}.$$

Taking the first derivative of $P(E_i \leq X_i)$ yields the probability density function (pdf) of pothole relative elevations, $p(x)$. Polynomial logistic regression was used to describe the cdf of the probability of observing a pothole at a particular $Z_{relative}$ and estimate the regression coefficients, β_k . In all reaches, the fifth-order polynomial provided the best fit based on the Akaike Information Criteria (AIC, Akaike, 1978). These pdfs from each reach were used to calculate the probability at all other surveyed points based on their relative elevations. Contour plots of probabilities were created using kriging in the terrain and surface modeling program Surfer.

5.4. Results

5.4.1. Inter-reach variability

The relationship between the pothole depth and radius follows a significant positive power function in all four reaches (Figure 5.4). Figure 5.4 shows the wide variability in pothole dimensions, which is also indicated by the low correlation coefficients in each reach ($r = 0.63, 0.62, 0.26, 0.20$, respectively). There is no clear distinction in these relationships between reaches; the coefficients and exponents are fairly consistent (Table 5.2). The exponents to these relationships in pothole dimensions reported by Springer et al. (2006) are two times as large as those reported here, and show much better correlations. Nonetheless, the exponents are consistently less than one in this study, indicating that pothole depth tends to increase faster than the radius.

Table 5.2. Dimension regression statistics ($R = aD^b$)

Reach	n	a	b	R2	p-value
1	105	4.21	0.47	0.40	<0.0001
2	296	4.83	0.48	0.39	<0.0001
3	176	5.50	0.46	0.26	<0.0001
4	146	5.69	0.38	0.20	<0.0001

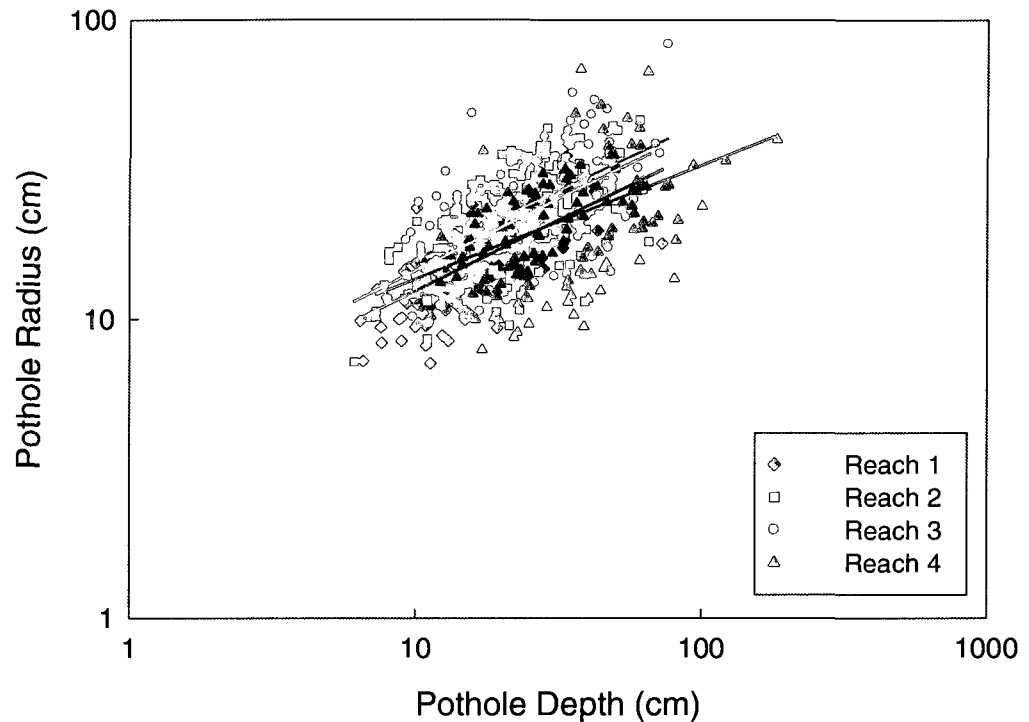


Figure 5.4. Pothole dimension relationships: Depth versus radius power functions for all four reaches. Statistics are reported in Table 5.2.

Comparing the pothole dimensions between the four reaches indicates that all dimensions in Reach 1 are significantly smaller than all four other reaches (Tukey HSD $p < 0.0001$). Reach 1 is the only reach of the four where the more densely jointed phyllite is the dominant substrate, as demonstrated in Chapter 3. Both the mean and maximum pothole depths are significantly different among all four reaches (Figure 5.5). These results support the hypothesis that pothole dimensions differ in the four reaches that vary in substrate characteristics (H1). The results also indicate that pothole dimensions vary in the direction expected (denser jointing results in smaller potholes).

The spatial patterns of potholes differ between the four reaches (Figure 5.6). At the smallest distances (1 to 10 m), the spatial pattern of potholes in all reaches is aggregated. The degree of aggregation is indicated by the K-functions as the level of

deviation above the 95 percent confidence limits of the simulated Poisson K-functions. Comparing the spatial patterns of all reaches at an intermediate distance of 30 m, the spatial pattern in Reach 1 is completely random based on the Cramér-von Mises goodness-of-fit ($p = 0.13$) and examination of the K-function. In all other reaches, the pattern of potholes was aggregated at a 30 m distance ($p < 0.0001$). These results support the hypothesis that the spatial patterns of potholes differ between reaches (H2) and show that potholes are more aggregated in reaches with more variable bed topography.

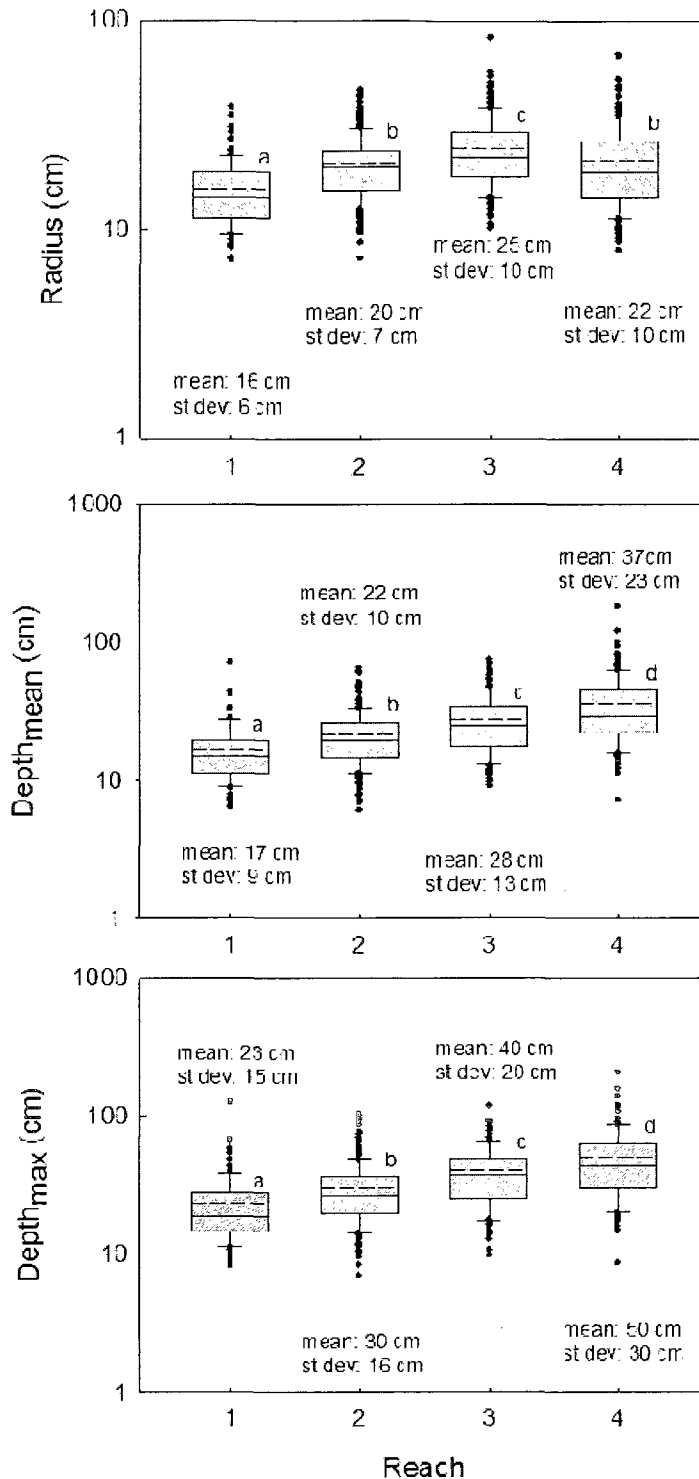


Figure 5.5. Boxplots comparing pothole dimensions between reaches (n = 105, 295, 176, and 146, respectively). a) pothole radius Significant pairwise differences in means (p<0.05) are indicated by contrasting letters above each box (Tukey's HSD following ANOVA on log transformed data). The box-plots indicate upper and lower quartiles as box ends, 10th and 90th percentiles as whiskers, and median values as the line within each box. Dots indicate values outside the 10th and 90th percentiles.

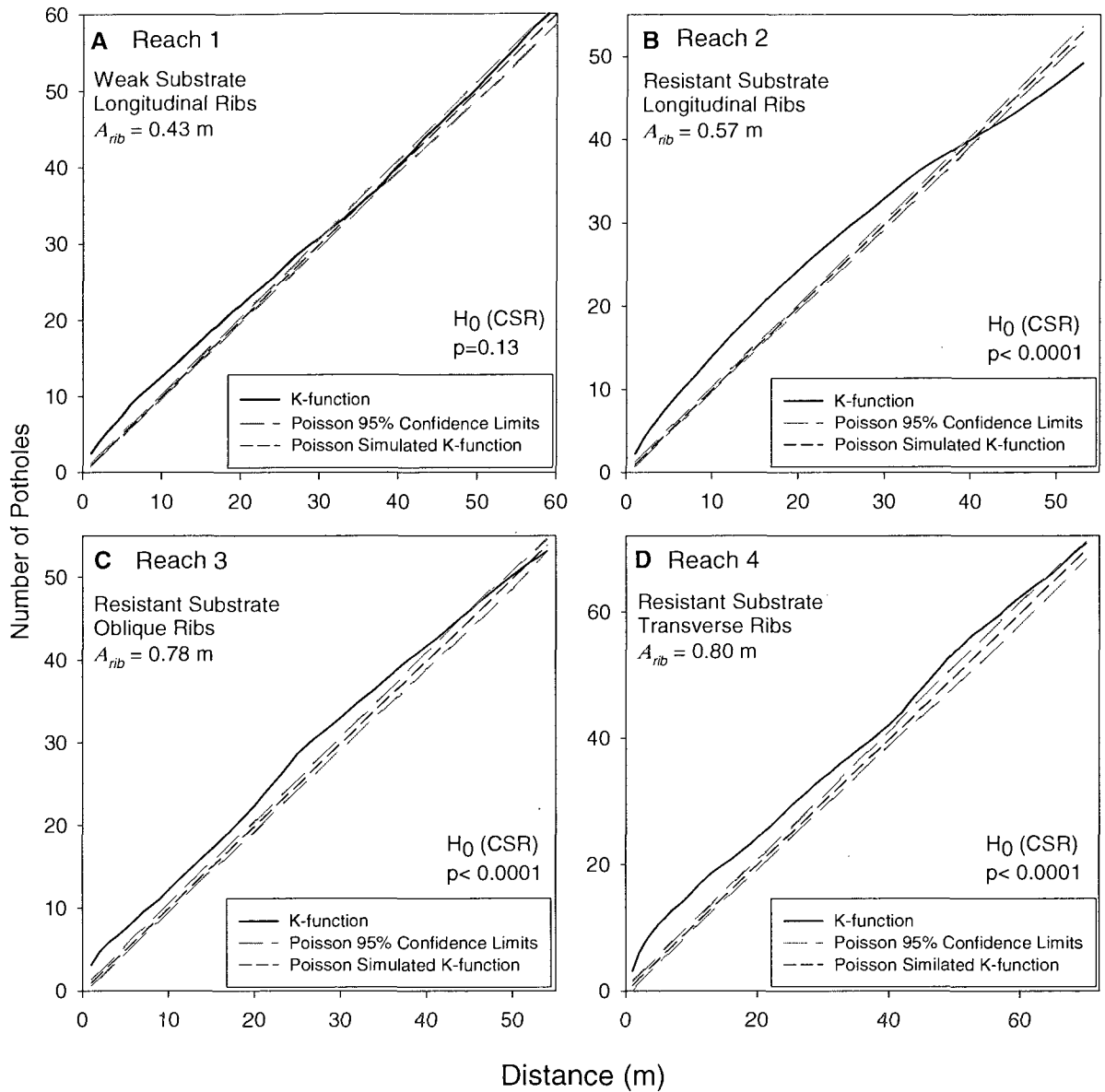


Figure 5.6. K-functions plotted in reference to simulated Poisson process based on 100 replications. Where the K-function plots above the Poisson envelopes, the potholes follow an aggregated spatial pattern; below the envelopes indicate a regular spatial pattern. The null hypothesis of complete spatial randomness is tested at a distance of 30 m in all reaches and indicated on each plot. A_{rib} is the mean bedrock rib amplitude in each reach.

5.4.2. Intra-reach variability

Potholes did not show consistent segregation or association by size in any of the four reaches (Table 5.3). Pothole spatial patterns were not significantly related to either depth or radius in Reach 1. This result is consistent to the interpretation of the K-function above, which indicated that at distances greater than 30 m, potholes in this reach were randomly distributed. In Reach 3, potholes of similar depth dimensions were positively segregated and associated (Pielou's Index = 0.889, $p < 0.0001$; MRPPA, $p = 0.001$). In this reach, nearest neighbor analysis (Pielou's Index) showed positive segregation according to pothole radius (Pielou's Index = 0.152, $p = 0.0258$), the weighted average testing all possible pairwise distances (MRPPA) showed that potholes of similar sized radii were associated ($p = 0.001$). The results thus partially support the hypothesis that potholes that follow an aggregated spatial pattern will be segregated according to dimensions (H3). In Reach 3 and Reach 4, where the greatest aggregation occurred (Figure 5.6), potholes were segregated by either depth or radius, although inconsistently.

Table 5.3. Summary statistics from segregation by size analysis

Reach	Pothole radius			Pothole depth		
	mmrpa (p-value)	Pielou's Index	p-value	mmrpa (p-value)	Pielou's Index	p-value
1	0.104	-0.043	0.69	0.023	0.171	0.130
2	0.278	0.047	0.24	0.132	0.083	<0.0001
3	0.412	0.152	0.0258	0.001	0.289	<0.0001
4	0.005	0.152	0.0086	0.195	0.131	0.09

Spatial patterns of potholes within each reach are best described in reference to the K-functions (Figure 5.6). In Reach 1, the potholes are aggregated at spatial scales up

to 30 m, beyond which the pattern is random. This is indicated by the observed K-function plotting within the simulated envelopes of a Poisson process. In Reach 2 (Figure 5.6b), where ribs are longitudinal to flow, of larger amplitude than in Reach 1, and the lithology is predominantly the more massive and resistant metagreywacke, the potholes follow an aggregated spatial pattern at spatial scales less than 40 m. This K-function plots below the Poisson envelopes at distances greater than 40 m, indicating that the clumps of potholes follow a regular pattern. In Reach 3 (Figure 5.6c), where ribs are oblique to flow, of larger amplitude than the former reaches, and lithology is more resistant, potholes are aggregated at distances up to 45 m. The observed K-function plots within the envelopes at this distance, indicating that the smaller scale clumps follow a random spatial pattern. In Reach 4 (Figure 5.6d), where the ribs are transverse to flow, of the greatest amplitude, and the rock is the most resistant (Schmidt hammer reading = 45, Table 5.1), the potholes are consistently aggregated at all scales.

5.4.3. Probability of pothole occurrence

The probability density functions of the pothole relative elevations are consistently centered at intermediate elevations in all reaches (Figure 5.7b). The spread and specific center of these distributions, however, differ among reaches. In Reach 1, the distribution is the narrowest, with a slight bulge in probability at lower relative elevations. The pdf of Reach 2 is centered consistently with the pdf of Reach 1, but the distribution is spread over a wider range of relative elevations. The pdf of Reach 3 is shifted to a center at slightly lower relative elevations, but has a similar spread to Reach 2. The pdf of Reach 4 shows the greatest spread in relative elevations.

When the relative elevations of all other survey points in each reach are applied to the pdfs generated from the pothole data, and these probabilities are plotted in space (Figure 5.8), the probabilities reflect the topography because they represent elevation. Mapping the actual locations of the potholes over these probabilities shows that potholes are consistently located in regions of greater likelihood. Notably, in Reach 1, the potholes follow the spatial pattern of the oblique ribs. The results thus support the hypothesis that the spatial occurrence of potholes is correlated to the bed elevation and, by inference, to the local hydraulics (H4).

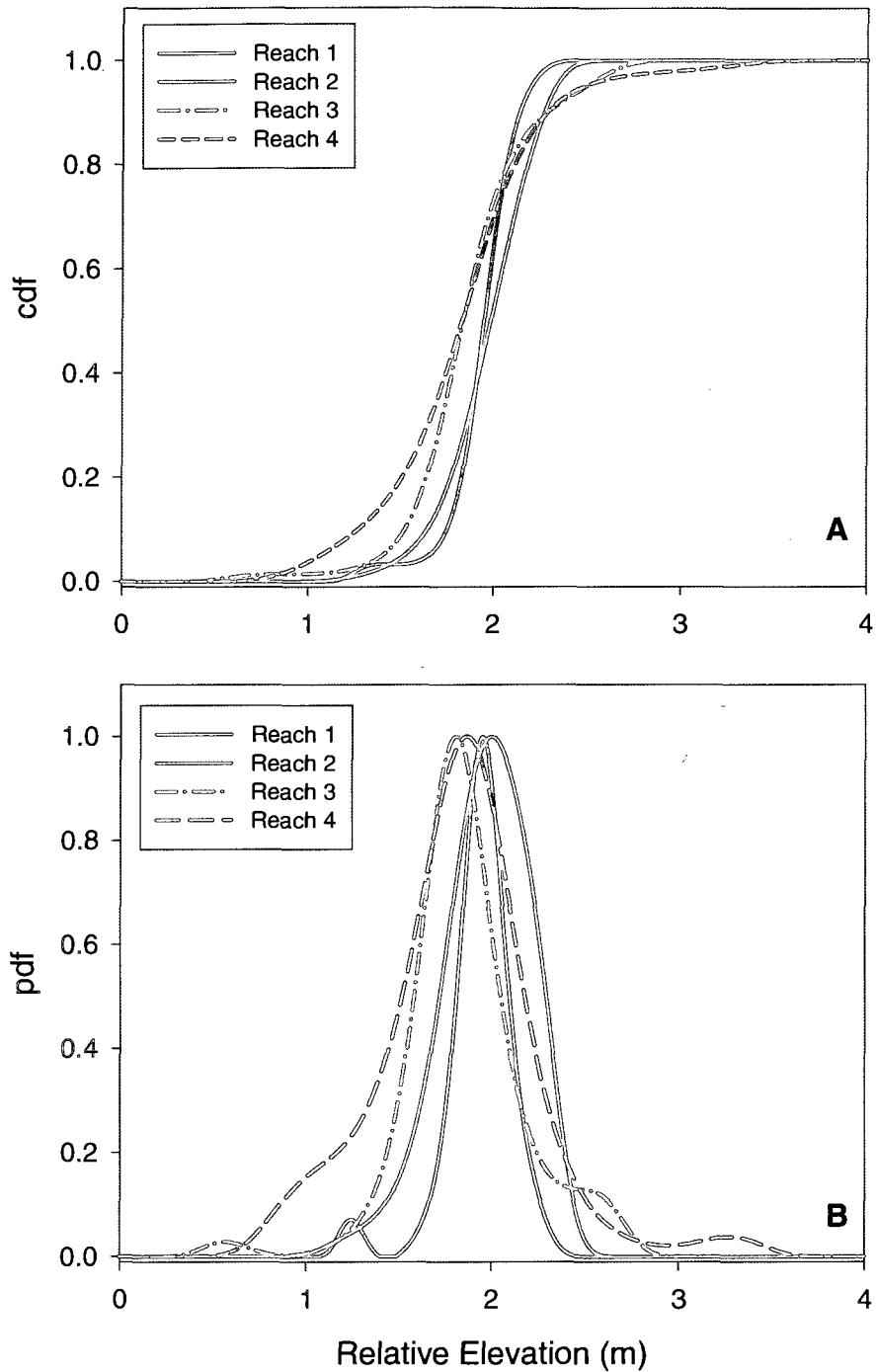


Figure 5.7 a) Cumulative distribution function of pothole elevations relative ($Z_{relative}$) to an arbitrary water surface elevation that parallels the mean bed slope (Figure 5.2). b) Probability density function pothole $Z_{relative}$ for all four reaches.

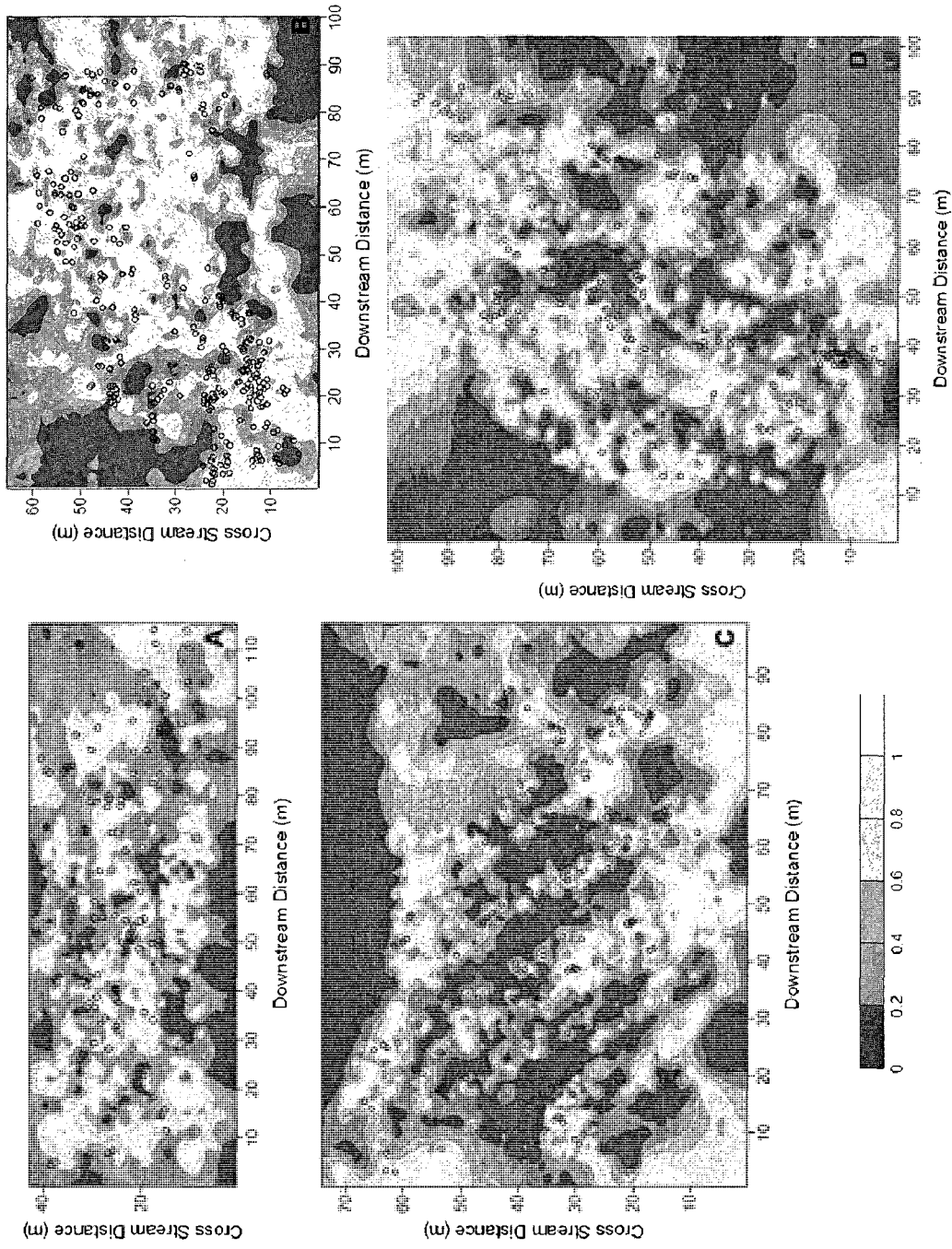


Figure 5.8. Probability plot of reach areas. Contours indicate probability of pothole occurrence based on the pdf's in Figure 5.7b; lighter colors indicate greater probability of observing a pothole. Actual locations of surveyed potholes are indicated by the black circles on each plot. Note that most of the potholes are located in regions of greater probability.

5.4.4. *Relative abrasional efficiency*

The size distribution of actual grinders excavated from a subset of surveyed potholes was significantly correlated with the size of the pothole radius (Figure 5.9). Of the 25 experimental grinders placed in the subset of fully excavated potholes, after the summer flow releases 64%, 88% and 84%, respectively, were retained in the three upstream reaches; and 52%, 80% and 76%, respectively, were retained after the winter flows. Grinders installed at Reach 4 were not used in this analysis because I observed disruption by recreational swimmers near the Olympic whitewater course. No correlations were found between experimental grinder abrasion and pothole dimensions after either recovery period (Figure 5.10). The greatest change in grinder size occurred within a small pothole (dimensions) in Reach 1, which was situated on a planar surface adjacent to the largest rib in this reach. This rib was composed of the more massive metagreywacke, whereas the pothole was incising into a more uniform surface of phyllite. Observations of the flow at this location during summer releases suggested relatively high velocities associated with the constriction formed by the rib. Prior to installing this grinder, the pothole contained a few well rounded gravel particles and a clearly abraded and polished interior. I was surprised to find that the grinder decreased in diameter by 35% after only 12 hours of flow at $45 \text{ m}^3/\text{s}$. Although the sample size is too small to conduct an analysis of grinder abrasion according to pothole location within each reach, this example illustrates the key role that the local environment plays in abrasion within a pothole. It also suggests that the channel is still actively incising, albeit at slow rates. If we focus our attention to the results from Reach 1, which had the most homogenous substrate, there is a positive correlation between pothole dimensions and

experimental grinder abrasion. In 2007, excluding the outlier discussed above, this relationship also appears.

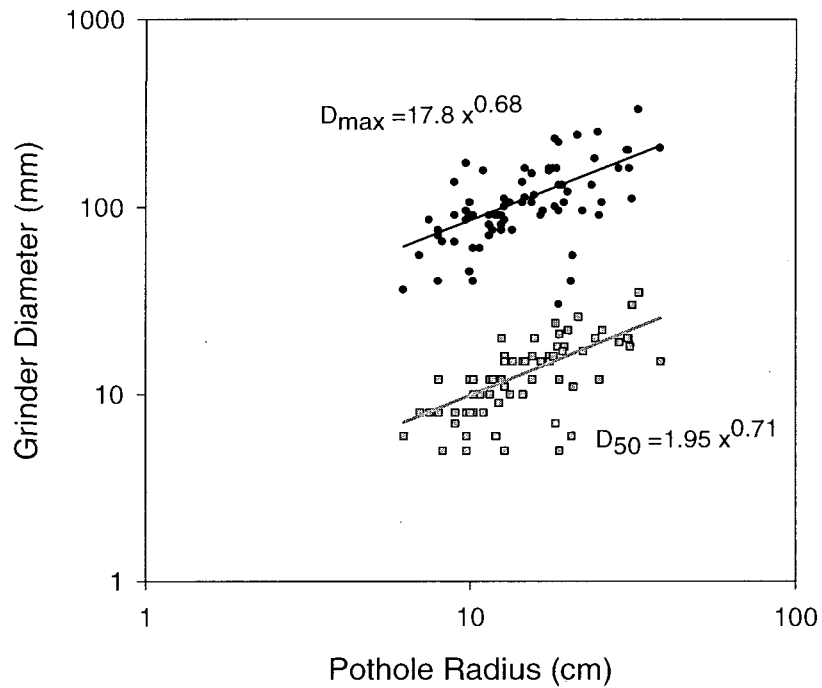


Figure 5.9. Relationship between grinder size and pothole radius. Data include the subset of selected potholes for all reaches for the experimental grinder analysis. D_{50} and D_{max} are based on a random sampling of 100 actual grinders excavated from each pothole.

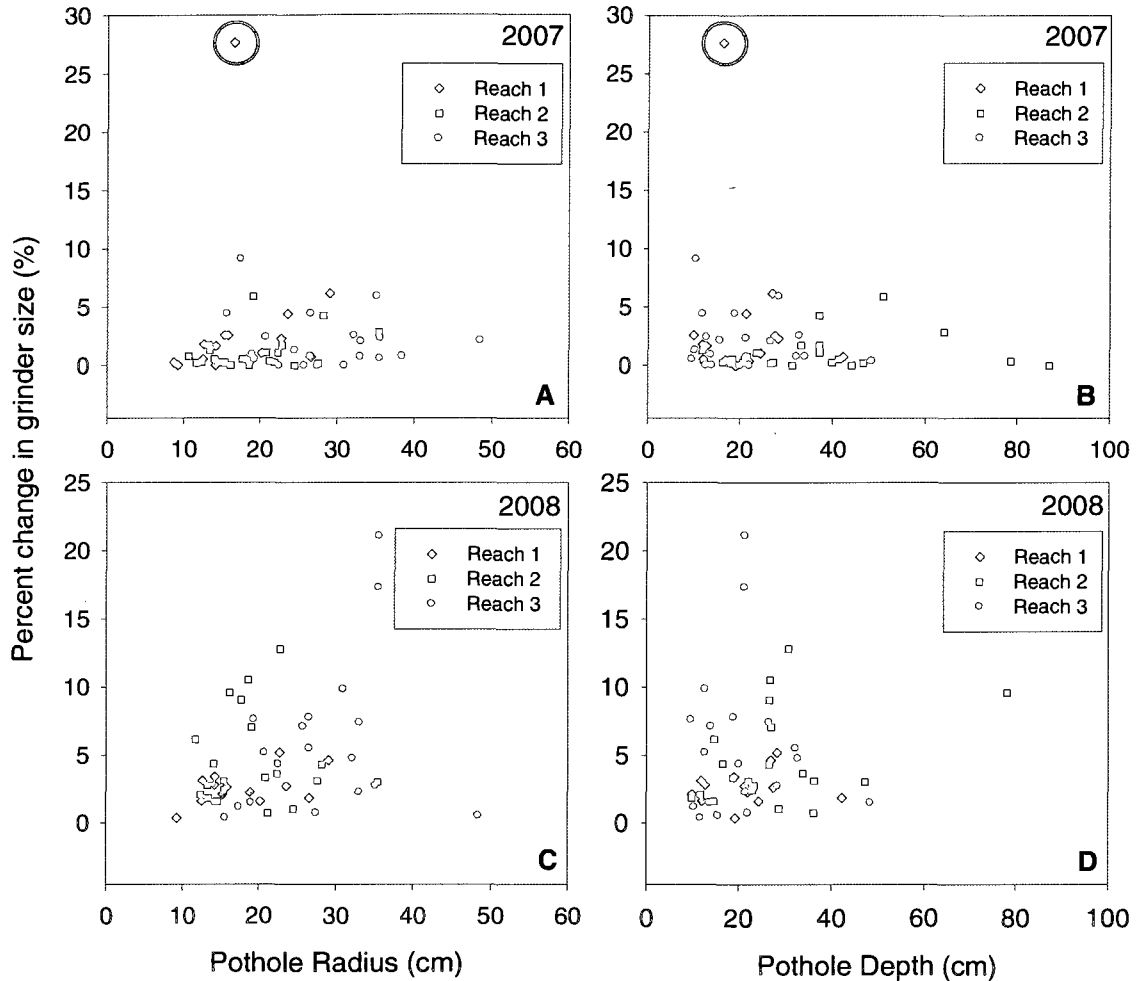


Figure 5.10. Relative experimental grinder abrasion. Circle indicates outlier in Reach 1, which was located in a uniform topographic and high velocity zone.

5.5. Discussion

Although pothole depth and radius were correlated based on positive power functions, there is a large degree of unexplained variability and the exponents determined in this study are nearly half the values found by Springer et al. (2005), indicating that potholes at the Ocoee site tend to be shallower and wider than those described along the Orange River in South Africa. These size differences may reflect the weaker lithology along the Ocoee River (Schmidt hammer readings ranging from 35 to 45) as opposed to

the Orange River (Schmidt hammer readings ranging from 60 to 70). If the relationship of pothole depth to radius is a representation of the local hydraulics within the pothole, then the unexplained variability in these relationships from the Ocoee River may be related more to the hydraulics around the pothole, which set up the internal hydraulic environment. The relationship between pothole depth and radius in Reach 1 explains the most variability in comparison to the other three reaches. This suggests that in reaches with greater substrate heterogeneity, differing erosional resistance limits the development of a consistent relationship between pothole depth and radius.

Lacking inner channel development, none of the reaches displayed active coalescence of potholes observed by other investigators of potholes associated with deep inner channels (Kale and Shingade, 1987; Wohl, 1993; Whipple et al., 2000b; Springer et al., 2005). In steeper sections of the Ocoee, ~ 5 km downstream of the study reaches, I observed more coalesced potholes where a thalweg was more defined. Therefore, it is likely that the large width-to-depth ratios, lack of an inner channel, relatively moderate bed slopes, and relatively weaker lithology have contributed to the small size of potholes along the Ocoee River study reaches compared to other reports of potholes dimensions (e.g., Springer et al., 2005).

5.5.1. Pothole variability as a function of rock characteristics: Reach-scale differences

Differences in pothole dimensions and spatial patterns appear to be related to inter-reach differences in rock properties and channel morphology, which suggests that lithology has an important influence on the dominant erosional mechanism. Reach 1, which has the lowest hydraulic roughness (Manning's n determined from hydraulic modeling and MSE from planar regressions; Chapter 3); Table 5.1), least variable

topography, and weakest rock (i.e., prevailing lithology densely jointed and foliated phyllite), also has the smallest potholes and random spatial pattern. Given its substrate characteristics, the fact that this is the only reach to show a random spacing of potholes suggests that rock properties influence the location and size of potholes. The significantly smaller pothole dimensions in Reach 1 and the dominance of the densely jointed phyllite suggest that hydraulic plucking is important in this reach. It is likely that the dense spacing of joints and foliations in this substrate promote plucking, which inhibits sustained pothole growth. This quantitative comparison is consistent with observations and suggestions of others (Angeby, 1951; Hancock et al., 1998; Whipple et al., 2000a), but not with Hartshorn et al. (2002), who reported the highest erosion rates in more continuously jointed and massive quartzite, compared to densely foliated schist. They attributed this difference to the efficient removal of large, joint bounded blocks of quartzite and to the greater elevational exposure of quartzite relative to the schist. Differences in erosion rates as a function of elevation are explored in the following section. Although I observed larger potholes in the reaches composed of metagreywacke and quartzite, I infer that differences in pothole size reflect the relative importance of abrasion versus plucking mechanisms in these reaches based on lithologic differences; I cannot extrapolate these results to differences in erosion rates.

The reaches also differ in bed slope; Reach 1 has the lowest slope and Reach 4 has the largest. Johnson and Whipple (2007) noted that potholes tended to form only on the steepest slopes tested in their flume, suggesting that a threshold in energy expenditure needs to be overcome to initiate pothole formation in a homogenous substrate. At steeper channel slopes and lower sediment supply rates, Finnegan et al. (2007) reported that

incision was focused in the channel center. Alternatively, at lower slopes and higher sediment supply rates, incision and transport were spread over the channel bed. Given the role of channel slope in controlling the interactions between incision rates and processes, differences in pothole dimensions and spatial patterns between reaches may be partly controlled by variations in bed slope. If rock properties provide an independent control on bed slope, these differences can be attributed predominantly to substrate characteristics.

5.5.2. *Relative elevation and optimal locations for pothole formation*

In order to function as abrasional tools, grinders must be delivered to potholes (Angeby, 1951). This flux in bedload sediment was documented in the flume by Johnson and Whipple (2007). They observed no static sediment maintained in potholes; potholes were eroded by sediment that entered the pothole as bedload and was moved out of the pothole after localized suspension by the upward-directed flow. In this study, I found that potholes are most likely to occur at intermediate elevations within a topographically variable channel bed. These results are consistent with the hypothesis that low elevations are preferentially filled with alluvial material and higher elevations are inaccessible for the bedload-sized grinders that form and maintain potholes. In a channel of similar metasedimentary lithology (i.e., schist and quartzite), but different in cross sectional shape (i.e., steep-walled and parabolic) than the reaches examined in this study, Hartshorn et al. (2002) reported a peak in erosion rates at higher elevations within the active channel. They propose infrequent but significant impacts of large saltating boulders and essentially continuous abrasion via very coarse sand in suspension as a mechanistic explanation for this peak in incision. This peak in erosion rates at

intermediate elevations is consistent with the probability distributions of the relative elevation of potholes, which suggests that intermediate elevations in a variable channel bed have the greatest probability for pothole formation and persistence. Both results are attributed to the vertical distribution of sediment transport.

5.5.3. *Interactions between potholes and bedrock ribs*

Bedrock channel wall forms have been suggested to form through pothole breaching and convergence (Wohl, 1993, 1998; Richardson and Carling, 2005). Carter and Anderson (2006), however, observed pothole formation in response to preexisting undulating wall forms, which created favorable hydraulic environments for pothole formation. Placing observations from the Ocoee River in the context of these experimental studies and qualitative interpretations, feedbacks likely operate between the formation of bedrock ribs via the convergence of potholes and pothole formation in response to bedrock ribs.

One interesting observation of the occurrence of potholes in all study reaches is the association of potholes with bedrock ribs (e.g., upstream, downstream or lateral margins). Reach 3 notably shows a consistent spatial relationship between pothole locations and bedrock ribs. In some cases I observed potholes formed in longitudinal succession adjacent to ribs. In reach 2, where ribs were longitudinal to the flow, I observed a cross stream spatial progression of potholes that appeared to be excavating the eventual rib troughs (Figure 5.11). This leads to the hypothesis that this spatial progression may represent a temporal evolution of rib geometry, where potholes coalesce and leave the ribs as intervening positive topographic features. This hypothesized process

is similar to observations of inner channel and canyon formation through the breaching and merging of potholes (Shepherd and Schumm, 1974; Wohl et al., 1999; Johnson and Whipple, 2007). These results point to the importance of feedbacks between these two forms and the local hydraulics and sediment transport dynamics.

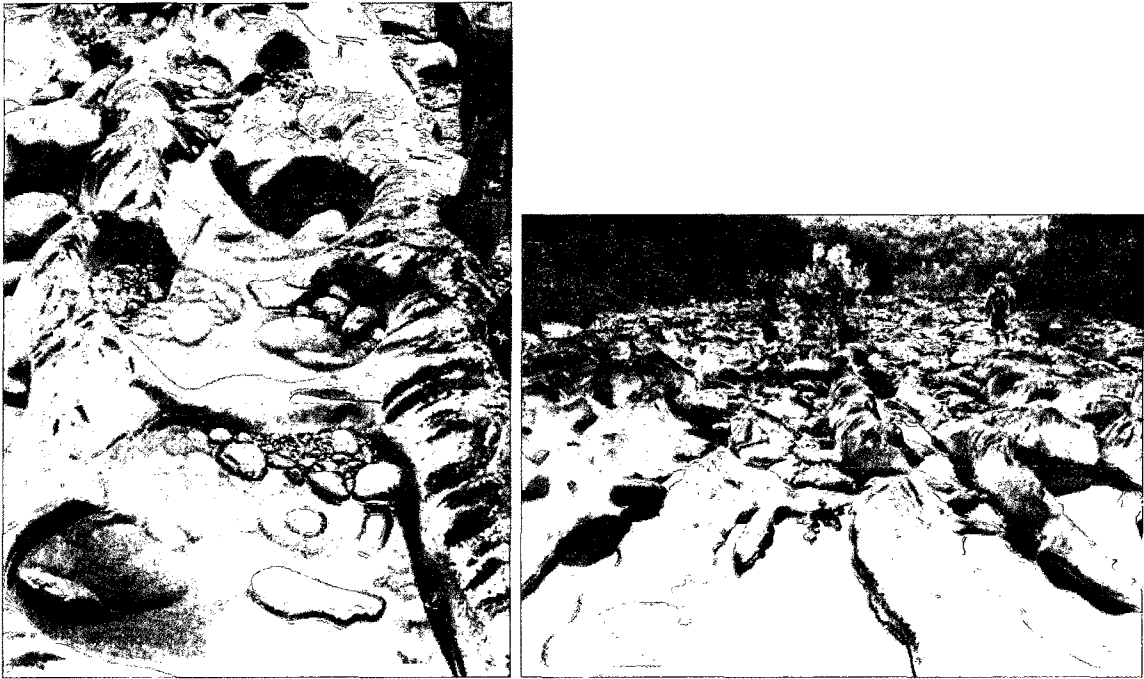


Figure 5.11. Coalesced potholes between longitudinal ribs. Flow is top to bottom.

Local hydraulics within potholes may be partly controlled by the potholes' internal dimensions, but the hydraulic environment around the pothole is likely to have an even larger influence on these dimensions. The experimental grinders showed that grinder abrasion was not significantly related to pothole dimensions, which suggests that the internal dimensions do not significantly control hydraulics. The early experiments of Alexander (1932) documented strong relationships between the strength of the recirculating vortex within a pothole and the angle of flow entrance. The kinetic energy, measured via the movement and angular velocity of grinding tools, was greatly reduced

as pothole depth increased. Through its influence on the local hydraulics around potholes, it is likely that variation in bed topography limits the ability to discern a clear relationship between pothole depth and grinder abrasion. However, I observed little evidence of abrasion of grinders in the deepest potholes (~1 m depth), whereas the shallowest potholes showed noticeable smoothing of the experimental grinder, thus indicating the effects of the recirculating vortex. In Reach 1, where the bed topography was the most homogenous, there appears to be the best relationship between pothole dimensions and experimental grinder abrasion, albeit statistically insignificant, which could partly be attributed to the limited sample size. Nonetheless, the lack of significant relationship between dimensions and experimental grinder abrasion points to other influences on the hydraulics within potholes. Considering these results in the context of the spatial patterns of potholes within each reach, it is likely that the topography surrounding an individual pothole and the relative elevation of the pothole are important influences on pothole dynamics.

5.6. Conclusion

This study demonstrates that complex-bed topography and substrate variability in a bedrock channel exert a major control on the abrasional sculpting by channel potholes. Lack of a defined thalweg precludes focused erosion in the center of the channel at the Ocoee study site. A comparison of four reaches with different substrate properties, bedrock rib orientation and amplitude indicates that, where the channel bed is more topographically homogenous, potholes follow a more random pattern. In contrast, potholes are aggregated in reaches that have high spatial variability in bed topography.

Within each reach, potholes are segregated by size and aggregations correspond to channel bed areas with the greatest topographic variation. Probability distributions show that potholes tend to be focused at intermediate bed elevations, which is conceptually supported by local and vertically oriented tools versus cover concepts applied to pothole formation. Potholes tend to be focused on the downstream sides of transverse ribs, and lateral to longitudinal ribs. Focused erosion in these locations is likely a result of flow separation associated with the rib forms. Because spatial aggregation of focused erosion in potholes does not vary systematically along the channel cross section, the results from this study will be useful for modeling the lateral component of bedrock incision.

References

- Akaike, H., (1973), Information theory and extension of the maximum likelihood principle. Pages 268-281. In: N. Petrov and F. Csaki, editors. Second International Symposium on Information Theory. Hungarian Academy Sciences, Budapest, Hungary. Reprinted 1992 in Breakthroughs in Statistics, S. Kotz and N. Johnson, editors, 1:610-624, Springer Verlag, New York, New York, USA.
- Alexander, H.S. (1932), Pothole erosion. *J. of Geology* 40, 305–337.
- Allen, J.R.L. (1971), Transverse erosional marks of mud and rock: their physical basis and geological significance. *Sedimentary Geology* 5, 165–385.
- Angeby, O. (1951), Pothole erosion in recent water-falls. Lund Studies in Geography. A 2, 1–34.
- Carter, C.L., and R.S. Anderson (2006), Fluvial erosion of physically modeled abrasion-dominated slot canyons, *Geomorphology* 81, 89-113, doi:10.1016/j.geomorph.2006.04.006
- Gilbert, G. K. (1877), Land sculpture, in The Geology of the Henry Mountains, Utah, edited by C. B. Hunt, chap. 5, *Mem. Geol. Soc. Am.*, 167, 99– 150.
- Gilbert, G.K. (1906), Moulin work under glaciers, *Geological Society of America Bulletin* 17, 317-320.
- Hancock, G., R. S. Anderson, and K. X. Whipple (1998), Beyond power: Bedrock river incision process and form, in *Rivers Over Rock: Fluvial Processes in Bedrock Channels*, edited by K. J. Tinkler and E. E. Wohl, Geophys. Monogr. Ser., vol. 107, pp. 35– 60, AGU, Washington, D. C.
- Hartshorn, K., N. Hovius, W.B. Dade, R.L. Slingerland (2002), Climate-driven bedrock incision in an active mountain belt. *Science* 297, 2036-2038.
- Johnson J.P., K.X. Whipple, and L.S. Sklar (2005), Field monitoring of bedrock channel erosion and morphology. *Eos Transactions AGU* 86(52) Fall Meeting Supplement: Abstract H52A-01.
- Johnson, J. P., and K. X. Whipple (2007), Feedbacks between erosion and sediment transport in experimental bedrock channels, *Earth Surf. Processes Landforms*, 32, 1048–1062.
- Kale, V. S., and B.S. Shingade (1987), A morphological study of potholes of Indrayani Knick Point (Maharashtra), in Datye, V. S., Diddec, J. N., Jog, S. R., and Patil, C. J. eds., Explorations in the tropics: Pune, India, Professor Dikshit Felicitation Committee, p. 206–214.

- Lorenc, M.W., P.M. Barco, and J. Saavedra (1994), The evolution of potholes in granite bedrock, W. Spain, *Catena* 22, 265-274.
- Matmon, A., P.R., Bierman, J. Larsen, S. Southworth, M. Pavich, M. Caffee, (2005), Temporally and spatially uniform rates of erosion in the southern Appalachian Great Smoky Mountains, *Geology* 31, 155-158.
- Mielke, Jr., P.W. (1986), Non-metric statistical analysis: Some metric alternatives, *Journal of Statistics Planning and Inference* 13, 377-387.
- Pielou, E. C. (1961), Segregation and symmetry in two species populations as studied by nearest neighbor relations, *Journal of Ecology* 49, 255-269.
- Reich, R.M. and D.B. Rideout (in press), Spatial distribution of lightning caused fires in the Black Hills National Forest
- Richardson, K., P.A. Carling (2005), A typology of sculpted forms in open bedrock channels. *GSA. Special Paper* 392. pp.108.
- Ripley, B.D., (1977), Modeling spatial patterns. *J. Royal Stat. Soc., Series B* 39, 172-192.
- Shepherd RG, and S.A.Schumm, (1974), Experimental study of river incision. *Geological Society of America Bulletin* 85, 257–268.
- Sklar, L. S., and W. E. Dietrich (1998), River longitudinal profiles and bedrock incision models: Stream power and the influence of sediment supply, in *River Over Rock: Fluvial Processes in Bedrock Channels, Rivers Over Rock, Geophys. Monogr. Ser.*, 107, edited by K. Tinkler and E. E. Wohl, pp. 237–260, AGU, Washington, D. C.
- Sklar, L., and W. E. Dietrich (2001), Sediment and rock strength controls on river incision into bedrock, *Geology*, 29, 1087– 1090, doi:10.1130/00917613
- Sklar, L., and W. E. Dietrich (2004), A mechanistic model for river incision into bedrock by saltating bed load, *Water Resources Research*, 40, W06301,doi:10.1029/2003WR002496.
- Springer G.S. and E.E. Wohl (2002), Empirical and theoretical investigations of sculpted forms in Buckeye Creek Cave, West Virginia. *Journal of Geology* 110, 469–481.
- Springer G.S., S. Tooth and E.E.Wohl (2005), Dynamics of pothole growth as defined by field data and geometrical description. *Journal of Geophysical Research-Earth Surface* 110, F04010. DOI: 10.1029/2005JF000321

- Springer G.S., S. Tooth, and E.E. Wohl, (2006), Theoretical modeling of stream potholes based upon empirical observations from the Orange River, Republic of South Africa, *Geomorphology* 82, 160-176.
- Stark CP. (2006), A self-regulating model of bedrock river channel geometry. *Geophysical Research Letters* 33, L04402. DOI: 10.1029/2005GL023193
- Sutton, S.J. (1991), Development of domainal slaty cleavage fabric at Ocoee Gorge, Tennessee. *J. of Geology* 99 (6) 789-800.
- Turowski, J.M., N. Hovius, H. Meng-Long, D. Lague, and C Men-Chiang (2008), Distribution of erosion across bedrock channels. *Earth Surface Processes and Landforms* 33, 353-363.
- Whipple, K. X., G. S. Hancock, and R. S. Anderson (2000a), River incision into bedrock: Mechanics and relative efficacy of plucking, abrasion, and cavitation, *Geol. Soc. Am. Bull.*, 112, 490
- Whipple, K.X., N.P. Snyder, and K. Dollenmayer (2000b), Rates and processes of bedrock incision by the Upper Ukak River since the 1912 Novarupta ash flow in the Valley of Ten Thousand Smokes, Alaska, *Geology* 28(9), 835-838.
- Wobus, C.W., G.E. Tucker, and R.S. Anderson (2006), Self-formed bedrock channels, *Geophysical Research Letters*, 33, L18408, doi:10.1029/2006GL027182
- Wohl, E. E. (1993), Bedrock channel incision along Piccaninny Creek, Australia, *Journal of Geology*, 101, 749– 761.
- Wohl, E.E. (1998), Bedrock channel morphology in relation to erosional processes, in *River Over Rock: Fluvial Processes in Bedrock Channels, Rivers Over Rock, Geophys. Monogr. Ser.*, 107, edited by K. Tinkler and E. E. Wohl, pp. 133-151, AGU, Washington, D. C.
- Wohl, E. E. and H. Ikeda (1997), Experimental simulation of channel incision into a cohesive substrate at varying gradients, *Geology*, 25, 295– 298.
- Wohl, E.E., D.M. Thompson, A.J. Miller (1999), Canyons with undulating walls. *Geological Society of America Bulletin* 111(7), 949-459.
- Zen E.A., and K.L. Prestegard (1994), Possible hydraulic significance of 2 kinds of potholes – examples from the Paleo-Potomac River. *Geology* 22, 47–50.

CHAPTER 6: CONCLUSIONS

The interactions and feedbacks among rock characteristics, hydraulics, sediment transport, incision processes and bedrock channel forms have been documented in experimental settings (Wohl and Ikeda, 1997; Johnson and Whipple, 2007; Finnegan et al., 2007) and inferred from field studies (Wohl, 1993; Wohl et al., 1999; Johnson and Whipple, 2005). However, most of these studies limited their scope to a few components of these interactions at a single scale. The research presented here provides new insights into these interactions by centering on the independent function of bedrock characteristics (i.e., resistance and spatial variability), and separately examining hydraulics, sediment transport and incision processes in this context at different spatial scales.

The Ocoee River study area offered a logical field setting for the research questions addressed in this dissertation. The channel displays bedforms that are undocumented in the literature, leading to an examination of the structural influence on hydraulic roughness, sediment transport and erosional mechanisms (i.e., potholing). The fact that the channel exhibits a large width-to-depth ratio and no well defined thalweg or inner channel development also allows investigation of these processes in a different context from the confined bedrock gorges or tectonically active regions that tend to dominate the current bedrock literature. This study was implemented by taking advantage of the dam operations followed for recreational flows by the TVA. A problem with field surveys on intermediate sized rivers (too large to take waded measurements, but too small for measurement by boat or bridge) is the feasibility of direct measurements. The

regulated regime allowed indirect examinations of sediment transport and pothole abrasion to be well constrained with respect to the flow regime.

In Chapter 3 the effects of substrate on channel form and the implications for reach-scale hydraulics were examined. The structurally influenced substrate that gives rise to what I term bedrock ribs reflects positive and negative feedbacks between rock properties and channel form, as schematically illustrated in the conceptual model below. The results of this component of the dissertation show that reach-scale differences in rock erodibility strongly correlate with channel geometry and hydraulics. Lower rock erodibility limits bed incision, resulting in increased slope relative to segments of channel bed with less resistant substrate. Local steepening of the profile effectively increases total stream power, thus enhancing hydraulic driving forces. The orientation of the bedrock ribs relative to flow direction in the study reaches appears to be an independent parameter that reflects the underlying bedrock structure. Steeper bed slopes also correlate with transversely oriented bedrock ribs of greater amplitude, which increase reach-scale hydraulic roughness. Increased hydraulic roughness presumably mediates the local increase in stream power along steeper reaches, providing a self-regulating feedback for flow energy available to perform work against the channel boundaries.

Chapter 4 demonstrates that complex-bed topography in a bedrock channel also exerts a major control on the transport dynamics of coarse material over at least relatively short temporal (circa 3 yr) and small spatial (10^2 m) scales. This complex bed topography in a bedrock channel appears to limit size-dependent transport distance by creating extreme spatial variability in the magnitude of hydraulic forces that influence sediment

entrainment and transport. A comparison of three reaches with different bedrock rib orientation and amplitude indicates that where ribs are longitudinal to flow and of lower amplitude transport is less obstructed, which leads to greater transport distances than in reaches where the ribs are oblique to flow and of larger amplitude. At the reach-scale, oblique or transverse ribs increase the reach-scale roughness and reduce reach-averaged velocity, which corresponds to lower transport distances. Because local-scale bedrock channel morphology correlates most strongly with transport distance, it likely plays a dominant role in the transport of coarse sediment. Ribs of greater amplitude create more localized zones of low velocity to shield clasts from entrainment.

Chapter 5 demonstrates that complex-bed topography and substrate variability exert a major control on abrasional sculpting by potholes. Lack of a defined thalweg precludes focused erosion in the center of the channel at the Ocoee study site. A comparison of four reaches with different substrate properties, bedrock rib orientation and amplitude indicates that, where the channel bed is more topographically homogenous, potholes follow a more random pattern. In contrast, potholes are aggregated in reaches that have high spatial variability in bed topography. Within each reach, potholes are segregated by size and aggregations correspond to channel bed areas with the greatest topographic variation. Probability distributions show that potholes tend to be focused at intermediate bed elevations, which is conceptually supported by applying local and vertically oriented tools versus cover concepts to pothole formation. Potholes tend to be focused on the downstream sides of transverse ribs, and lateral to longitudinal ribs. Focused erosion in these locations is likely a result of flow separation associated with the rib forms. Because spatial aggregation of focused erosion in potholes does not vary

systematically along the channel cross section, the results from this study will be useful for modeling the lateral component of bedrock incision.

Linking the results of the three field studies elucidates the interactions among hydraulics, sediment transport, and incision processes with the central independent control of substrate properties (Figure 6.1).

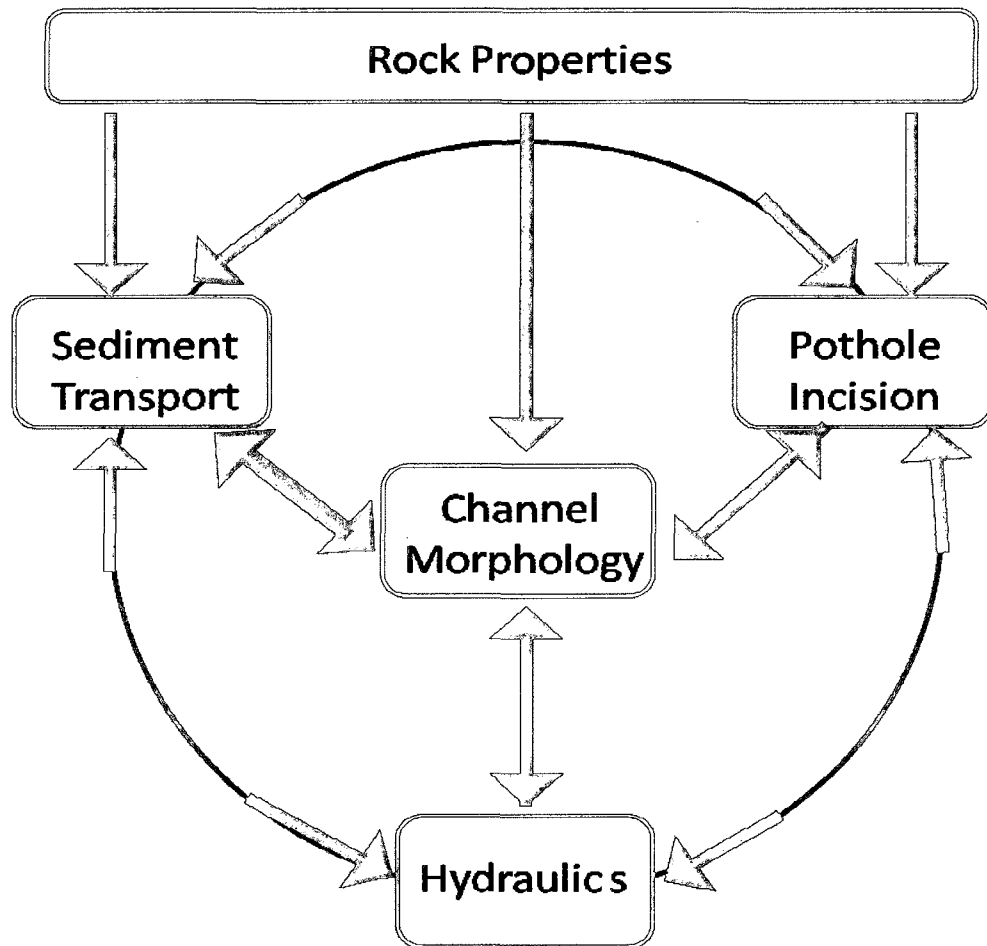


Figure 6.1. Flow diagram of the interactions among channel morphology, sediment transport, pothole incision, and hydraulics, which are all influenced directly or indirectly by rock properties.

The independent rock properties (lithology and structure) have a direct effect on channel morphology in the Ocoee River and other Blue Ridge streams examined in Chapter 3. The underlying folded structure and variation between metagreywacke and

phyllite creates differences in the orientation and amplitude of bedrock ribs in the channel bed. The bedrock lithology also controls the size and lithology of the coarse sediment transported in the Ocoee River. Differences in rock resistance between the two dominant lithologies also directly lead to differences in the size and spatial patterns of potholes, which appear to be the most effective incision process in this bedrock system. Through the other interactions, rock properties lead to differences in hydraulics examined at the reach scale.

As shown in Figure 6.1, channel morphology, pothole incision, hydraulics and sediment transport are all interconnected, with channel morphology as the overall control. The three outer circle components were separately the focus of the three key study chapters. Summarizing these interactions is complicated, so it is best to focus on channel morphology and follow a single path through these interactions, despite the many potential directions. This discussion follows the progression of the three study chapters.

The hydraulics within this bedrock system are intricately linked to the differences in bedrock rib morphology; transverse, higher amplitude ribs are associated with the greatest hydraulic resistance quantified by the Manning's roughness coefficient, n . Hydraulic differences at both the inter-reach and intra-reach scales produce variations in sediment transport distances, and the greatest transport distances are associated with the longitudinal ribs, greatest reach-averaged velocity, and least interference of transport at the smallest scales. Hydraulics and pothole incision also show a direct interaction, as potholes are more likely located at intermediate elevations. Indirectly, hydraulics influence sediment transport processes, which provide the flux of tools to initiate and maintain potholes. Both pothole incision process and sediment transport, through the

mechanism of abrasion, are important for shaping the bedrock morphology, thereby closing the interaction loop. Overall, by separately examining these components to the extent possible in the field, new insight is gained regarding these interactions, which adds to and supports the experimental work of others (Johnson and Whipple, 2007; Finnegan et al., 2007; Chatanantavet and Parker, 2008).

6.1. Future directions

There are still many unanswered questions regarding the forms and processes within bedrock channels dominated by abrasional processes. Based on the research presented in this dissertation, several directions for future study can be suggested that would build on these results. Given the new recognition of the bedrock rib morphology examined here, it would be beneficial to further examine the presence of this morphology in other contexts. Several streams in the Blue Ridge Province displayed this morphology, but reporting the existence of these features in other regions dominated by metasediments or by other lithologies would enhance the broad applicability of the results reported here.

The high width-to-depth ratio and lack of an inner channel pose the question of whether there are field settings in which threshold slopes, values of stream powers, rock resistance and/or uplift rates, cause the formation of an inner channel, and analogous combinations of these variables that preclude the formation of an inner channel. Other investigators have interpreted the presence of an inner channel as a mechanism of focused erosion in response to greater substrate resistance or relative base level fall, and the relatively non-resistant substrates and stable base level of the field area supports this

interpretation. Much remains to be done, however, before we can quantitatively predict the conditions under which an inner channel will or will not form.

The high variability of sediment transport in this system suggests that much more research is needed to predict sediment transport processes, especially given the importance of bedload material in shaping bedrock channels. If pothole abrasion is the most effective mechanism of bedrock incision in massive substrates, then more research on the mechanics and spatial variability of pothole erosion is needed to improve the shallow literature in this area. Focusing on smaller scale hydraulics around ribs and within potholes, as well as sediment flux through potholes at different flows, would likely provide useful insights.

Given the recent advancements in bedrock river studies, and recognition of the importance of these systems within the whole landscape, future studies will continue to constrain concepts of bedrock channel form and process. Our knowledge of these systems might one day be on par with that of their alluvial counterparts.

APPENDIX A:
CROSS SECTION PLOTS

